

# Testing and monitoring of an energy efficient indirect evaporative CO<sub>2</sub> refrigeration system at a Coles supermarket

Final report



## RACE for Business

**Research Theme:** BT2: Decarbonising businesses and supply chains

ISBN: 978-1-922746-54-2

Industry Report

Testing and monitoring of an energy efficient indirect evaporative CO<sub>2</sub> refrigeration system at a Coles supermarket

### Citation

Lau, T., Alemu, A., Bruno, F., Chuvan, T., Evans, M., Gilbert, R., J., Leak, J., Leonardis, C., Liddle, R., Liu, A., Rainey, T., Semsarilar, H., Xing, K. (2024).

Testing and monitoring of an energy efficient indirect evaporative CO<sub>2</sub> refrigeration system at a Coles supermarket

Prepared for RACE for 2030

July 2024

## Project team

UniSA

- Dr Timothy Lau
- A/Prof Ke Xing
- Dr Michael Evans
- Prof Frank Bruno
- Mr Hesam Semsarilar
- Mr Raymond Liddle

QUT

- Dr Aaron Liu
- A/Prof Thomas Rainey
- Dr Alireza Taghipour
- Mr Thuy Chuvan

Seeley International

- Mr Rob Gilbert
- Mr Clint Leonardis

Australian Alliance for Energy Productivity (A2EP)

- Mr Jarrod Leak

## Project partners



## Acknowledgements

The research team would like to thank the industry reference group participants from the following organisations: Australian Institute of Refrigeration, Air Conditioning and Heating (AIRAH), Alfa Laval, Australian Meat Processing Corporation (AMPC), Coca Cola Amatil, Dairy Australia, Health Infrastructure (NSW), Mater Group and the Refrigerated Warehouse and Transport Association.

## Acknowledgement of Country

The authors of this report would like to respectfully acknowledge the Traditional Owners of the ancestral lands throughout Australia and their connection to land, sea and community. We recognise their continuing connection to the land, waters and culture and pay our respects to them, their cultures and to their Elders past, present, and emerging.

## What is RACE for 2030?

RACE for 2030 CRC is a 10-year co-operative research centre with AUD350 million of resources to fund research towards a reliable, affordable, and clean energy future. <https://www.racefor2030.com.au>

## Disclaimer

The authors have used all due care and skill to ensure the material is accurate as at the date of this report. The authors do not accept any responsibility for any loss that may arise by anyone relying upon its contents.

## Executive Summary

A first of a kind dew point CO<sub>2</sub> refrigeration system was successfully designed, manufactured, installed and commissioned at a Coles supermarket in Norwood, South Australia. The DP-CO<sub>2</sub> system is comprised of 3 gas cooler units which integrate 12 Seeley International CW-15S dew point coolers to provide the required heat rejection capacity for Coles' refrigeration system. The DP-CO<sub>2</sub> system was also integrated with a custom-built monitoring system, comprised of 115 sensors which measure key properties such as temperature, pressure and energy across multiple locations and points within the system. These sensors record the data every 10 seconds and upload it to a secure server at the end of each week for use by the research team. The DP-CO<sub>2</sub> system was commissioned between January to May 2023, and the Coles store opened successfully on the 21<sup>st</sup> of June 2023.

Both the DP-CO<sub>2</sub> system and the monitoring system functioned as expected, albeit with a few minor issues, including a sub-optimal placement of the ambient temperature sensor too close to the dew point cooler outlets (which resulted in errors in the ambient temperature reading), and the sub-optimal selection of an approach temperature for the gas cooler outlets. Additionally, it was found that the original changeover procedures between the flash gas bypass mode and the parallel compression mode was sub-optimal, resulting in slightly lower system efficiencies. These issues have been rectified, with further details found in Section 6.

These minor issues notwithstanding, the DP-CO<sub>2</sub> system performed strongly. Based on the 8-month monitoring period between July 2023 and February 2024, the system was able to deliver cool 17°C temperature air to the gas coolers despite the ambient temperature exceeding 40°C, which significantly reduced refrigeration energy consumption. The average difference between the ambient air temperature and the air temperature supplied to the gas coolers was 9.8°C, which is impressive given that this includes cooler overnight temperatures, together with the fact that a significant proportion of the monitoring period occurred during the cooler months.

During the monitoring period, measurements show that there was a large range of ambient temperatures, ranging from 5°C to 40°C. Despite this, the supply air temperature was more narrowly distributed between 5°C and 22°C. The supply air temperatures closely matched the ambient dew point temperature, which implies that the DP-CO<sub>2</sub> system is most effective in climates where the dew point temperatures are typically low (regardless of the ambient dry bulb temperature). Importantly, for the monitored system the supply air temperature was below 20°C for 98.4% of the time. That is, the implementation of the dew point cooler to the CO<sub>2</sub> refrigeration system allowed the system to operate in the (more efficient) sub-critical mode for close to 99% of the time.

A computational model of the DP-CO<sub>2</sub> system was also developed as part of the current project. This model uses a range of sub-models, including sub-models for the dew point coolers and the CO<sub>2</sub> refrigeration system, together with the ambient weather conditions and the expected refrigeration loads, to predict the thermodynamic details, energy consumption and water consumption of the DP-CO<sub>2</sub> system as a function of time. The model was then validated against previously measured CO<sub>2</sub> refrigeration data, with the DP-CO<sub>2</sub> energy consumption predicted by the model shown to match the monitored data from the Coles system to within 7%.

The model was then used to compare the energy consumption of the Coles DP-CO<sub>2</sub> system with that of a more conventional spray-type adiabatically cooled CO<sub>2</sub> refrigeration system. The results for a typical meteorological year in Adelaide show that the DP-CO<sub>2</sub> system reduces energy consumption by 19.6% across the whole year, with the greatest reduction in energy consumption occurring in summer, where a 37% reduction is predicted. The model was also used to estimate the performance of the DP-CO<sub>2</sub> system in

different sectors and across different climates. The results show that for a typical hospital kitchen room in Brisbane, the DP-CO<sub>2</sub> system can reduce energy consumption due to refrigeration by 20-25% during the summer months compared to a conventional R134a system. However, the DP-CO<sub>2</sub> system is less efficient in the cooler months, such that the total energy consumption across the whole year is approximately equal for both systems. Additionally, the model was also applied to a typical abattoir, but with the location varied to represent sites across Australia. The results show that the DP-CO<sub>2</sub> system reduces energy consumption by 4-27%, depending on location, compared to a conventional adiabatic CO<sub>2</sub> refrigeration system. The most significant reduction occurs in hot, dry climates, such as those found in central and western Australia.

However, while these results demonstrate the capability of the DP-CO<sub>2</sub> system to operate more efficiently than a conventional CO<sub>2</sub> system, the early termination of the project 6 months prior to its original due date because of the withdrawal of an industry partner meant that a more detailed analysis of the system was not achieved. Notably, a full 12 month monitoring period (encompassing all seasons) was not achieved, which in turn impacted the research team's ability to fully validate the computational model and to conduct a full detailed analysis of the monitored DP-CO<sub>2</sub> system. Notably, further improvements in the performance of the DP-CO<sub>2</sub> system may be realised through further detailed analysis of the measurements from the monitored system.



# Contents

EXECUTIVE SUMMARY	3
LIST OF FIGURES	6
LIST OF TABLES	10
NOMENCLATURE	11
<b>1 INTRODUCTION</b>	<b>13</b>
1.1 Project Aims	13
1.2 Background	14
<b>2 INSTALLED REFRIGERATION &amp; MONITORING SYSTEM</b>	<b>18</b>
2.1 Description of Installed Refrigeration System at Coles	18
2.2 Refrigeration Monitoring System Design	20
<b>3 COMPUTATIONAL MODEL ARCHITECTURE</b>	<b>34</b>
3.1 Introduction	34
3.2 Model Architecture	34
3.3 Description of Model Algorithms	40
<b>4 EXTENSION OF THE MODEL TO VARIOUS APPLICATIONS</b>	<b>46</b>
4.1 Modelling Validation	46
4.2 Model for Extended Applications	53
<b>5 MONITORING SYSTEM PERFORMANCE</b>	<b>59</b>
5.1 Monitoring System Architecture	59
5.2 Monitoring System Performance	62
<b>6 DP-CO<sub>2</sub> SYSTEM PERFORMANCE</b>	<b>64</b>
6.1 Dew Point Cooler Efficiency	64
6.2 CO <sub>2</sub> Refrigeration System Performance	67
<b>7 CONCLUSION</b>	<b>72</b>
REFERENCES	74
APPENDIX A: PIPING AND INSTRUMENTATION DIAGRAMS (P & ID) OF THE DP-CO <sub>2</sub> SYSTEM	76
APPENDIX B: DP-CO <sub>2</sub> MONITORING EQUIPMENT SCHEDULE	78
APPENDIX C: EXTRACT FROM MODEL EXPORT FILE	92
APPENDIX D: SUMMARY OF IRG MEETINGS	93
IRG Meeting #1	93
IRG Meeting #2	94
IRG Meeting #3	94
IRG Meeting #4	95

# List of Figures

Figure 1: Schematic of a basic vapour-compression system (left) and its corresponding pressure-enthalpy diagram (right) .....14

Figure 2 A pressure-enthalpy (P-h) diagram of a basic CO<sub>2</sub> refrigeration cycle operating in trans-critical (TC) and sub-critical (SC) modes..... 15

Figure 3 Schematic of the Dew Point Cooler (DPC) .....16

Figure 4 Illustration of the different condenser temperatures achievable with different types of condenser cooling ..... 17

Figure 5 Bitzer CO<sub>2</sub> refrigeration rack..... 17

Figure 6 Coles Norwood supermarket. .... 18

Figure 7 The three DP-CO<sub>2</sub> modules installed at Coles Norwood..... 19

Figure 8 Process and Instrument Diagram (P&ID) of the CO<sub>2</sub> Rack installed at Coles..... 20

Figure 9: Line diagram of the installed CO<sub>2</sub> system for the Coles supermarket (Bitzer) ..... 24

Figure 10: An indicative pressure-enthalpy (P-H) diagram of the installed DP-CO<sub>2</sub> system. In this present case, the DP-CO<sub>2</sub> system is operating in the trans-critical mode. Note that the pressure and enthalpy values may change depending on conditions, and that this figure is intended for illustrative purposes only..... 24

Figure 11: Psychrometric chart and process cycle for the installed dew point cooler. This is for illustrative purposes only, with actual values of temperature and humidity dependent on the instantaneous conditions (operating and ambient)..... 25

Figure 12 Location of temperature and pressure sensors on Unit A. .... 26

Figure 13 Supply air velocity, temperature and pressure sensors..... 27

Figure 14 Ambient air temperature and relative humidity sensor..... 28

Figure 15 Water sump valves, access point and differential pressure sensor location..... 28

Figure 16 Evaporate pad wetting pumps and tank level sensors/ switches. .... 29

Figure 17 Plant room, Glaciem Electrical box with PLC, HMI attached on the left-hand side of the CO<sub>2</sub> Rack. .... 30

Figure 18 IFM pressure sensor mounted to SCM pressure manifold..... 31

Figure 19 High pressure expansion valve CO<sub>2</sub> temperature sensor and IFM converter module..... 31

Figure 20 Electrical board- Electrical breakers, PLC and DENT power meter. .... 32

Figure 21 Snapshot of live feed from Scada..... 33

Figure 22 Schematic of the modelling procedure. Note that the “Climate Wizard” refers to the dew point (indirect evaporative) cooler. The data in the orange box are inputs required from the user..... 35

Figure 23 Sample “system specification” page..... 37

Figure 24 Sample VBA code with 3 modules for psychrometric, CO <sub>2</sub> and compressor calculations.....	38
Figure 25: Example output page .....	40
Figure 26 Flow diagram of modelling procedure.....	41
Figure 27: Pressure-enthalpy (P-h) diagram of the modelled refrigeration cycle. The points here are for a single snapshot in time; the exact values of the state points will vary with time (and conditions). The numbered points here refer to the locations within the DP-CO <sub>2</sub> system, as shown schematically in Figure 9. ....	42
Figure 28 Schematic overview of the CO <sub>2</sub> refrigeration plant in a subtropical aquarium .....	47
Figure 29 The measured and simulated total compressor power of the CO <sub>2</sub> refrigeration system in a subtropical aquarium for a 12 hour period on 06/12/2021 .....	48
Figure 30 Comparison of monitored and modelled total compressor power for a 21-day period in July 2022 for the CO <sub>2</sub> refrigeration system in a subtropical aquarium. ....	48
Figure 31 Correlation between modelled and monitored total compressor power for the CO <sub>2</sub> refrigeration system in a subtropical aquarium. The data points here were taken from hourly-averaged data across a 21-day period in July 2021 .....	49
Figure 32 A piping and instrumentation diagram of the trans-critical CO <sub>2</sub> refrigeration system with TES located at an apple-packing site.....	50
Figure 33 The measured and modelled total compressor power from the refrigeration system at the at the apple-packing site recorded over an 8 hour period on 01/06/2022.....	52
Figure 34 Comparison of monitored and modelled compressor data (hourly averages) for the first week of June 2022 for the refrigeration system at the apple-packing site.....	52
Figure 35 Modelled versus monitored total compressor power for the refrigeration system at the apple-packing site for the first week of June, 2022. Data points are hourly-averaged data. The dotted line shows a linear curve fit to the data. ....	53
Figure 36 Monthly electricity usage (in kWh) over one year for a modelled 14 kW <sub>t</sub> DP-CO <sub>2</sub> refrigeration system (blue) compared against measurements of an existing refrigeration system (green) at the hospital location in Case Study 1. Maximum measured temperatures of each month are also shown (orange curve).....	54
Figure 37 Histograms of temperature and humidity ratio measured at the three hospital locations (Hornsby, Tamworth and Griffith) in Case Study 2. ....	55
Figure 38 Mean monthly power consumption for the same DP-CO <sub>2</sub> system installed at three different hospital locations for Case Study 2. ....	56
Figure 39 The ratio of the annual energy consumption of the refrigeration system for the abattoir case study for the adiabatic spray pre-cooling system vs the DP-CO <sub>2</sub> for different regions across Australia.....	58
Figure 40 Compressor Model.....	60
Figure 41: Refrigeration cycle- cooling energy, compressor work and total heat rejection .....	60
Figure 42: Psychrometric chart and process cycle for the dew point cooler.....	61

Figure 43 Visualisation of the gas cooler performance overlaid on a P-h diagram. The numbered points here refer to the locations within the DP-CO <sub>2</sub> system, as shown schematically in Figure 9.....	63
Figure 44: Ambient and supply air temperatures for the installed system at Coles. Data was taken from the 23rd of January, 2024.....	64
Figure 45 Air temperatures across the dew point cooler for DP-CO <sub>2</sub> system installed at Coles. Data taken from the 26 <sup>th</sup> of January, 2024.....	65
Figure 46 Probability distribution function (PDF) of the ambient and supply air temperatures. Data taken from the first 8 months of the monitoring period. ....	65
Figure 47 Probability distribution function of the difference between the ambient and supply air temperatures, $\Delta T_{\text{pre-cooling}}$ . Data taken from the first 8 months of the monitoring period. ....	66
Figure 48 Daily average water consumption vs daily maximum ambient air temperature. ....	67
Figure 49 Measured discharge pressure vs supply air temperature for the installed DP-CO <sub>2</sub> system at Coles....	68
Figure 50 Modelled vs monitored electrical consumption for the Coles DP-CO <sub>2</sub> refrigeration system. ....	70
Figure 51: Modelled vs monitored monthly water consumption for the Coles DP-CO <sub>2</sub> refrigeration system.....	70
Figure 52 Modelled monthly energy consumption for DP-CO <sub>2</sub> and adiabatically-cooled CO <sub>2</sub> systems. The values here are for the current Coles system, under Adelaide weather conditions.....	71
Figure 53: Piping and instrumentation (P & ID) diagram of the proposed Coles DP-CO <sub>2</sub> refrigeration system ...	76
Figure 54: Piping and instrumentation diagram of the condensers and dew-point cooling units.....	77
Figure 55: IFM PT series pressure transducer.....	85
Figure 56 IFM TA2262 temperature sensor (RTD).....	86
Figure 57 IFM TS4759 temperature sensor (RTD).....	87
Figure 58 IFM TP3231 evaluation unit.....	87
Figure 59 IFM TA2537 temperature sensor RTD.....	88
Figure 60 Dwyer RHP-2R11 humidity sensor.....	88
Figure 61 Dwyer 607D-04 pressure differential sensor.....	89
Figure 62 Dwyer MS2-W102 Pressure differential sensor.....	89
Figure 63 XPS Ultima switch capacitive level switch.....	90
Figure 64: IFM LRO50 radar guided level sensor.....	90
Figure 65 IFM SM8030 Magnetic water flow meter.....	90
Figure 66: Dent Power Meter PS48.....	91
Figure 67: Dent HSC-20 Mini Hinged current transformer.....	91



Figure 68 Extract from the detailed data export file. Here, each row represents one time period (usually 1 hour). Each column represents values calculated by the model. Note that only a selected number of rows and columns are shown for brevity..... 92

## List of Tables

Table 1 Suction group.....	19
Table 2: CO <sub>2</sub> Booster Rack Instrumentation. Acronyms: RTD = resistive temperature detector, CT = current transformer, LT = low temperature, MT = medium temperature and HT = high temperature.....	22
Table 3 Indirect evaporative gas cooler instrumentation.....	23
Table 4 Measurement derived from the temperature sensors. ....	26
Table 5 Measurement derived from the differential pressure sensors.....	26
Table 6: An Example of a Weather Input file (first 7 hours only) for Adelaide (AD). Here DB refers to the dry-bulb temperature. ....	36
Table 7: Sample load data file used in the modelling of the Coles site. Here LT, MT and HT refer to low, medium and high temperatures, respectively.....	37
Table 8 Refrigeration Cycle stages and required energy on state equations. The State points are also illustrated in Figure 29. ....	43
Table 9 Comparison of annual energy and water usage for the same DP-CO <sub>2</sub> system installed at three different hospital locations for Case Study 2. Total electrical consumption of a DP-CO <sub>2</sub> is the sum of the compressor and DP cooler consumptions. ....	56
Table 10 Brewery case study model results. ....	57
Table 11 Power consumption and water usage for a 1MW <sub>t</sub> abattoir at each capital city in Australia.....	57
Table 12: Schedule of monitoring equipment for the proposed DP-CO <sub>2</sub> system .....	78

# Nomenclature

## List of symbols

$\varepsilon$	effectiveness
$\rho$	fluid density, kg/m <sup>3</sup>
C <sub>p</sub>	specific heat, kJ/(kg·K)

## Subscripts

ANCIL	ancillary
COMP	compressor
C	condenser
pb	dry bulb
dp	dew point
EXH	exhaust
EV	evaporator
in	entering, in, inlet
LT	low temperature
MT	medium temperature
out	leaving, out, outlet
TOT	total

## List of abbreviations

CO <sub>2</sub> , R744	Carbon dioxide refrigerant
ATD	approach temperature difference
COP	coefficient of performance
DB	dry bulb
DP	dew point
DPC	dew point cooler/cooling (see context)
DP-CO <sub>2</sub>	Dew point- CO <sub>2</sub> system
FG	flash gas
HVAC	Heating, ventilation and air conditioning

HP	high pressure
HTF	heat transfer fluid
IHX	internal heat exchanger
LT	low temperature
MT	medium temperature
SST	saturation suction temperature
WB	wet bulb



# 1 Introduction

Despite recent advances, the HVAC-R sector remains a highly energy-intensive sector. Heating, ventilation and air conditioning (HVAC) contributes significantly to business energy use and operating costs, typically consuming the largest proportion of energy in commercial buildings. In a commercial building, HVAC electricity consumption can typically account for around 40 per cent of total building consumption and around 70 per cent of base building electricity consumption (Lecamwasam et al., 2012).

As of 2017, HVAC-R systems account for 61,000 GWh (23.6%) of Australia's annual electricity production, with cooling alone contributing to 58.7 Mt CO<sub>2-eq</sub> (11.5%) of Australia's total greenhouse gas emissions (Brodribb and McCann, 2018). HVAC-R systems are also a major contributor to peak energy demand, and therefore directly contribute to Australia's already high network operating costs.

The RACE for 2030 Transforming energy productivity through value chains (B1) Opportunity Assessment (OA) (Denham et al., 2021) has identified Australian's food cold chain, which is estimated to consume 19,600 GWh of electricity per annum, as a sector with significant potential for improved energy productivity. The OA estimated that a 30% reduction in energy consumption can be realised through the use of high-performance refrigeration systems and recommended a demonstration project as a high priority.

This project therefore aimed to monitor and validate the performance of a new-generation indirect evaporative (or dew-point) CO<sub>2</sub> (DP-CO<sub>2</sub>) refrigeration system in a Coles supermarket. Coles operates more than 1,500 outlets across Australia and is Australia's 12th largest electricity user (annual usage at 1.61 billion kWh of electricity). The DP-CO<sub>2</sub> system has already been shown to reduce peak demand by 24% and average annual energy consumption by 16%, relative to conventional CO<sub>2</sub> systems, under lab-scale conditions relevant to Australia's challenging climate (Belusko et al., 2019).

While the performance of the DP-CO<sub>2</sub> had already been demonstrated at lab-scale, it has yet to be confirmed at larger, commercial scale conditions. These commercial scale conditions may differ from those at lab-scale, which may in turn impact the performance of the system. For example, in real-world conditions the internal load profile (i.e., the amount of people within the store) and the operational strategies employed may be different to smaller scale systems. As such, this project aimed to monitor the performance of the novel DP-CO<sub>2</sub> system on site under large scale, commercial, real-world conditions.

## 1.1 Project Aims

The project aimed to model, monitor and validate the performance of a new-generation indirect evaporative (or dew-point) CO<sub>2</sub> (DP-CO<sub>2</sub>) refrigeration system at scale, providing direct evidence of the efficacy and viability of the technology under real-world conditions.

In particular, this project aimed to:

1. Continuously monitor the performance of the DP-CO<sub>2</sub> system in a Coles supermarket across three major seasons (summer, winter and shoulder);
2. Develop a model to reliably estimate the reduction in energy consumption, CO<sub>2</sub> emissions and water usage that can be realised under a range of operating conditions and climates;
3. Provide recommendations to optimise the operation and control of DP-CO<sub>2</sub> systems;
4. Demonstrate the viability and efficacy of the DP-CO<sub>2</sub> system in Australian conditions and commercial supermarket loads.

## 1.2 Background

Refrigeration systems typically use a vapour-compression system whereby a heat transfer fluid (typically called a refrigerant) is continually compressed and expanded in a closed system (see Figure 1). In these systems, heat from the high temperature compressed refrigerant is rejected in the condenser, while heat is absorbed from the environment by the cold expanded refrigerant in the evaporator. Electrical energy is primarily consumed by the compressor and by the fans for the condenser and evaporator.

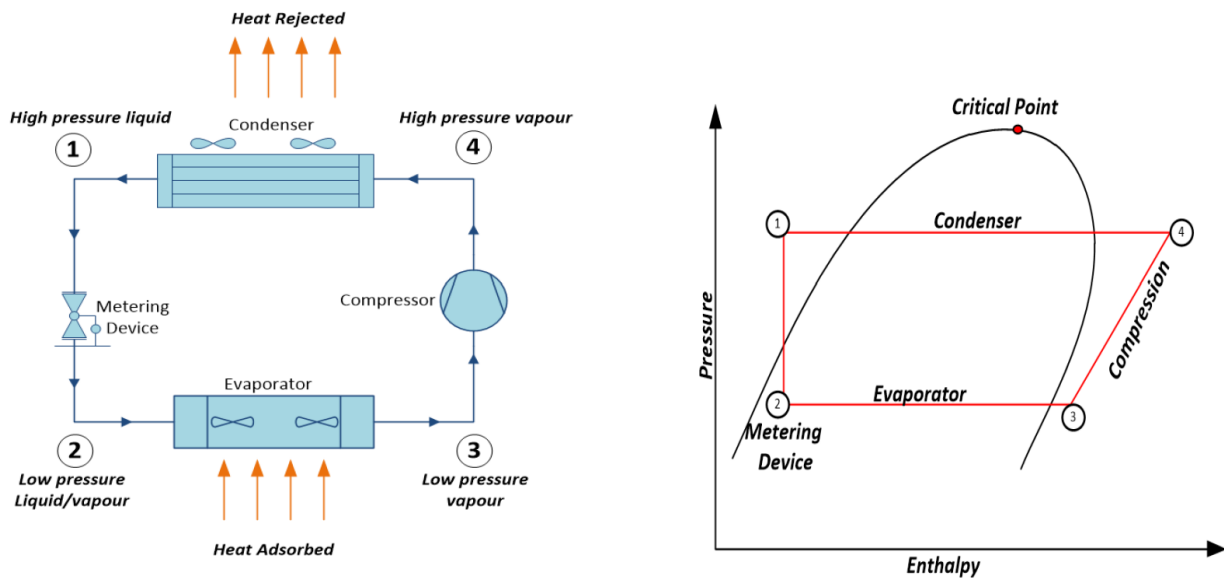


Figure 1: Schematic of a basic vapour-compression system (left) and its corresponding pressure-enthalpy diagram (right)

Among the several natural and synthetic commercially available refrigerants, one of the refrigerants which is growing in popularity is CO<sub>2</sub> (R744), due to its low global warming potential (GWP), zero ozone depleting potential (ODP), and the fact that it is non-toxic and relatively abundant. One of the distinct features of a CO<sub>2</sub> refrigeration system is its low critical temperature of 31°C, which results in the CO<sub>2</sub> refrigerant operating in a supercritical state as it passes through the air-cooled condenser if the ambient temperatures are approximately 30°C or higher.

Operating with CO<sub>2</sub> in the super-critical state is typically disadvantageous, as its ability to transfer heat is significantly reduced compared to CO<sub>2</sub> in the sub-critical state. As a result, the efficiency (or coefficient of performance, COP) of conventional CO<sub>2</sub> refrigeration systems typically significantly reduced when the ambient conditions are sufficiently hot such that the CO<sub>2</sub> becomes super-critical. This mode of operating refrigeration systems is called the trans-critical mode.

The predominant method of minimising the impact of trans-critical operation is by modifying the refrigeration cycle using parallel compression (Bellos and Tzivanidis, 2019; Sarkar and Agrawal, 2010) or the use of a mechanical expander or ejector (Li and Groll, 2005). These methods may bring marginal performance improvements during trans-critical operation. Similarly, heat rejected by the gas cooler can be recovered for other applications such as water or space heating for improved overall efficiency (Ge and Tassou, 2014). However, heat recovery for other purposes is not always technically and or economically viable, as it requires the installation of additional heat exchangers and pipework, as well as a source of utilising heat (i.e. a heat load).

Another alternative to improve the performance of a CO<sub>2</sub> refrigeration system is by maintaining the temperature of the condensing medium (in this case, air passing over the CO<sub>2</sub> condenser coil) below the

critical temperature of 31°C as much as possible to enable the sub-critical operation of the CO<sub>2</sub> system. Figure 2 illustrates the differences between operating the CO<sub>2</sub> system in sub-critical and trans-critical modes using a pressure-enthalpy diagram. Here, the total (useful) work done by the evaporator (i.e. the indoor fridges and freezers) is  $Q_{evap}$ , while the work done by the compressor (i.e. the input energy) is  $W_{comp}$ . The coefficient of performance of the system is

$$COP = \frac{Q_{evap}}{W_{comp}}$$

As can be seen, operating the system in a trans-critical (TC) mode (the red line) uses significantly more compressor work,  $W_{comp}$ , than in a sub-critical (SC) mode (the blue line), and results in a lower refrigeration capacity ( $Q_{evap}$ ), which in turn results in poorer energy efficiency. By contrast, maintaining a lower condensing media temperature allows the peak refrigerant temperature to be reduced, which in turn reduces the compressor discharge pressure (and therefore the work the compressor needs to do). If the condensing media temperature is sufficiently low, the refrigeration system may be able to operate in the sub-critical regime (i.e. below the critical point), which in turn results in higher efficiencies.

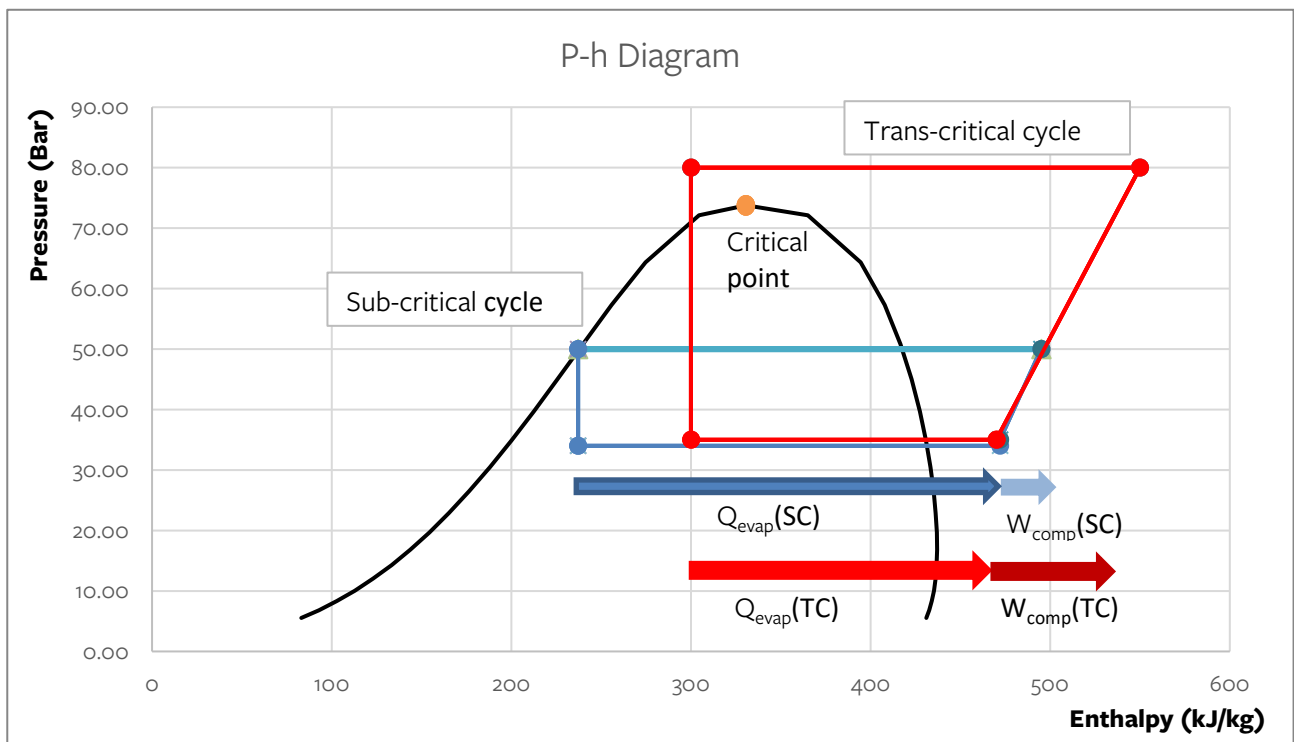


Figure 2 A pressure-enthalpy (P-h) diagram of a basic CO<sub>2</sub> refrigeration cycle operating in trans-critical (TC) and sub-critical (SC) modes.

A novel system has been developed where CO<sub>2</sub> refrigeration is integrated with existing Dewpoint (or indirect evaporative) Cooling (DPC) technology. Based on preliminary lab-scale results derived from simulations of the indirect evaporative CO<sub>2</sub> (DP-CO<sub>2</sub>) refrigeration system, this system has been found to be very energy efficient even under high ambient temperature conditions (Belusko et al., 2019). It has also superior performance in winter compared to the conventional trans-critical CO<sub>2</sub> systems with parallel compression.

In this section of the report a background of the refrigeration system that was evaluated and monitored as part of the project will be discussed.

### 1.2.1 Dew Point Cooling

The indirect evaporative cooling of the air through the condenser/ gas cooler is achieved using Seeley's Climate Wizard dew point coolers. As illustrated in Figure 3, these DPCs achieve their performance based on the Maisotsenko cycle (Mahmood et al., 2016). In this system, primary air is drawn through the primary, dry channels to a plenum chamber. From the plenum chamber, a portion of the air is supplied as supply air. An optimally selected proportion of the primary air (typically around 35%) which maximises the COP of the DPC is drawn back to separate wet channels of the heat exchanger and leaves the heat exchanger through the exhaust. The air traveling through these channels is cooled through an evaporation process. This evaporatively cooled portion of air then cools the air in the dry channels (i.e. the primary air). In the meantime, the air in the wet channels absorbs heat from the primary stream, such that it increases in temperature. The end result is that the portion of the primary air leaving the dry channels will exit close to its dew point temperature, while the portion of the air leaving the wet channels through the exhaust will be warm and very humid.

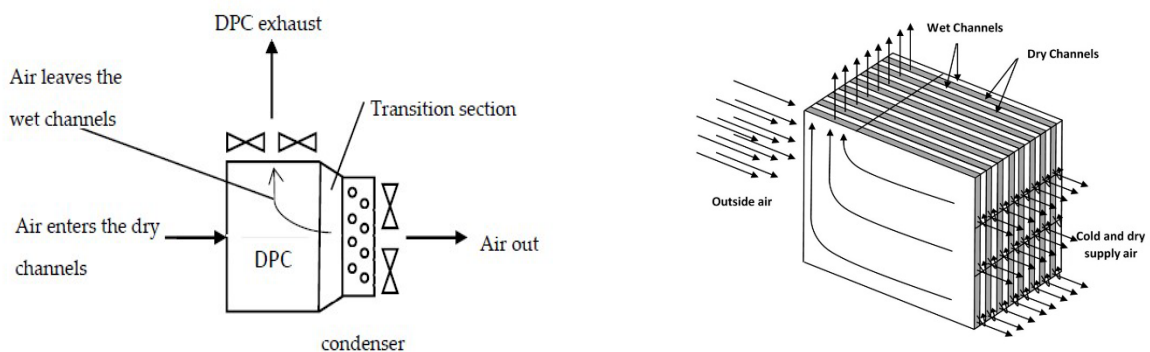


Figure 3 Schematic of the Dew Point Cooler (DPC)

Figure 4 illustrates the different potential condenser inlet temperatures under three different systems of condenser heat rejection (cooling). The three different systems are:

- No pre-cooling (point 1) – in typical systems, no pre-cooling of the air passed over the condenser of the refrigeration system is employed. For these cases, the condenser air inlet temperature is equal to the dry bulb temperature (point 1), i.e., the ambient air temperature;
- Adiabatic (evaporative) pre-cooling (process 1-2') – in this system, ambient air is evaporatively cooled towards the wet-bulb temperature (point 2'). The wet-bulb temperature is always cooler than the ambient dry-bulb temperature, and hence this system allows a reduction in the condenser temperature;
- Dew-point (indirect evaporative) cooling (process 1-2-3) – in this system, the ambient air is cooled towards the dew-point temperature of the ambient air (point 2), which is significantly cooler than the wet-bulb temperature. Additionally, the Seeley International system also has an additional evaporative cooling stage downstream of the indirect evaporative cooling, which further decreases the air temperature around the condenser (point 3). That is, the use of this new dew point cooling technology is capable of reducing the condenser air temperature significantly, which in turn will increase the efficiency of the refrigeration system.



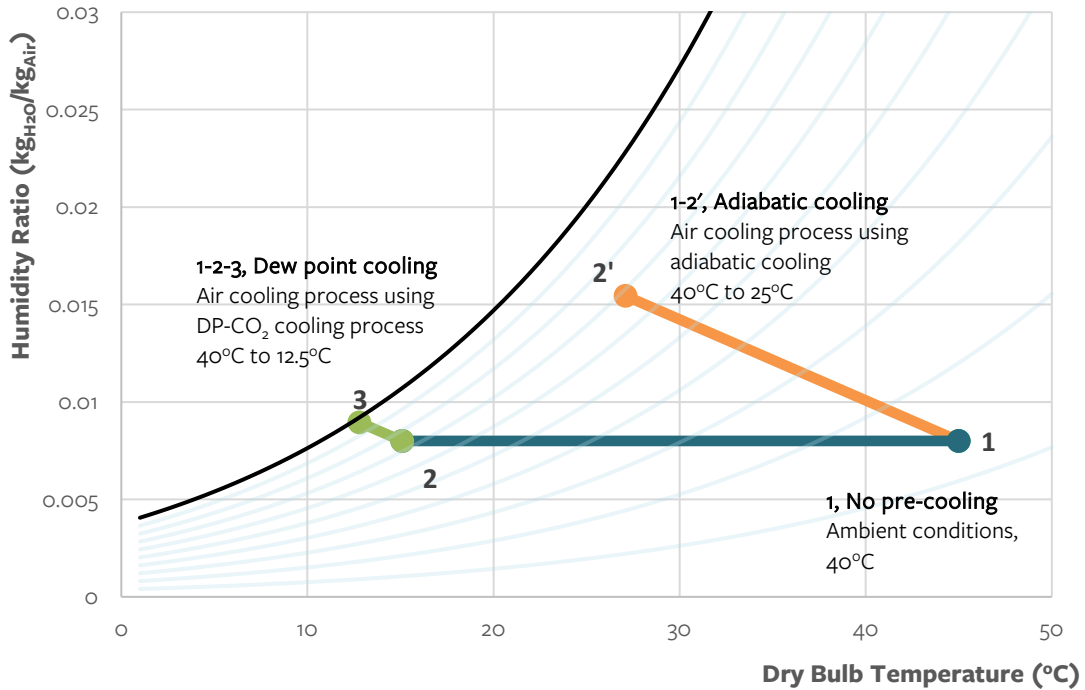


Figure 4 Illustration of the different condenser temperatures achievable with different types of condenser cooling.

### 1.2.2 Trans-critical CO<sub>2</sub> rack with parallel compressors

In a typical multi-stage CO<sub>2</sub> refrigeration system, multiple compressors may be used to provide the required refrigerant compression, particularly for supermarket applications where different temperatures are required for freezers (low temperature - LT), cool rooms (medium temperature - MT), display cases (LT and MT), and air conditioning (AC). One such example of a typical trans-critical CO<sub>2</sub> rack with parallel compressors providing the refrigeration and air conditioning is shown in Figure 5. Notably, these systems are the low-GWP substitutes for the older R134a/R4004A cascade racks (which have very high GWP) currently used in many supermarkets. Note that in this example, which represents typical CO<sub>2</sub> systems used in supermarkets, the refrigerant will usually become super-critical under high ambient temperature conditions.

The goal of this project was therefore to combine the DPC technology outlined in section 1.2.1 with “typical” CO<sub>2</sub> refrigerant systems employing parallel compressors to enable the system to run in sub-critical mode for as much of the year as possible.

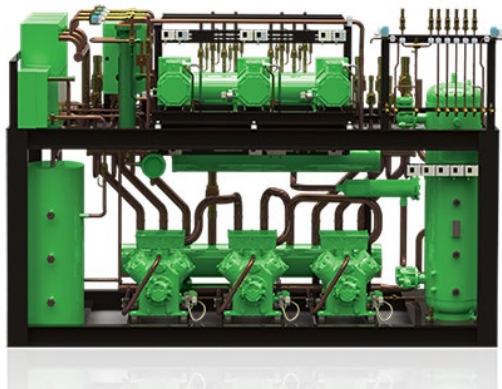


Figure 5 Bitzer CO<sub>2</sub> refrigeration rack

## 2 Installed Refrigeration & Monitoring System

### 2.1 Description of Installed Refrigeration System at Coles

#### 2.1.1 Introduction

This project aimed to monitor and validate the performance of a new-generation DP-CO<sub>2</sub> system in a Coles supermarket. Coles operates more than 1,500 outlets across Australia and is Australia's 12th largest electricity user (annual usage at 1.61 billion kWh of electricity). The DP-CO<sub>2</sub> system has already been shown to reduce peak demand by 24% and average annual energy consumption by 16%, relative to conventional CO<sub>2</sub> systems, under lab-scale conditions relevant to Australia's challenging climate (Belusko et al., 2019).

Therefore, to demonstrate the capability of the DP-CO<sub>2</sub> system under practical conditions, a custom built DP-CO<sub>2</sub> system was built and installed in a "greenfield" Coles supermarket store in Norwood, South Australia. The system was installed and commissioned in the first half of 2023. The Coles supermarket officially opened successfully on the 21<sup>st</sup> June 2023 (see Figure 6).



Figure 6 Coles Norwood supermarket.

#### 2.1.2 Dew Point Coolers

The dew point CO<sub>2</sub> (DP-CO<sub>2</sub>) gas cooler used at the Coles Norwood is a fourth generation, advanced air precooling system, designed to improve the operating performance of a trans-critical CO<sub>2</sub> refrigeration system. The system uses a total of 12 indirect evaporative coolers (Seeley International Climate Wizard CW-15s) to condition the air approaching the air side of six CO<sub>2</sub> separate gas coolers that, together, reject heat from the CO<sub>2</sub> refrigeration system.



Figure 7 The three DP-CO<sub>2</sub> modules installed at Coles Norwood.

The gas cooler packs, shown in Figure 7, were arranged in 3 modular packs. Each pack contains 4 dew point coolers and 2 gas coolers.

### 2.1.3 CO<sub>2</sub> Refrigeration Rack

The gas coolers provide condensing/gas cooling to the Coles supermarket CO<sub>2</sub> refrigeration rack. The CO<sub>2</sub> rack consists of three suction groups for the purpose of cooling:

Table 1 Suction group

Suction Group	Application	# of Compressors
Low Temperature (LT)	Freezer applications	2
Medium Temperature (MT)	Refrigeration and display case applications	4
High Temperature (HT)	Parallel compression/ AC loads	4

The CO<sub>2</sub> rack also contains a desuperheater for the purpose of providing supplementary hot water heating to the store. A gas boiler – separate to the refrigeration system and outside the scope of this project - provides the primary hot water heating. A schematic of the refrigeration system at the Coles supermarket (as installed) is shown in Figure 8.

The gas cooler pack can be controlled by either its own PLC or the Danfoss controller of the refrigeration rack.



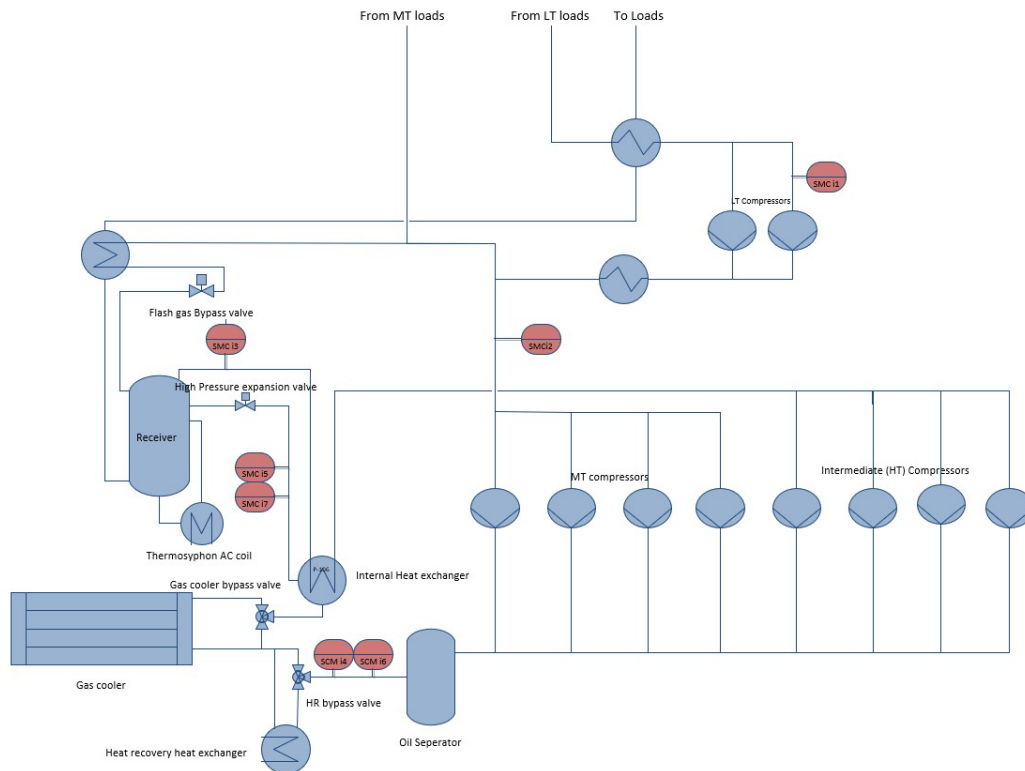


**Figure 8 Process and Instrument Diagram (P&ID) of the CO<sub>2</sub> Rack installed at Coles**

## 2.2 Refrigeration Monitoring System Design

### 2.2.1 Instrument selection

Instrument and component selection has been performed by the project team, with the view to maximising accuracy and reliability, which were paramount for the success of this project. In particular, measuring data accurately is crucial for both the optimisation of the DP-CO<sub>2</sub> system and for the verification of the model. Instruments have been selected from lists of devices that have shown to be reliable<sup>1</sup> in past projects, providing confidence that they will be suitable for this project.

As the main aim of this project was to establish the performance of DP-CO<sub>2</sub> refrigeration systems, we therefore needed to define, measure and optimise the efficiency of the system and substantiate that the model can accurately predict the efficiency of the system.

It should be noted that the project team was responsible for the selection of the instruments that were installed on the indirect evaporative condenser, but not the CO<sub>2</sub> rack, which were selected by the entity responsible for design and implementation of the CO<sub>2</sub> rack (separate to the project). The project team was able to access a limited number of values measured by these sensors through the communication between the operating systems. As the sensors on the CO<sub>2</sub> rack were required for control and day-to-day operation of the refrigeration system, and since the control system requires a higher sensor accuracy than the model validation, it was anticipated that these sensors will be sufficient to meet the current project's requirements.

---

<sup>1</sup> These instruments have been used by the project team previously in multiple refrigeration systems in the past 5-6 years without any issues or faults.



As the monitoring of literally every single physical property of the DP-CO<sub>2</sub> system was not feasible, the project team prioritised the measurement of key parameters that were required to understand and optimise the performance DP-CO<sub>2</sub> system, and to validate the computational model of the system. The description of the parameters measured are discussed below.

#### 2.2.1.1 Efficiency

A key parameter that is required to be measured is the efficiency of a refrigeration system, defined as the refrigeration power divided by the electrical energy required for it, i.e.,

$$\eta = \frac{P_{\text{refrigeration}}}{P_{\text{in}}}$$

where  $P_{\text{refrigeration}}$  is the rate at which heat removed from the refrigeration system, and  $P_{\text{in}}$  is the total electrical input power, which includes the input power to the fans and compressors. The accumulation (integral) of power over time is energy. Therefore, the average efficiency of system over a period of time can be defined as:

$$\bar{\eta} = \frac{E_{\text{refrigeration}}}{E_{\text{in}}}$$

where  $E_{\text{refrigeration}}$  is the total heat removed from the product or process, and  $E_{\text{in}}$  is the total input energy over a defined period of time. Efficiency can be also stated as the Coefficient of Performance (COP). This term can be used for both individual compressors or for the entire system.

In the present system, the electrical input power,  $E_{\text{in}}$ , was measured directly using power meters (see section 2.2.3.1), while the refrigeration energy,  $E_{\text{refrigeration}}$  was inferred from the measurement of compressor suction and discharge pressures and temperatures, as well as the compressor frequency (see also section 3.3.3).

#### 2.2.1.2 Instrument Function

Table 2 contains a list of measurable variables, together with their corresponding derived variables, which are used either as an input to the model or to quantify the performance of the DP-CO<sub>2</sub> system. The “state” of each of the measure variables relates to the state of the CO<sub>2</sub> throughout the refrigeration cycle. The numbering format labelled with the square brackets [] references the points in the CO<sub>2</sub> refrigeration system as shown in Figure 9 (with its corresponding pressure-enthalpy diagram shown in Figure 10), while the numbers in the triangular brackets <> references the psychrometric state of the dew-point cooler system, as shown in Figure 11.

**Table 2: CO<sub>2</sub> Booster Rack Instrumentation.** Acronyms: RTD = resistive temperature detector, CT = current transformer, LT = low temperature, MT = medium temperature and HT = high temperature.

CO<sub>2</sub> Booster Rack Instruments

Measured variable [State]	Instrument type/ validation	Derived variables
LT liquid Temperature (subcooled) [11]	Pack controller setpoint	
LT Temperature at Evaporator [12]	Pack controller setpoint	
LT suction Temperature at compressors [1]	Pack controller setpoint	
LT suction pressure [1]	Pressure transducer	LT refrigeration load
LT compressor Discharge Temperature [2]	Compressor model output	
LT compressor Discharge Pressure [2]	Pressure transducer	
Lead LT compressor Frequency [1-2]	Inverter analogue signal	
LT compressors running status [1-2]	One digital signal per compressor	
MT Temperature at Evaporator [14]	Deduced from pressure transducers	
MT suction Temperature at Compressors [5]	Pack controller setpoint	
MT suction pressure [5]	Pressure transducer	MT refrigeration load
MT compressor Discharge Temperature [6]	Compressor model output	
Lead MT compressor Frequency [5-6]	Inverter analogue signal	
MT compressors running status [5-6]	One digital signal per compressor	
HT suction Temperature at compressors [5]	RTD	
HT suction pressure [5]	Pressure transducer	
HT compressor Discharge Temperature [6]	Compressor model output	HT refrigeration load
Lead HT compressor Frequency [5-6]	Inverter analogue signal	
HT compressors running status [5-6]	One digital signal per compressor	
MT, HT Discharge Pressure temperature [6]	Pressure transducer	
MT, HT Liquid temperature [8]	RTD	
Receiver Pressure [9a]	Pressure transducer	MT, HT refrigeration load
Subcooled condensate Temperature [9]	RTD	
Flash gas Temperature [16]	RTD	
Superheated Flash gas temperature [17]	RTD	

Chilled water HX inlet Temperature	Danfoss Pack controller	
Chilled water HX outlet Temperature	Danfoss Pack controller	HT load /Flash gas load
Chilled water flow rate	Flow meter	
LT compressors input power [1-2]	Power meter /CT	
MT compressors input power [5-6]	Power meter /CT	Refrigeration system efficiency
HT compressors input power [17-18]	Power meter /CT	
Total Rack input power	Power meter /CT	

Table 3 Indirect evaporative gas cooler instrumentation. States with <#> are derived from Figure 42, States with [#] are derived from Figure 11.

Indirect evaporative Gas cooler

Measured variable [state]	Instrument type	derived variables
Main CO <sub>2</sub> discharge temperature [18]	RTD	
Main CO <sub>2</sub> gas return temperature [8]	RTD	MT, HT Refrigeration load (Back up)
Discharge pressure transducer [6]	Pressure transducer	
Gas cooler coil CO <sub>2</sub> inlet temperature	RTD	Gas cooler CO <sub>2</sub> energy transfer
Gas cooler coil CO <sub>2</sub> outlet temperature	RTD	
Ambient air humidity <1>	RTD + Humidity sensor	Cooling performance of cooler
Indirect cooled air Temperature <2>	RTD	Air cooler indirect pad performance
Exhaust air temperature (humid air) <2'>	RTD	
Gas cooler coil supply air temperature <3>	RTD	Air cooler direct pad performance
Gas cooler coil discharge air temperature <4>	RTD	Gas cooler air energy transfer
Cooler fan air pressure	Differential pressure transducer	Air cooler flow rate
Air pressure-drop of indirect pads	Differential pressure transducer	
Air pressure-drop of direct pad	Differential pressure transducer	Air cooler flow ratio
Air pressure-drop of air filters	Differential pressure transducer	
Water tank low level switch	Liquid level switch	Air cooler water consumption
Water tank High level switch	Liquid level switch	

Water tank Level sensor	Liquid level switch	
Makeup water flow	Flow meter	
Gas cooler fan power	Power meter /CT	Gas cooler efficiency
Gas cooler pump input power	Power meter /CT	

A detailed list of the selected instruments is included in [Appendix B](#). The positions of these instruments are tagged on the associated P&ID diagram shown in [Appendix A](#).

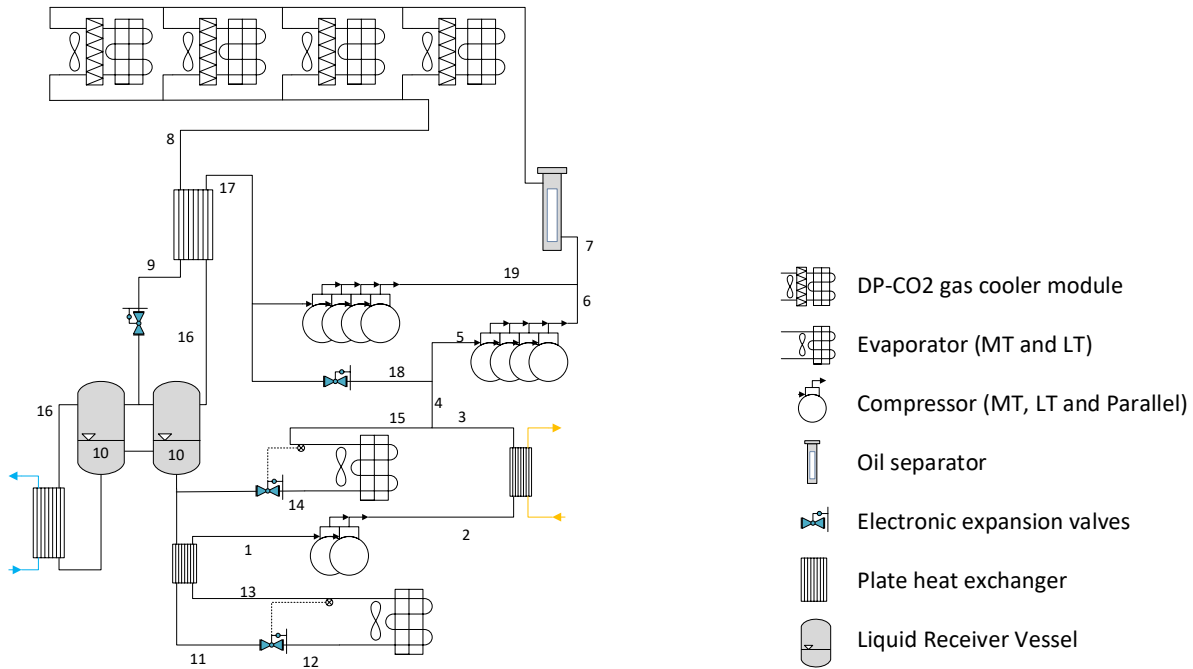


Figure 9: Line diagram of the installed CO<sub>2</sub> system for the Coles supermarket (Bitzer)

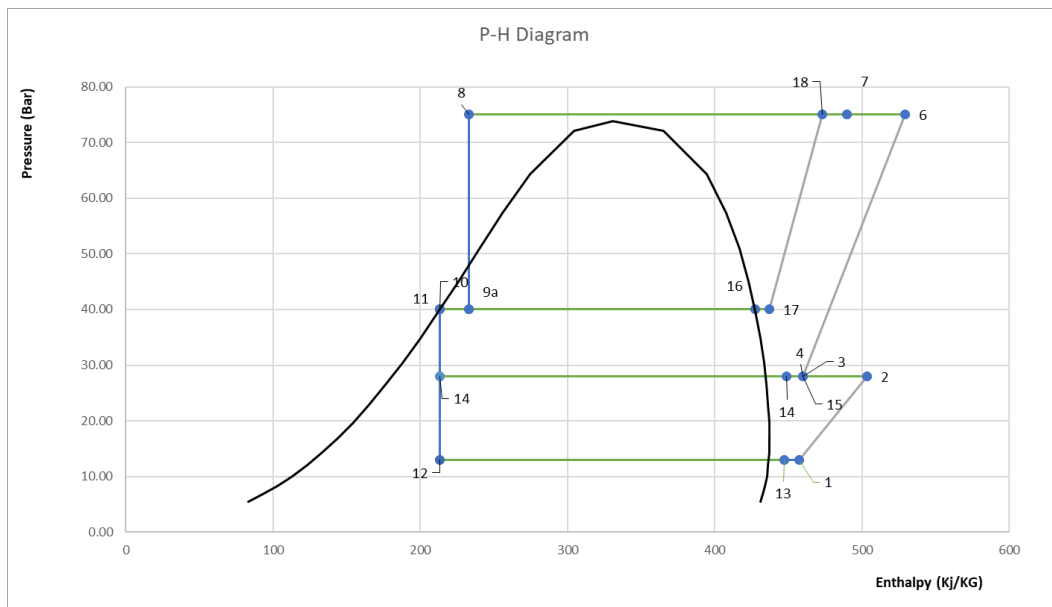
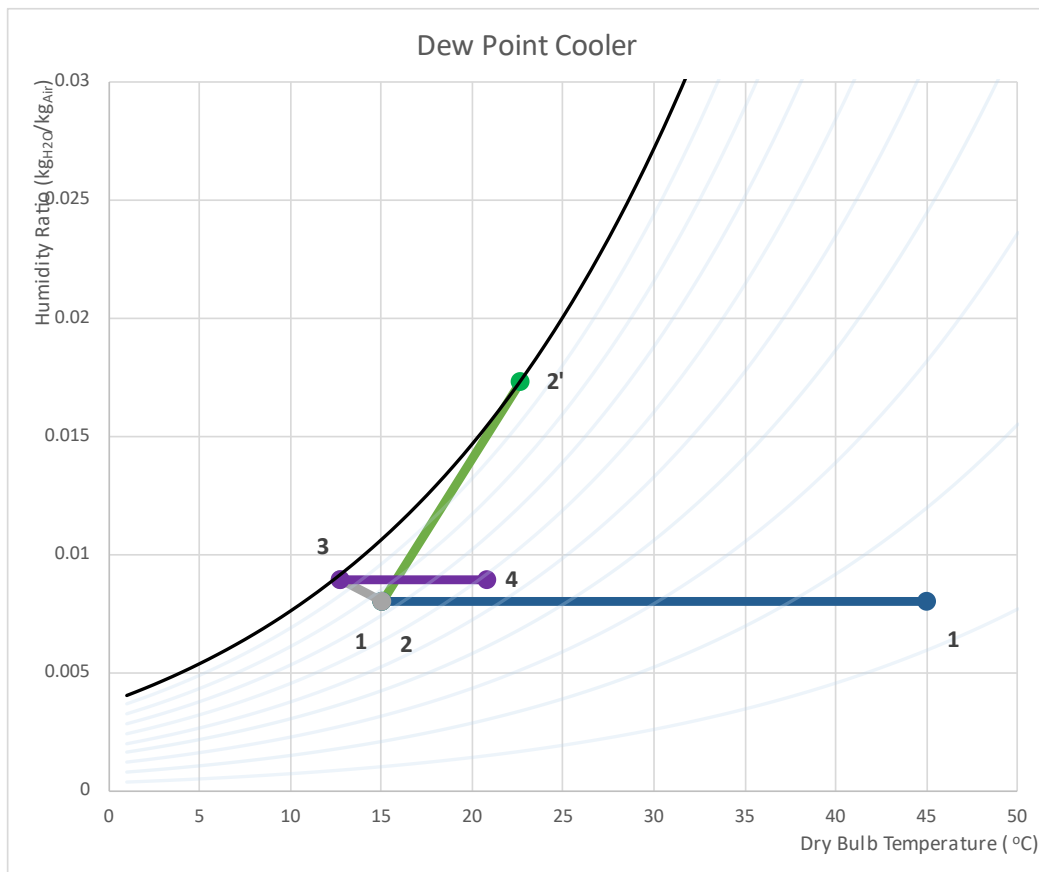


Figure 10: An indicative pressure-enthalpy (P-H) diagram of the installed DP-CO<sub>2</sub> system. In this present case, the DP-CO<sub>2</sub> system is operating in the trans-critical mode. Note that the pressure and enthalpy values may change depending on conditions, and that this figure is intended for illustrative purposes only.



**Figure 11: Psychrometric chart and process cycle for the installed dew point cooler. This is for illustrative purposes only, with actual values of temperature and humidity dependent on the instantaneous conditions (operating and ambient).**

### 2.2.2 Sensor Locations on the Dew Point Coolers

To further reduce instrumentation costs and noting that the gas cooler system comprises of 3 identical racks, the project team decided to fully instrument one of these racks (called Unit A), while only minimally instrumenting the other two racks (Units B and C).

Figure 12 illustrates the locations of the air temperature probes and differential pressure sensors on Unit A. While Unit B and C were fitted with temperature sensors to measure the supply air and gas cooler CO<sub>2</sub> outlet temperatures, Unit A is used to investigate, in detail, the performance of the dew point coolers. Air temperatures are recorded for both the bottom and the top assemblies of Unit A. The flow diagram as displayed on the top unit of Figure 12 shows the location of the temperature sensors in relation to the main components in the module while the flow diagram on the bottom module shows the location of the pressure sensors. Table 4 and Table 5 summarise the process measurements that can be obtained using these sensors. Air velocity meters in the transition piece will be used in conjunction with these sensors to calculate the heat capacity of each process.

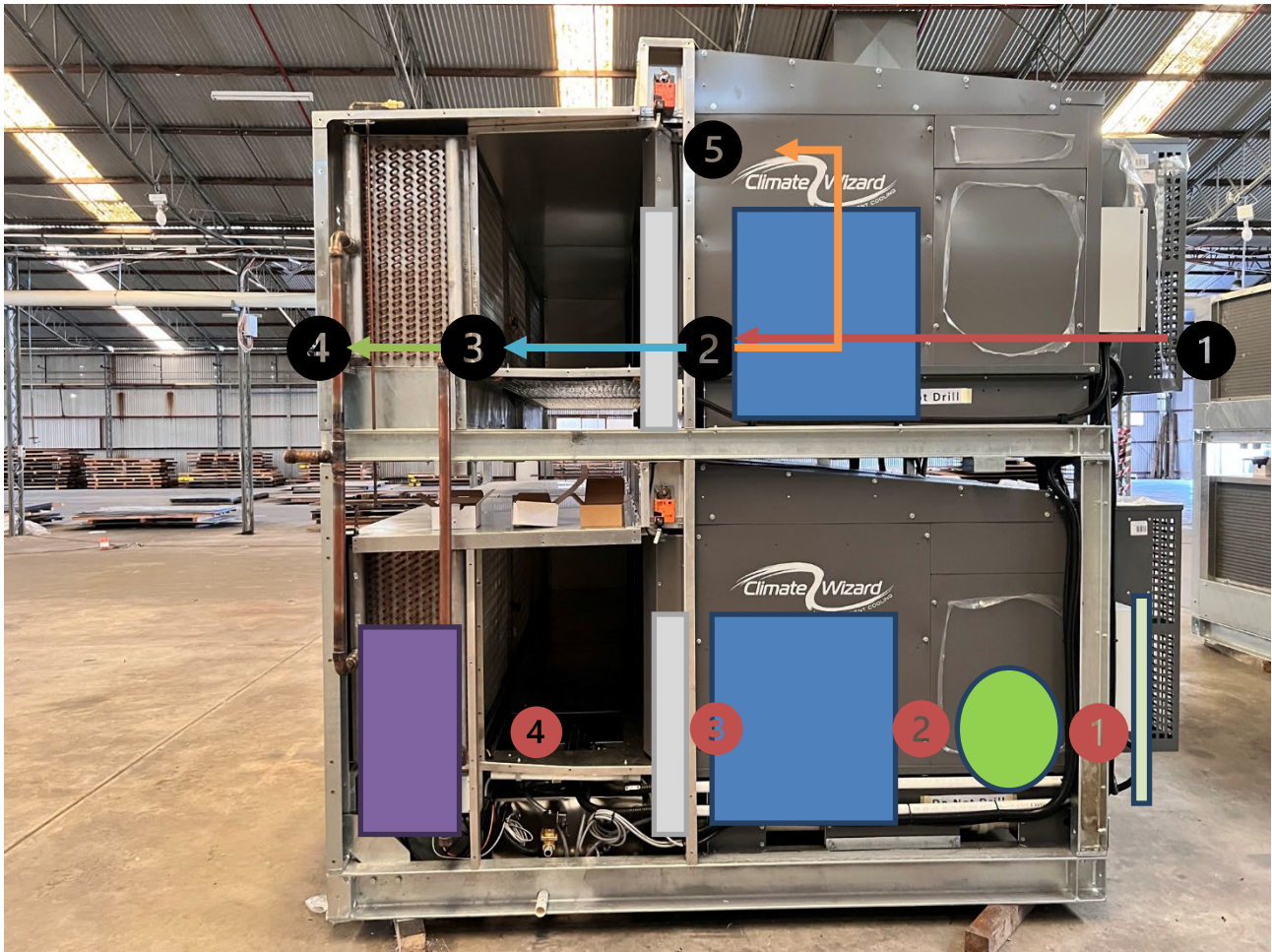


Figure 12 Location of temperature and pressure sensors on Unit A.

Table 4 Measurement derived from the temperature sensors.

Temperature sensors	Process measured
1 → 2	Temperature difference across the “dry” side of the indirect evaporative pad
2 → 3	Temperature difference across the direct evaporative pad
3 → 4	Temperature difference across the gas cooler coil
2 → 5	Temperature difference across the “wet” side of the indirect evaporative pad to the exhaust
1 → 3	Total temperature difference between the ambient air and supply air

Table 5 Measurement derived from the differential pressure sensors.

Pressure sensors	Differential pressure measured
1	Filter pressure drop
1 → 2	Fan differential pressure
2 → 3	Pressure drop across the indirect evaporate pad
3 → 4	Pressure drop across the direct evaporate pad



It should also be noted that the measurements taken from Unit A also allowed researchers to analyse the performance of Seeley's dew point coolers independently from the CO<sub>2</sub> refrigeration system, which in turn provided further useful information for the optimised the design and implementation of the systems.

Figure 13 to Figure 16 show the final installation positions of the sensors installed on Unit A. These sensors were installed by UniSA staff and the wiring of the sensors was performed by Electrical Solutions.

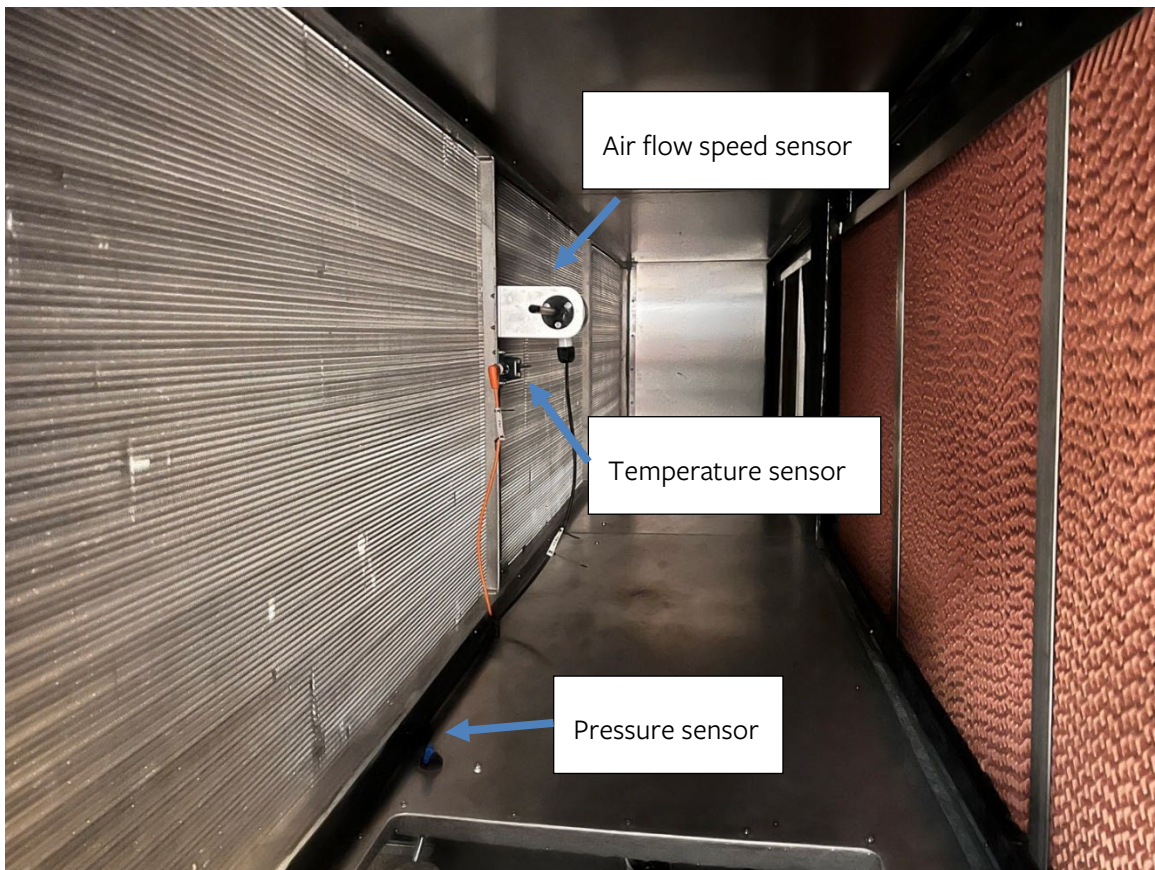


Figure 13 Supply air velocity, temperature and pressure sensors.



Figure 14 Ambient air temperature and relative humidity sensor.

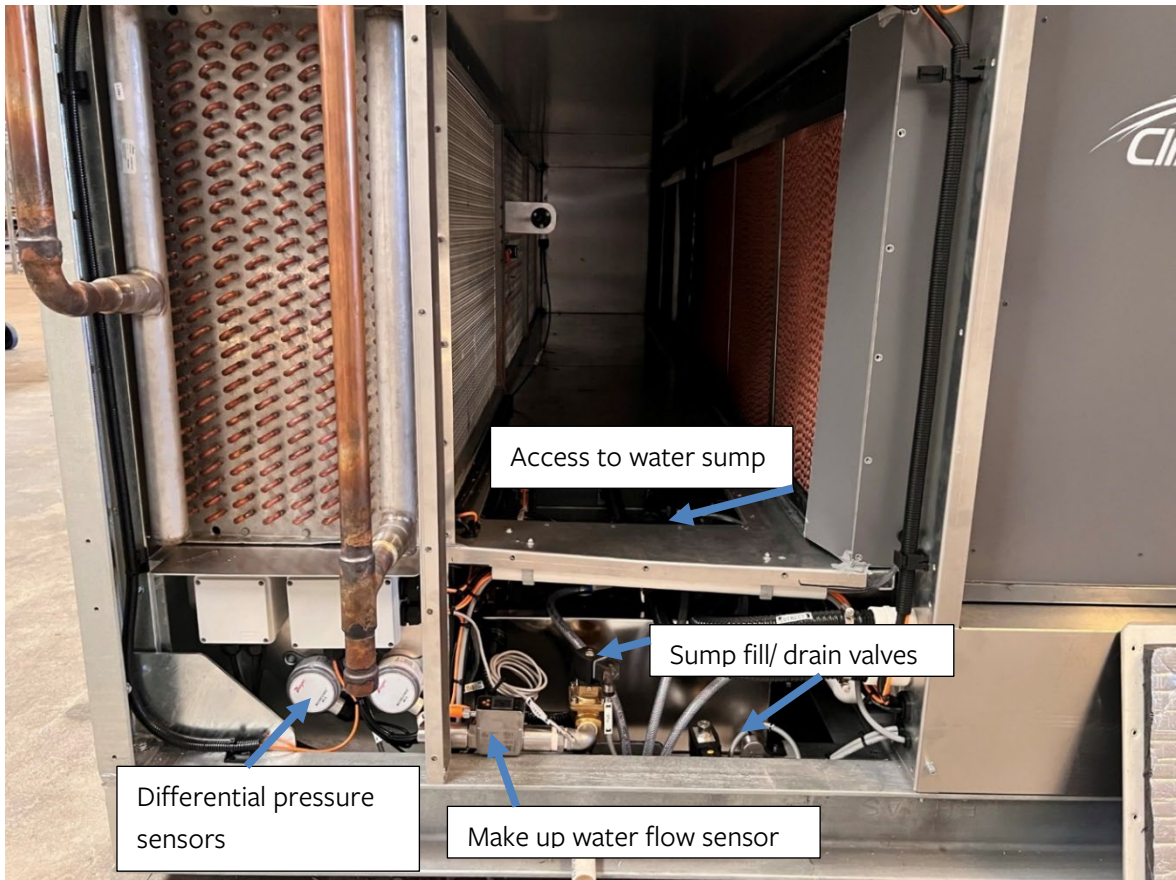
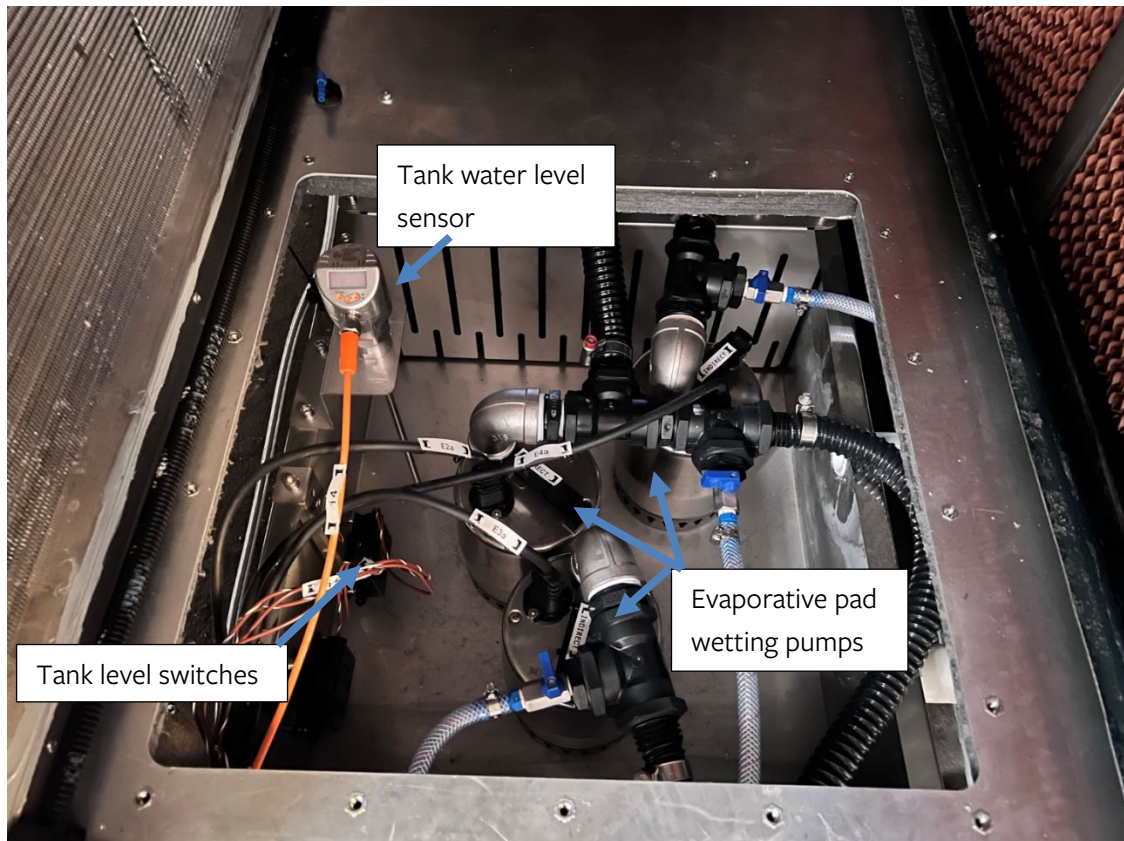


Figure 15 Water sump valves, access point and differential pressure sensor location.





**Figure 16** Evaporate pad wetting pumps and tank level sensors/ switches.

### 2.2.3 Sensor locations on the CO<sub>2</sub> Rack

The installation of the CO<sub>2</sub> refrigeration rack was conducted by third party supplier SCM. The rack, shown in its installed form in Figure 17 is controlled by a Danfoss pack controller. The Danfoss pack controllers are a great option for control for supermarkets as they are specifically designed for this type of refrigeration purposes. While it is beneficial to use these controllers as they are cheaper and designed to integrate the typical applications and systems present in a supermarket CO<sub>2</sub> system, they are not designed for atypical setups, such as the use of the DP-CO<sub>2</sub> systems. In particular, the pack controller does not provide sufficient data for the compressors for detailed data analysis. To ensure there is enough detail in the monitoring of the complete system, researchers have added additional pressure (Figure 18) and temperature (Figure 19) sensors to critical parts of the refrigeration rack.



Figure 17 Plant room, Glaciem Electrical box with PLC, HMI attached on the left-hand side of the CO<sub>2</sub> Rack.

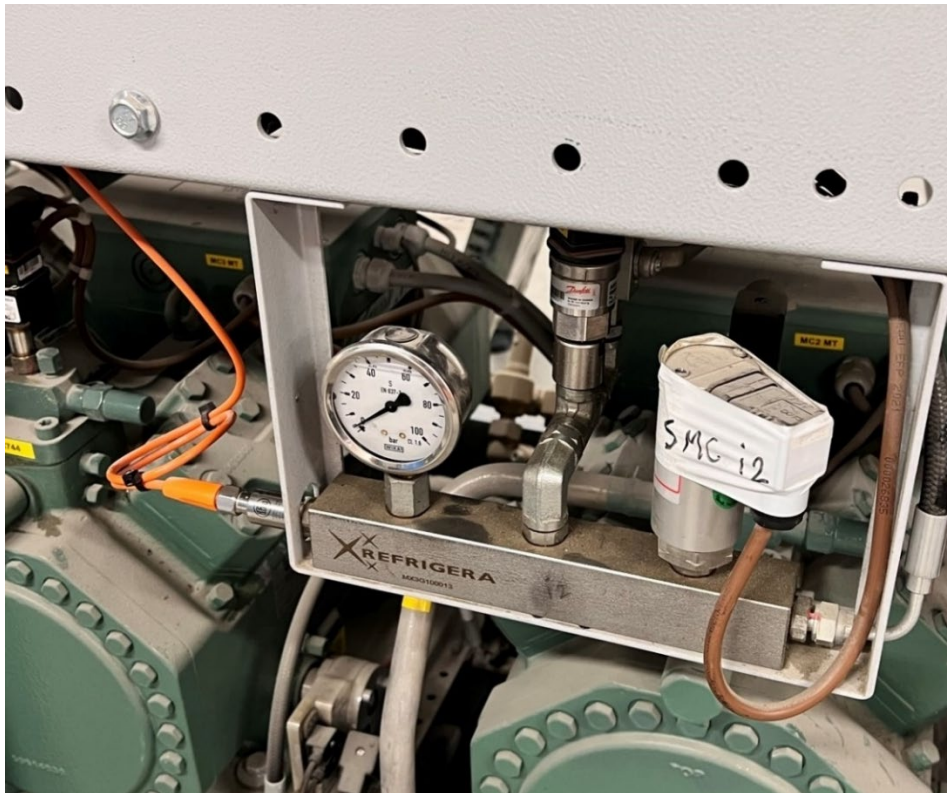


**Figure 18 IFM pressure sensor mounted to SCM pressure manifold.**



**Figure 19 High pressure expansion valve CO<sub>2</sub> temperature sensor and IFM converter module.**

The overall performance of the system and the effect of the dew point coolers on the system was established from the monitoring data specified above. The monitoring system however was not designed to provide complete insight into the performance of the lower pressure suction groups. In addition to the pressure and temperature sensors installed on the rack, several 0-10V channels on the pack controller were specifically dedicated to outputting data to the gas cooler PLC for monitoring and control purposes. Furthermore, an additional Dent power meter was also installed to provide accurate power data for each of the 10 compressors in the system (Figure 20).





**Figure 20 Electrical board- Electrical breakers, PLC and DENT power meter.**

The results from the entire monitoring system, which includes 146 sensors and component state logs from the DP-CO<sub>2</sub> system, including the compressor rack and power meters, were exported continuously to the graphical-based dashboard. This data was updated every second. Data from the sensors were recorded every 10 seconds and uploaded to a password-protected cloud server weekly, enabling researchers to access the data remotely.

#### 2.2.3.1 Instrument Types

Selection considerations such as measuring range, response time, accuracy, output signal, mounting, and cost are taken into consideration when selecting each of the sensors. A complete specification sheet for each sensor is provided in Appendix B of this report along with a brief list of the types of sensors that were used in the project.

#### 2.2.4 Summary of the Monitoring System Design

A piping and instrumentation diagram of the complete design of the DP-CO<sub>2</sub> system including the monitoring points is shown in Appendix A.

A schedule of the monitoring instruments and sensors is summarised in Appendix B.

## 2.2.5 Summary of the Control System and Monitoring System Design

The base for the control of the system as well as collection of the monitored data is an onboard allocated Programmable Logic Controller (PLC). PLCs and Supervisory Control and Data Acquisition (SCADA) systems are widely used in commercial and industrial scale, because they are a proven technology which is robust, reliable and meet the required industry standards. Amongst the multitude of options, we have chosen a Schneider PLC with its associated SCADA system provided by CITECT. These are commonly used devices in the Australian industry which brings a peace of mind when it comes to availability of spare parts and technical support. Moreover, this was consistent with the operating system of the main CO<sub>2</sub> rack supplied by Coles.

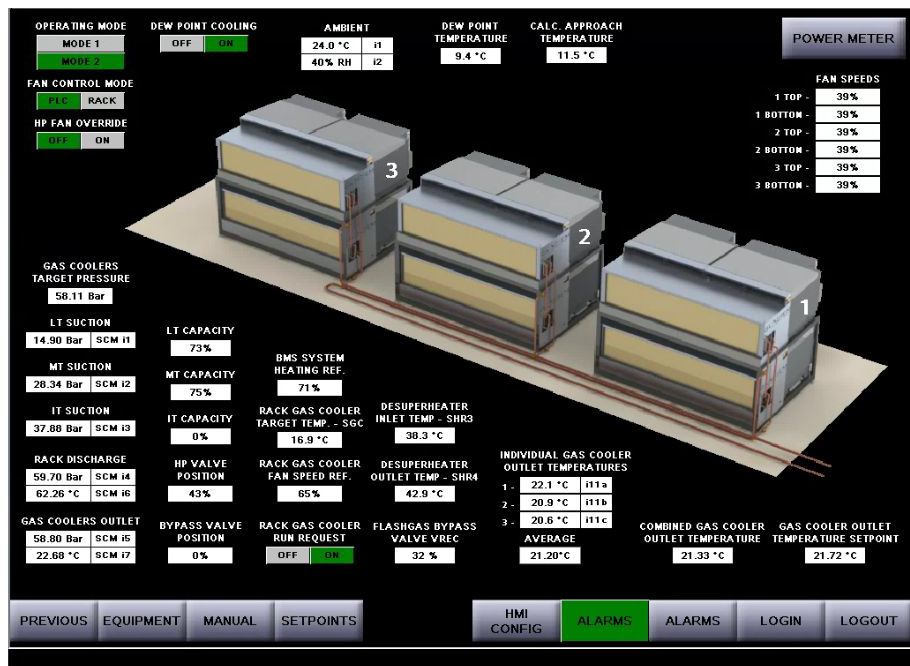


Figure 21 Snapshot of live feed from Scada.

The DP-CO<sub>2</sub> system PLC was programmed to monitor and control the performance of the gas coolers directly. It communicates with the main pack controller of the CO<sub>2</sub> system through digital and 0-10V analog signals. Communication to the allocated power meter and the individual I/O units on each of the dew point cooler modules was through the Modbus communication protocol. For the purposes of monitoring, data was collected every 10 seconds by the PLC and stored on a computer on site. This data could be accessed live via an internet connection through the SCADA software, CITECT. Remote real-time monitoring and analysis of the system performance was enabled by the CITECT user interface, Webgate, through the internet. Example snapshots of the interface of the installed system are shown in Figure 21. In addition, batched data was uploaded to the cloud weekly, enabling researchers to analyse the performance over the desired period of operation.

## 3 Computational Model Architecture

### 3.1 Introduction

A key part of the project involved modelling the performance of the combined dew point cooling and CO<sub>2</sub> refrigeration systems. The numerical model developed as part of this project was designed for three major roles, namely:

- As a design and sizing tool to enable engineers to size compressors, heat exchangers and major system components based on the year-round performance of the system in various climate zones;
- As a performance estimation and comparison tool. The model was developed to estimate the annual energy and water consumption of the system under various operating and ambient conditions. Therefore, the model can also be used to compare the performance of the DP-CO<sub>2</sub> system to more conventional condenser-based CO<sub>2</sub> systems; and
- As an optimisation tool, to enable the testing of various operating protocols and control system methodologies which optimise the system's performance. This includes the operation limits of the dew point coolers' water and air distribution systems (e.g. how much water to use for indirect and direct evaporation), the condenser fan set points (e.g. when and under what conditions do the fans turn on) and the refrigeration systems' mode of operation (e.g. whether it is more beneficial to temporarily operate in the super-critical mode to save on fan power).

The modelling of the DP-CO<sub>2</sub> system has been designed to be as flexible as possible, allowing for the adoption of the model to different climates and different applications. The model focusses on the detailed performance analysis of the dew point cooler and the CO<sub>2</sub> refrigeration system's compressors, together with the optimisation of the operation of the combined system.

Previous research into the performance of the DP-CO<sub>2</sub> system showed that the optimal performance of the system was achieved by considering the play off in power consumption between the dew point cooler fans and the refrigeration system's compressor power (Belusko et al., 2019). The optimal performance was therefore dependent on the ambient weather conditions, refrigeration load and operating parameters. To ensure adequate system performance modelling, these operating conditions are used as inputs to the model.

In this project, the modelling work was divided into two components:

- A Coles-specific model, which was based on the components and system specifically relevant to the chosen Coles supermarket site; and
- A more generalised model, where the preliminary model was extended so that it can be applied to a broader range of applications and climate conditions.

Section 3.2 provides an overview of the architecture of the model.

### 3.2 Model Architecture

The model has been designed as a Microsoft Excel spreadsheet to be used for a variety of different cooling applications in varying climates. To provide a high flexibility within the model, a modular code was chosen. The model contains a number of input files which feed into the optimisation files. An output file aggregates the results of the model in hourly, monthly, seasonally, and yearly formats. Figure 22 illustrates the structure and generic format of the model. Descriptions of each component present in Figure 22 can be found in the proceeding sub-sections.

The model requires three sets of inputs, namely weather data, site specific design information and site load data. These are discussed in more detail in Section 3.2.1.

The weather, system design and load data files are input into the model as discrete input files. This allows for the model to quickly and easily be modified to suit different climate zones and applications. The core model contains a numerical model of the dew point cooler and the CO<sub>2</sub> refrigeration system. The system operating conditions and the climate data are supplied to the core model and the performance of the system is simulated for each hour of the year. An output “dashboard” page provides high level performance statistics and the option to export a file containing the detailed operating parameters from the model for further analysis.

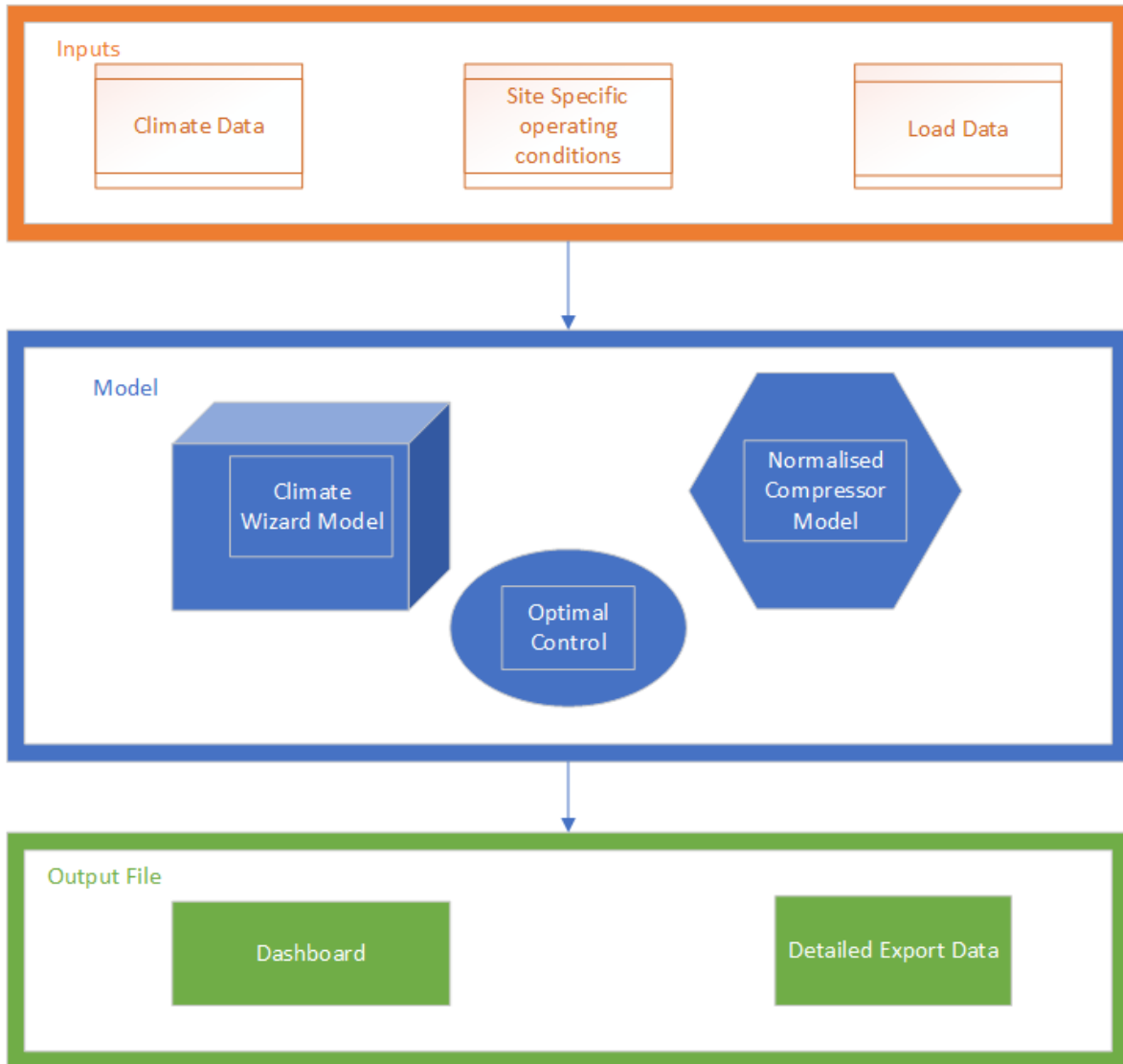


Figure 22 Schematic of the modelling procedure. Note that the “Climate Wizard” refers to the dew point (indirect evaporative) cooler. The data in the orange box are inputs required from the user.

### 3.2.1 Inputs

The modelling inputs comprise of the climate data, the site-specific operating conditions and the load profiles. Details of these inputs are explained in the sub-sections below.

### 3.2.1.1 Climate Data

The model requires climate (ambient) weather conditions in the typical meteorological year (TMY) file format, which is the standard file format used by building and energy modellers across the globe. More specifically, the model requires the dry-bulb temperature and the humidity (moisture content) on an hourly basis across the year starting at midnight on the 1<sup>st</sup> of January, up to the 11 pm on the 31<sup>st</sup> of December (see Table 6 for an example). For major Australian cities and towns, TMY data can be obtained from the Australian Bureau of Meteorology. Alternatively, for Australian conditions, NatHERS climate files can also be used as useful weather input files as they provide localised climate data. Any TMY format files can be used as long as they are in the required format for input weather files.

**Table 6: An example of a Weather Input file (first 7 hours only) for Adelaide (AD). Here DB refers to the dry-bulb temperature.**

City	Year	Month	Day	Hour	DB x 10 (°C)	Moisture (g/kg) x 10
AD	89	1	1	0	185	88
AD	89	1	1	1	186	86
AD	89	1	1	2	190	84
AD	89	1	1	3	189	81
AD	89	1	1	4	191	79
AD	89	1	1	5	184	78
AD	89	1	1	6	197	79
AD	89	1	1	7	203	80

### 3.2.1.2 Load Data

The model also requires data on the refrigeration loads of the refrigeration system, i.e., the amount of cooling required (in terms of thermal energy), the time at which this cooling is required, and the required cooling temperature(s). For most accurate results, the model requires refrigeration load data on an hourly basis continuously across an entire year. However, most sites requiring refrigeration will not monitor refrigeration load or refrigeration power consumption in enough detail to be able to input data into this model. Therefore, to overcome the lack of detailed data, the model allows for several methods that can be used to obtain the real time load data. In particular, the model has provisions for:

- Using available refrigeration system power consumption data (where available) and then estimating the refrigeration load using the refrigeration system coefficient-of-performance values (obtained from the manufacturers);
- Using industry standard load profiles. These “standard” load profiles vary between sectors and industries, and typically comprise of educated estimates and/or rules-of-thumb based on the experiences of refrigeration engineers and operators within each sector. In the present project, these load profiles are estimated through engaging with individual members of the Industry Reference Group (IRG);
- Using short term (e.g. 1 week, 1 month) monitored data (organised by the site owner).

For cases where a full 12-month period of load data cannot be obtained, extrapolation of data using climate statistics and/or expected load variations can provide a reasonable estimate for year-round load data.

In the case of the Coles site, the model had been input with load data supplied by Coles. This data was adapted from their temperature-based load profiles. A load data file was created for a 12-month period with hourly load profile data. The timesteps of the load data match the timesteps of the climate data above. This provided



the model with the expected operating conditions of the refrigeration system for every hour of the year. A sample of the load data is shown in Table 7.

Table 7: Sample load data file used in the modelling of the Coles site. Here LT, MT and HT refer to low, medium and high temperatures, respectively.

Timestep	Dry Bulb Temperature (°C)	LT Load (kW)	MT Load (kW)	HT Load (kW)	Total Cooling Load (kW)
1/01/2000 0:00	18.5	20	100	40	160
1/01/2000 1:00	18.6	20	115	30	165
1/01/2000 2:00	19.0	20	115	30	165
1/01/2000 3:00	18.9	20	200	25	245
1/01/2000 4:00	19.1	20	200	60	280
1/01/2000 5:00	18.4	30	100	50	180
1/01/2000 6:00	19.7	40	150	40	270

### 3.2.1.3 Site-specific Operating Conditions

The model considers site-specific details including the refrigeration process cycle used and the control of the system components (including degree of superheat/ subcooling, operating hours and limits). The configuration of the refrigeration system, the operating parameters and ambient conditions for any site can be input into the model through the “System Specifications” page. This page is where the weather and load profiles are also selected. The system type is then selected, which opens options to modify the site-specific layouts and operating controls such as:

- Compressor selection
- Suction pressure set points
- Intermediate pressure
- Operating hours
- Heat exchanger operating parameters
- Condenser operating parameters

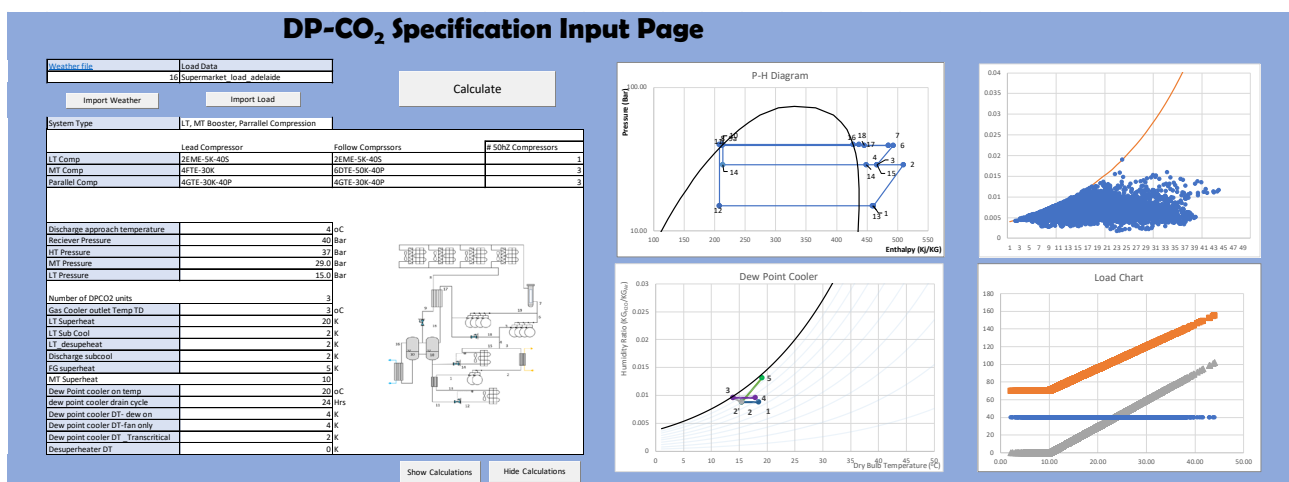


Figure 23 Sample “system specification” page

Figure 23 provides a view of the system specifications input page. For the basic user, the site-specific specifications page and the output page will be the only pages accessible. All other pages will be hidden as they will not need editing. A base scenario will be presented on start-up with default details input for each of the

above controls. The user can then deviate away from the default values where required, changing compressors, temperature, pressures where required.

### 3.2.2 Model

The model uses the input file data to optimise and evaluate the performance of the refrigeration system for each hour of the year.

Specific worksheets become available depending on the choice of system type and the input data provided. For the Coles model, the dewpoint cooler model and compressor model become available. These worksheets provide the backbone for the mathematical calculations based on the specific layout of the system.

The overall model uses sub-models and algorithms to perform the necessary background calculations. In particular, three visual basic (VBA) modules have been created within Excel to perform the background calculations for:

- Psychrometric properties air properties
- CO<sub>2</sub> energy of state calculations
- Compressor performance.

The three VBA modules, comprising over 85 separately-coded VBA functions are used to calculate properties such as air moisture content, CO<sub>2</sub> enthalpy at different states (i.e. pressures and temperatures) and compressor performance for differing load conditions (for example, see Figure 24). These functions are then referenced in the climate wizard and compressor model worksheets. Key features of these sub-models are explained in more detail below.

```

Option Base 1
Option Explicit

Const RGASco2 = 0.188924      ' Universal gas constant in J/mol/K
Const MOLMASSco2 = 44.0098   ' mean molar mass of dry air in kg/mol
Const Rmco2 = 8.31451        ' kJ/kmolK universal gas constant
Const Ttco2 = 216.592        'triple point temperature in K
Const Pttco2 = 0.51795       'triple point Pressure in MPa

'Calculation of Saturation pressure as a function of saturation temperature
'Critical point properties of CO2
Const PC = 7.3773            'MPa
Const Tco2 = 298.15          'reference temperature
Const Pcco2 = 0.101325       'reference pressure

Const Tc = 304.1282         'Kelvin
Const rhoc = 467.6          'kg/m3

'reference
Const T0co2 = 298.15         'K reference temperature
Const p0co2 = 0.1013258     'MPa reference pressure
Const ho_ig = 0              'reference enthalpy in the ideal gas state at To , kJ/kg
Const so_ig = 0              'reference entropy in the ideal gas state at To , kJ/k kg
Const delta_h = 506.777     'kJ/kg offset to IRR reference state
Const delta_s = 2.739       'kJ/kg K offset to IRR reference state

Function h_pt(ByVal P As Variant, ByVal T_K As Variant) As Variant

Dim d As Variant
Dim T As Variant
    
```

Figure 24 Sample VBA code with 3 modules for psychrometric, CO<sub>2</sub> and compressor calculations

#### 3.2.2.1 Climate Wizard model

A sub-model has been developed for the Climate wizard system. The model includes the performance of specific aspects of the dew point cooler including:

- The dew point efficiency at various ambient conditions (i.e. dry bulb temperatures and relative humidities)
  - Indirect evaporative component
  - Direct evaporative component
- The fan power/ air flow rate curve
  - Ventilation only mode
  - Evaporative cooling mode
- Fan air flow and fan power based on condenser heat of rejection
- Water consumption

#### 3.2.2.2 Compressor data

The compressor data worksheet models the entire refrigeration cycle. Initial values for the suction pressure groups and discharge pressure are input from the system specification page and initial calculations performed on the dew point cooler page. These data are used to model the refrigeration cycle. At each point in the cycle, the pressure, enthalpy, temperature, density, and entropy are calculated. From this point the mass flow rate of refrigerant is calculated based on the normalised compressor data for the specific compressors, pressure ratio and refrigerant density. The number of compressors and their variable frequency drive (VFD) frequency to meet the load for each hour of operation are calculated and the electrical power is then modelled. Finally, the heat of rejection through the condenser is determined which in turn is used in the Climate wizard model to calculate the fan air flow rate, fan power consumption and dew point cooler water consumption.

#### 3.2.3 Output file

The output file aggregates the performance of the system and details the operating performance of the system throughout the year. These data are provided in hourly, monthly, seasonal, and yearly formats. Data provided in the output page includes:

- Compressor power
- Dew point cooler power
- System COP
- Water Consumption

## DP-CO<sub>2</sub> Performance Output Page

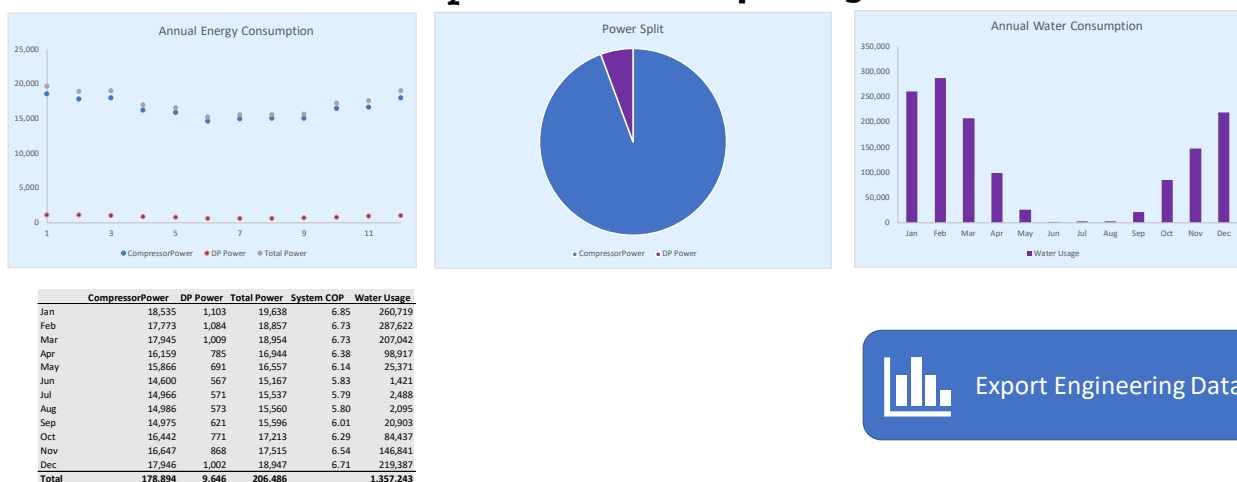


Figure 25: Example output page

Figure 25 provides an example of the output page. This output page summarises key data of the refrigeration system energy and water consumption (monthly), thereby providing an overview of the performance of the system and how it operates seasonally. From this page there will be an option to export the detailed operating and performance data to a new excel file (see Figure 68 in Appendix C for an example) for expert user analyses. The exported file will contain all of the calculated parameters for the simulation at each timestep. This will include:

- Dew point cooler operating conditions
  - Ambient air conditions
  - Indirect evaporator outlet conditions
  - Direct evaporative cooler outlet conditions/ condenser inlet conditions
  - Fan electrical power consumption
- Compressor rack operating conditions
  - Complete CO<sub>2</sub> cycle pressure and enthalpy values
  - Compressor operating state
  - Number of compressors operating
  - Frequency of any VFD controlled compressors
  - Compressor power consumption

The detailed data will enable engineers to perform detailed analysis of the system. This detailed analysis will be vital for the correct sizing and optimisation of systems, including part load analysis of the system. Part load analysis is often overlooked in engineering and annual system performance is often significantly affected by the lack of scrutiny it receives.

### 3.3 Description of Model Algorithms

The model has been developed in a modular format. The separation of inputs, dew point cooler performance, CO<sub>2</sub> cycle properties and compressor performance calculations simplifies the extension of the model to different applications. The exchanging of modules (e.g. the dew point cooler with an adiabatic cooler) allows for rapid comparative modelling of multiple systems. Similarly, exchanging load and weather input data allows the model to be used for different applications and climate zones. Figure 26 provides an overview of the mathematical process within the model. Input files (orange) provide data points for the models (blue squares)

which interact with each other to provide output (green) data for monthly and yearly total energy and water usages.

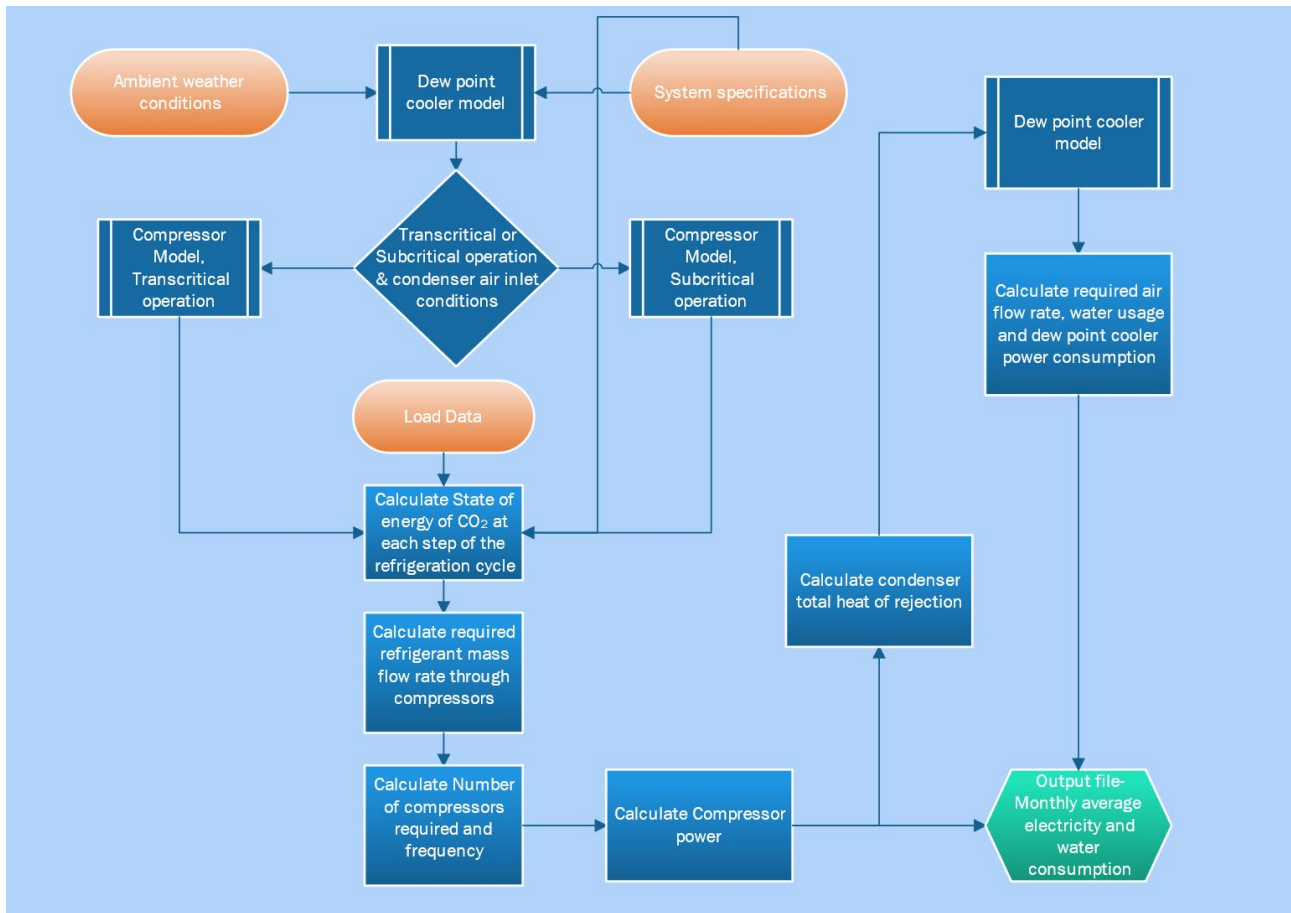


Figure 26 Flow diagram of modelling procedure

### 3.3.1 Dew point cooler calculations

The model of the dew point cooler performance is based on the model published by Belusko et al. (2019). In this sub-model, the performance of the cooler can be divided into two main components, namely the thermal performance and the power consumption of the dew point cooler system. The thermal performance is calculated first. This determines the condenser outlet conditions of the refrigeration system as one of the parameters required for the calculation of the refrigeration system performance. Power performance is calculated after the performance of the refrigeration system is attained. This allows for the power required to meet the condenser load to be added to the calculation of the dew point cooler power consumption.

Calculation of the dew point thermal process starts with the ambient air conditions. Using the calculation methodology developed by Belusko et al., the indirect evaporative process outlet air temperature,  $T_2$ , can be predicted using the following linear regression equation:

$$T_2 = 0.055T_{DB} + 0.289V + 923W + 4.8$$

where  $T_{DB}$  is the ambient dry bulb temperature (in °C),  $V$  is the volumetric flow rate of air through the condenser (in  $m^3/s$ ) and  $W$  is the ambient moisture content (in kg of moisture / kg of dry air).

The condenser air inlet condition ( $T_3$ ) is obtained by determining the outlet conditions of the adiabatic pads. This is calculated using a specified wet bulb effectiveness of the pads,

$$T_3 = T_{WB,2} + (1 - WB_{eff})(T_2 - T_{WB})$$

where  $T_{WB,2}$  is the wet bulb temperature at state 2,  $WB_{eff}$  is the web bulb effectiveness of the adiabatic cooling pads.

The condenser air inlet condition, ( $T_3$ ) is then input into the refrigeration system model.

The condenser load can be determined from the performance of the refrigeration system. The required fan power and water usage for the dew point cooler can then be calculated.

The water consumption is estimated at the end of the modelling process using the required mass flow rate of air to meet the total heat of rejection of the condenser. The mass flow rate through the exhaust stream of the dew point cooler and the mass flow rate across the direct evaporative pads can be calculated. The water consumption is estimated to be the water added to the air streams due to evaporation in both air streams.

### 3.3.2 Refrigeration system model

The model of the refrigeration cycle uses input data in the system specification page to set the operating conditions. The values for the state of the process (as described in Figure 27 and Table 8) at the discharge of the condenser (point 8 of Figure 27) is determined by the system specifications and the dew point cooler model. From there, calculations of the CO<sub>2</sub> properties at each stage of the refrigeration cycle are determined using a calculation methodology specified by Span & Wagner (1996). The methodology for the calculation of change of state follows that described by Wang et al. (2022) with the addition of modified compressor efficiency and power calculations, allowing a more versatile and automated calculation of performance. Table 8 outlines the calculations at each step of the cycle.

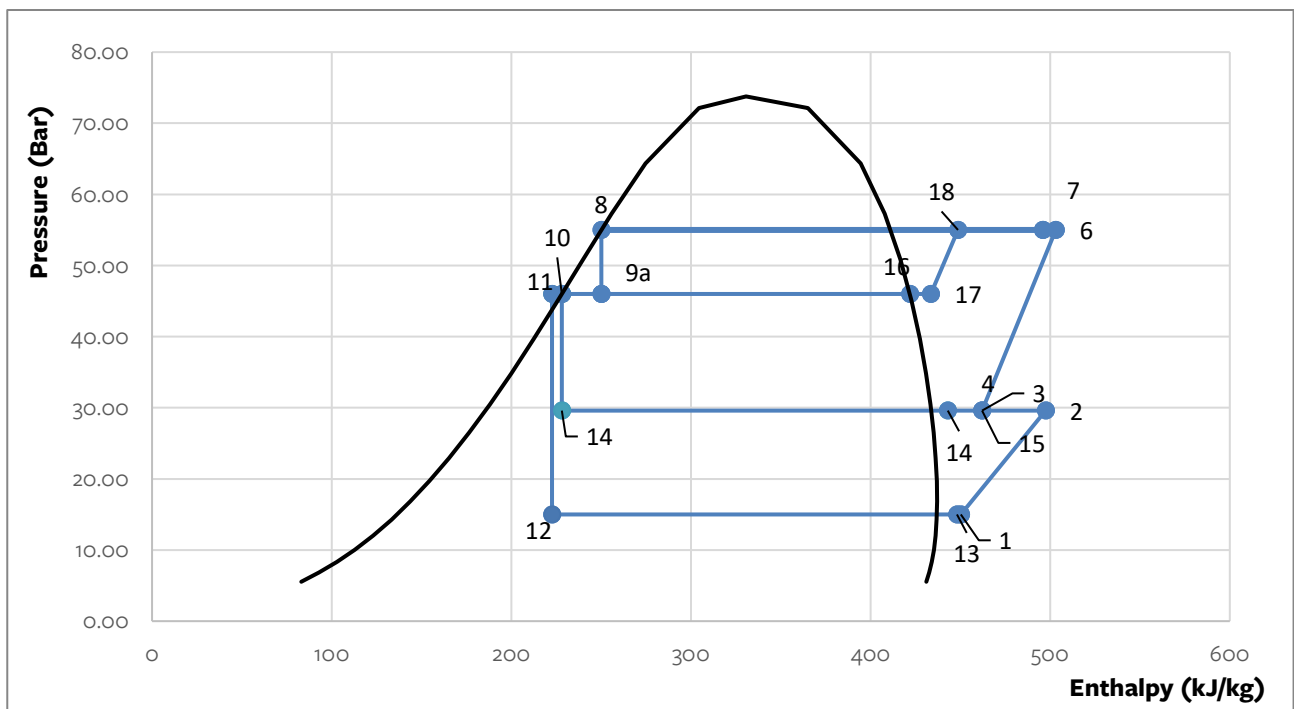


Figure 27: Pressure-enthalpy (P-h) diagram of the modelled refrigeration cycle. The points here are for a single snapshot in time; the exact values of the state points will vary with time (and conditions). The numbered points here refer to the locations within the DP-CO<sub>2</sub> system, as shown schematically in Figure 9.

Table 8 Refrigeration Cycle stages and required energy on state equations. The State points are also illustrated in Figure 9, with its equivalent P-h diagram shown in Figure 27.

State	State description	Required data	Calculated derived from
8	Condenser discharge, $Cond_{dis}$	$P, SCT/T_{gco}, h$	Derived from Dew point cooler condenser inlet temperature Subcritical – discharge pressure, Saturated liquid properties Trans-critical- Optimal discharge Pressure
9	Receiver	$P, X, h$	System specified Pressure, vapor fraction relating to the enthalpy at $Cond_{dis}$
10	Receiver, liquid outlet	$P, h$	Saturated liquid properties at receiver pressure
11	LT IHX sub cooling	$P, h$	Include sub cooling to receiver Saturated liquid properties
12	LT TX valve outlet	$P, h$	$CO_2$ properties at $h_{11}$ , system specification $P_{LT}$
13	LT Evaporator outlet	$P, h$	$CO_2$ properties for saturated vapor, specified $P_{LT}$ , specified $LT_{superheat}$
1	LT IHX superheat/ LT Compressor inlet	$P, h, m, s, t$	$CO_2$ properties for saturated vapor, specified $P_{LT}$ , specified $LT_{superheat}$ DT LT IHX
2	LT compressor outlet	$P, h, m, s, t, Compressor Data$	Compressor calculation. See section 3.3.3
3	LT compressor outlet-cooled	$P, h$	Derived from compressor outlet – DT cooler
14	MT Evaporator outlet	$P, h, m$	$CO_2$ properties for saturated vapor, specified $P_{MT}$ , specified $MT_{superheat}$

15	MT superheat	P, h, m	CO <sub>2</sub> properties for saturated vapor, specified P <sub>MT</sub> , specified LT <sub>superheat</sub> , m calculated from load and h <sub>15</sub> -h <sub>9</sub>
4	MT compressor inlet (LT/MT mixed flow)	P, h	Calculated from the mixed flow rates and temperatures of state 3 & 15
6	MT compressor outlet	P, h, m, s, t, Compressor Data	Compressor calculation. See section 3.3.3
16	Receiver flash gas/ air conditioning load out	P, h	Specified P <sub>Parallel</sub> , saturated vapor properties superheat
17	Parallel Compressor inlet	P, h, m	m, from air con load and h <sub>16</sub> -h <sub>9</sub> , m <sub>MT</sub> and m <sub>LT</sub>
18	Parallel Compressor outlet	P, h, m, s, t, Compressor Data	Compressor calculation. See section 3.3.3
7	Mixed MT comp, Parallel Comp flow	P, h, m. MTcomp, m. PARALLELcomp	Calculated from the mixed flow rates and temperatures of state 6 & 18

---



### 3.3.3 Compressor model

For each suction group, the compressors are modelled. The volumetric and isentropic efficiency of the compressors are calculated for the specific load and operating conditions through an iterative process.

Firstly, the inlet conditions are calculated as described in Section 3.3.2. The required inlet CO<sub>2</sub> parameters are:

- Enthalpy
- Mass flow rate
- Superheat temperature
- Entropy
- Density

The CO<sub>2</sub> mass flow rate and density are used to calculate the required volume flow rate.

The volumetric efficiency of each compressor is calculated for the pressure ratio between compressor inlet and outlet, the degree of superheat and the frequency of the compressor. The calculation of the volumetric efficiency is performed using an equation developed through regression analysis of publicly available Bitzer compressor data.

A theoretical volume flow rate for compressor frequencies of 30, 50 and 60 Hz is then calculated to determine the number of compressors and frequency of compressors required to meet the required volume flow rate for the load. This calculation is an iterative process and uses the Newton Raphson Method (Garrett, 2015), to estimate the number of compressors required and the frequency of any Variable Frequency Drive (VFD) driven compressors.

The power consumption of the compressors can then be estimated using equations developed through regression analysis of publicly available Bitzer compressor data. These equations use the regression equation, a known power usage at set condition for that compressor and the pressure or temperature of the suction and discharge of the compressor.

### 3.3.4 Output page and file

The output page provides aggregated monthly data for:

- Compressor power
- Dew point cooler power
- Total power
- Water consumption and
- Coefficient of Performance (COP)

Power values are the summation of the hourly power consumption for each month. Indicated COP values are the monthly average value.

### 3.3.5 Export output file

There is an option for advanced users to export the mathematical results for each timestep. This includes the input data (temperatures and loads) as well as the refrigeration cycle properties and electrical and water consumption. This data is useful for engineers when sizing system components. This data can also be used to perform a detailed financial analysis based on time of use electrical energy costs.

## 4 Extension of the Model to Various Applications

The original model (as described in Section 3) was designed to calculate the performance of the DP-CO<sub>2</sub> system in a supermarket at a specific location. However, the architecture of the model was developed to allow for the evolution of the model to be used as a tool to predict the performance of the DP-CO<sub>2</sub> system in a number of applications in various locations. To fully enable the model to be applied more generally to other sectors where CO<sub>2</sub> refrigeration may be employed, the following modifications were made:

- 1) A library of different types of compressors, including their performance data and operating windows, were added to the model database. This information was obtained from manufacturers' specifications;
- 2) The model's system specification page was modified to allow a larger range of different configurations of CO<sub>2</sub> refrigeration systems. Most notably, the model was modified to allow the LT, MT and HT loads to be used optionally (whereas these were a "must" for the Coles model) and modified to allow the use of flash gas bypass systems. Different types of condenser types (e.g. no pre-cooling, adiabatic pre-cooling) were also added to the model.

The tool therefore has the capability to predict the performance of the DP-CO<sub>2</sub> system in a range of different sectors across Australia (and the world), including supermarkets, aquariums, food processing, cold storage, breweries, meat processing and buildings.

In this section, we will apply the model to a number of different configurations outside of a Coles supermarket. The model will be applied to a hospital kitchen cool room (Section 4.2.1), a hospital HVAC system (Section 4.2.2), a brewery (Section 4.2.3) and an abattoir (Section 4.2.4).

However, prior to using the model, the model will have to be first validated using known (measured) data. The model validation process is discussed in Section 4.1.

### 4.1 Modelling Validation

Data from two specific case studies (obtained separately to the current project) are used for model validation of the CO<sub>2</sub> cycle model, used in conjunction with the previously validated dew point evaporative cooling model (Belusko et al., 2019). These case studies involve measurements from the CO<sub>2</sub> refrigeration systems in a public aquarium and in an agricultural cold storage facility.

Both case studies use adiabatic coolers and recorded useful data that is used to validate the model. The data used include compressor power, ambient temperatures, Saturated Suction Temperatures (SSTs), Condenser Discharge Temperatures (CDTs) and thermal loads.

The two validation cases are discussed separately below.

#### 4.1.1 Validation case study I: Public Aquarium

##### 4.1.1.1 System description

A large public aquarium used chillers to provide chilled water-based air conditioning for their building and to provide 4 million litres of chilled seawater to their two main aquarium tanks which were maintained at 28°C for optimum marine life conditions. The site is located in a subtropical region in northern Australia and had a total solar PV capacity of 256 kW. The system used for validation comprised of:

- 1.2 MWh of thermal energy storage system (TES) using Phase Change Materials (PCMs);
- An integrated thermal energy storage and CO<sub>2</sub> heat pump system which runs in parallel with the existing HVAC-R systems;
- An Advanced Control & Forecasting Algorithm (ACFA) (Cirocco, 2022) integrated with the site's Building Management System (BMS) to allow the system to dynamically control the usage and storage of the site's renewable energy.

The overall HVAC-R plant on-site consisted of an ammonia refrigeration plant and CO<sub>2</sub> heat pump. A schematic of the CO<sub>2</sub> refrigeration subsystem is shown in Figure 28. For validation purposes, only data relating to the CO<sub>2</sub> plant was assessed. The present model was modified such that it simulates the aquarium refrigeration cycle, including its three CO<sub>2</sub> compressors, evaporator attached to the heat transfer loop between the refrigeration system, the TES, the chilled water loop and the desuperheater/gas cooler.

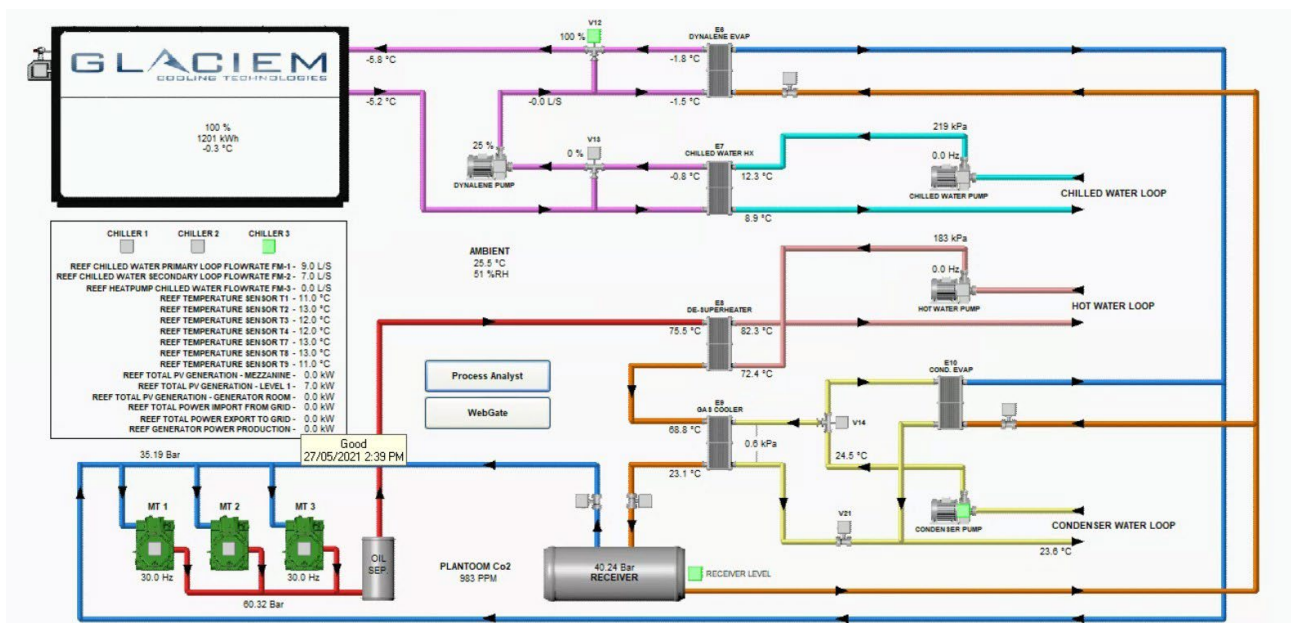


Figure 28 Schematic overview of the CO<sub>2</sub> refrigeration plant in a subtropical aquarium

#### 4.1.1.2 Results

The first stage of the validation was to compare the monitored data to the simulation results over the course of a typical summer day for a 12-hour period (on a minute-by-minute basis). The chosen date was 6th December 2021, i.e. a typical summer day. As seen in Figure 29, the results for the total compressor power obtained from the model closely matches that of the recorded data. The model data does, however, underestimate the total compressor power by approximately 8% towards the evening, which is attributed to the fact that the model makes a number of simplifications and idealised assumptions (see Section 3). Importantly, the model does strongly predict the overall temporal profile, including the significant ramp-up in compressor power in the morning and the sudden drop in power in the late morning.



Figure 29 The measured and simulated total compressor power of the CO<sub>2</sub> refrigeration system in a subtropical aquarium for a 12 hour period on 06/12/2021

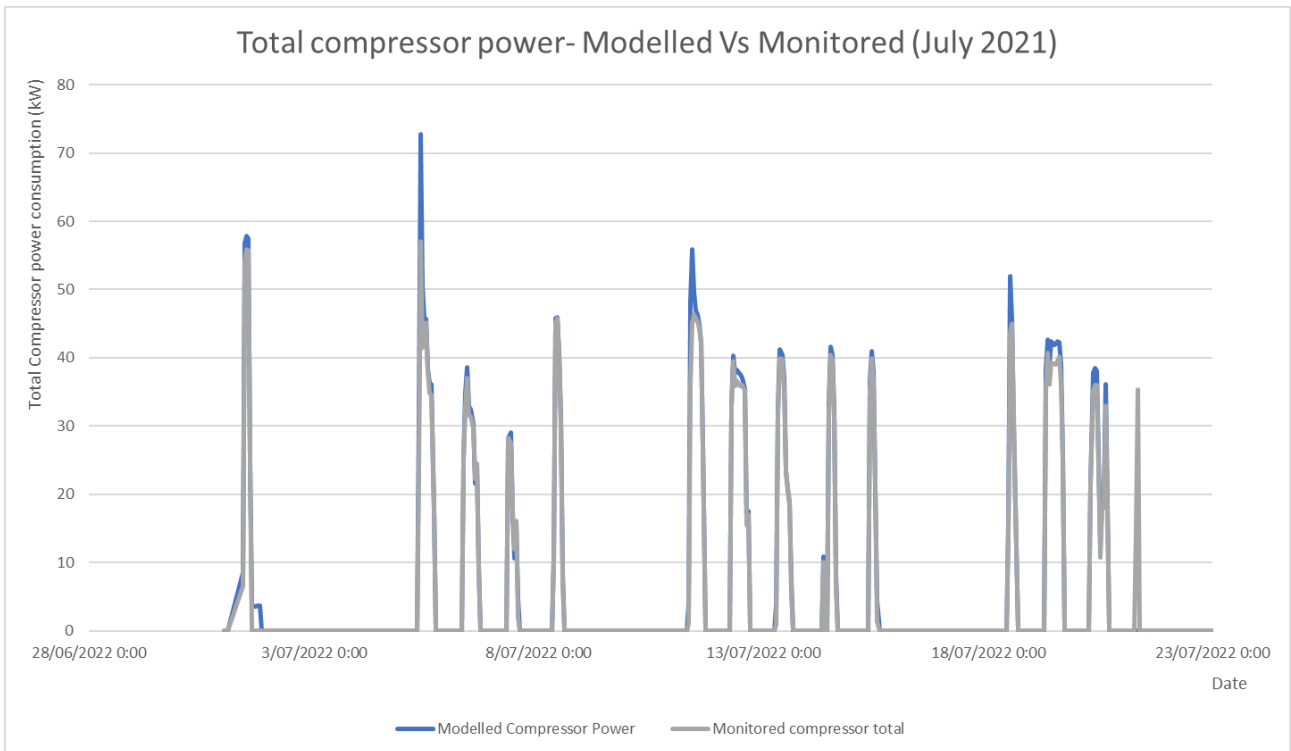


Figure 30 Comparison of monitored and modelled total compressor power for a 21-day period in July 2022 for the CO<sub>2</sub> refrigeration system in a subtropical aquarium.

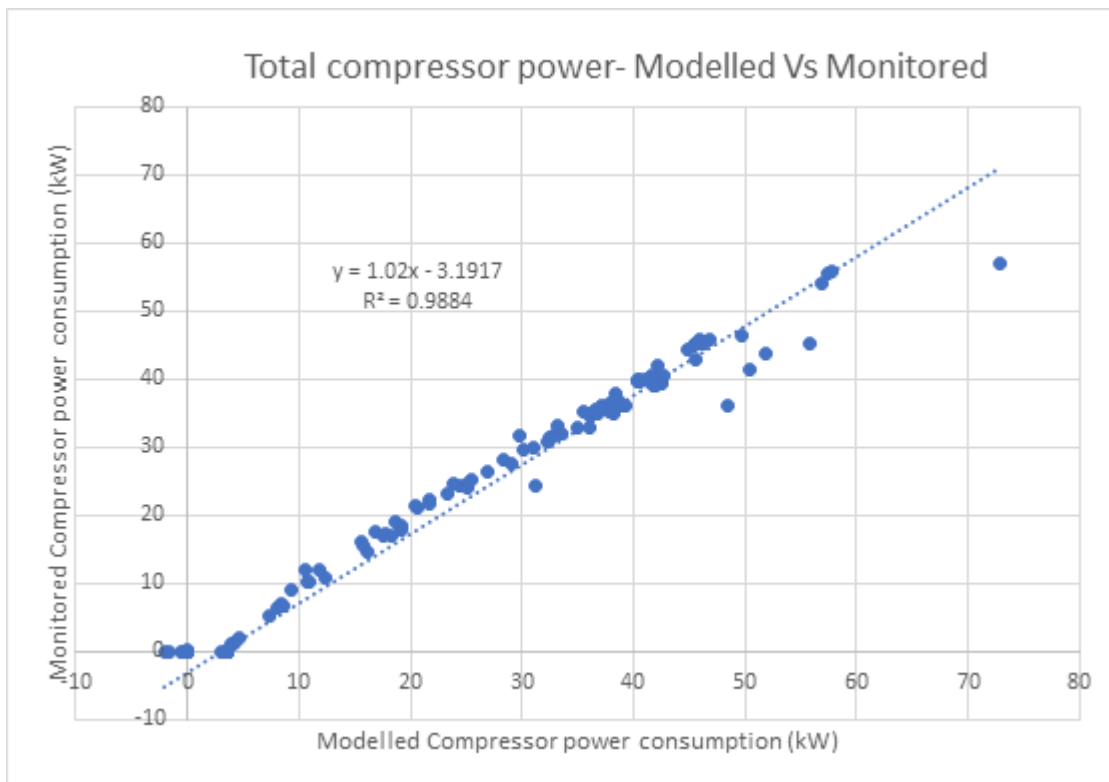


Figure 31 Correlation between modelled and monitored total compressor power for the CO<sub>2</sub> refrigeration system in a subtropical aquarium. The data points here were taken from hourly-averaged data across a 21-day period in July 2021

The same model was then modified to accept hourly-averaged data from the monitoring system. The measured and modelled results for the total compressor power consumption over the course of a 21-day period (in July 2021) is shown in Figure 30. This date was chosen as it represents typical winter operation. As can be seen, there is a strong correlation between the modelled and measured compressor power consumption, with an average difference between the two of less than 4.5%.

Figure 31 presents a direct plot of the measured versus modelled compressor power for the same 21-day period. As can be clearly seen, there is a strong, linear correlation between the two results (with a goodness-of-fit value of  $R^2 = 0.9884$ ), which provides evidence that the model is capable of accurately modelling a CO<sub>2</sub> refrigeration system under dynamic loads and changing weather conditions.

#### 4.1.2 Validation case study II: Agricultural cold storage

##### 4.1.2.1 System Design

The second case study is an apple packaging and cold storage facility in south-east Australia. The region has a temperate oceanic climate. The packaging plant capable of processing 227 million apples a year.

A trans-critical CO<sub>2</sub> heat pump system incorporating a thermal energy storage (TES) system designed to deliver 718 kW of heating for the hot water system was installed on site. For added efficiency, the heat pump is used to provide cooling to the storage facility and when the heating load exceeds the cooling load, the TES system is used to store the additional cooling provided for use at time outside of apple processing hours. A schematic of the refrigeration system, including the TES system, but excluding the hot water system, is shown in Figure 32.

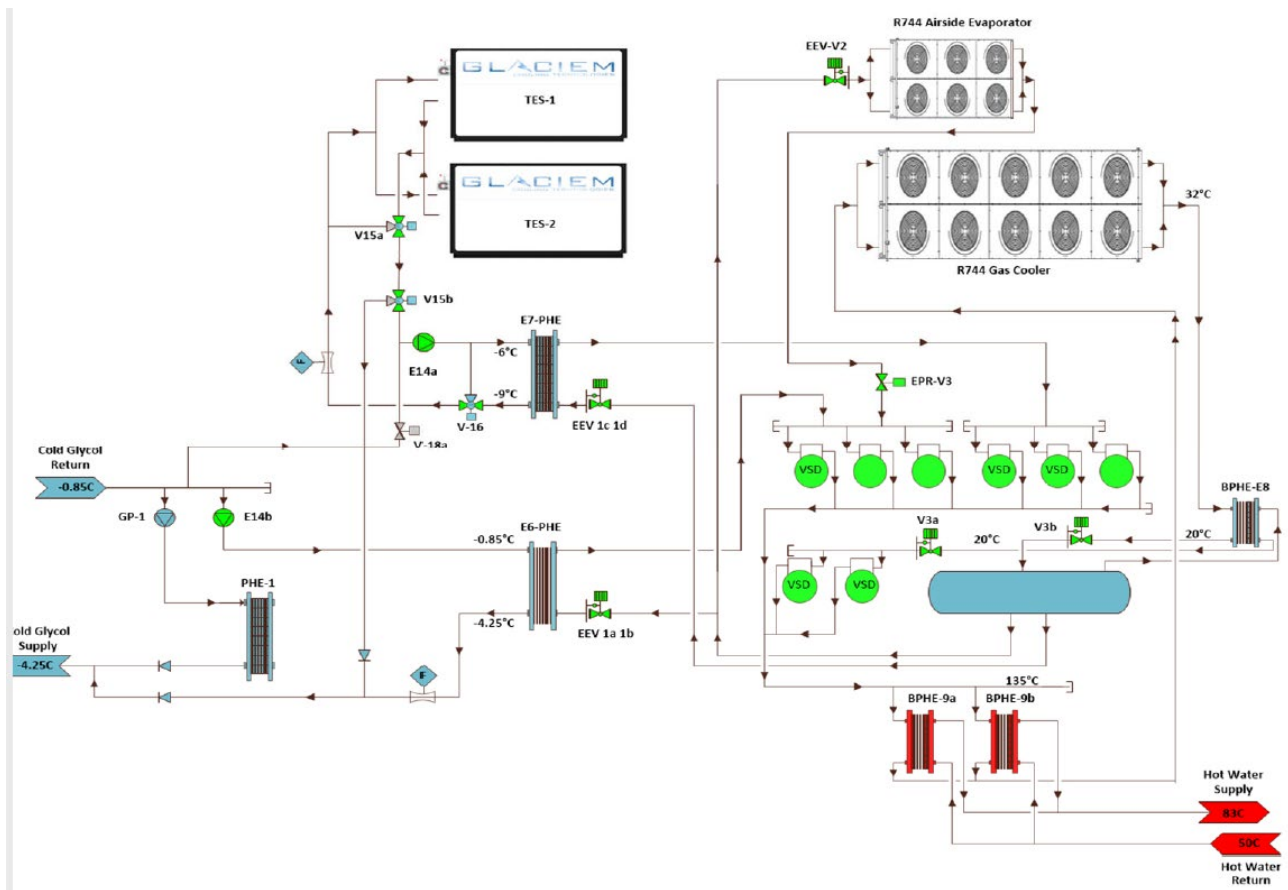


Figure 32 A piping and instrumentation diagram of the trans-critical CO<sub>2</sub> refrigeration system with TES located at an apple-packing site.

The system was designed predominantly as a heat pump. The cooling refrigeration was a secondary concept. As such the heating load was often larger than the cooling load and occurred at different times. To ensure there was always sufficient evaporator load at all times for the heat pump, the compressors were split into two groups:

Group A: 3 trans-critical compressors with designed to meet evaporator loads;

- Supply cooling to the main glycol secondary cooling loop
- Charge the PCM TES operating at -12°C (saturation suction temperature)

Group B: 3 trans-critical compressors designed with designed evaporator loads:

- Supply cooling to the main glycol secondary cooling loop
- Excess cooling load provided by a CO<sub>2</sub> airside evaporator

The system also includes 2 x Bitzer 6DTE-40K compressors running in parallel, with these compressors designed to compress the flash gas created by the trans-critical heating cycle.

All three compressor groups were connected to a common discharge allowing the heat pump to operate in several different modes depending on the hot water heating demand, the cooling load on the main glycol system and the PCM state of charge. The site also includes two TES tanks were installed with a storage capacity of 4 MWhr.

For simplification and accuracy of results the mathematical model of this system focused on the operation of the plant when only the group A parallel compressors were in use. This ensured the energy balance was maintained as there was no method for measuring any energy expelled from the airside evaporator.

#### 4.1.2.2 Results

A single day's worth of data was used to compare the monitored compressor power to the modelled power prediction. The installed CO<sub>2</sub> system is predominantly a heat pump. This classification means that the control strategy around the system is based around the desuperheater and its ability to produce hot water. The current model was not developed to be controlled as a heat pump. As such, additional information was used from the monitored data and only the refrigeration system was included in the validation. The monitored data that was used in this case was the:

- Ambient air temperature
- Ambient humidity
- Evaporator load
- Discharge pressure
- Suction pressure

System specific details such as compressors and suction groups were input into the specifications page of the model.

The model calculated the performance of the system for a typical winter day for every minute over an 8-hour period on the 1st of June 2022 (winter). Both the measured and modelled total compressor power for this period is presented in Figure 33. As can be seen, there is a strong correlation between the modelled and measured data. Although the modelled data slightly underestimates total compressor power, the overall profile of the compressor power across the day, including the various fluctuations in power, are ably captured by the model.

The same model was then modified to accept hourly averaged data from the monitored data. The results for compressor power across a week in early July 2022 is shown in Figure 34. The results show that the model is broadly capable of predicted compressor power, however there are some significant discrepancies between the model and the measured data. In particular, on 6th June the model underestimated the compressor power by approximately 55%, which is a significant underestimation. The reason for this discrepancy is because the current model is designed specifically for refrigeration only and does not use heat pumps. Nevertheless, the results for the measured and predicted compressor power over the course of a week, presented in Figure 35, show that in general, there is a strong linear correlation ( $R^2 = 0.9918$ ) between the two results, with the modelled data, on average, underestimating the compressor power by approximately 8.8% (as indicated by the gradient of the linear curve fit presented in Figure 35). The inclusion of heat pump modelling and control systems will be considered during further extensions of the tool, however, the computations required may become too taxing for many standard computers and operating systems.



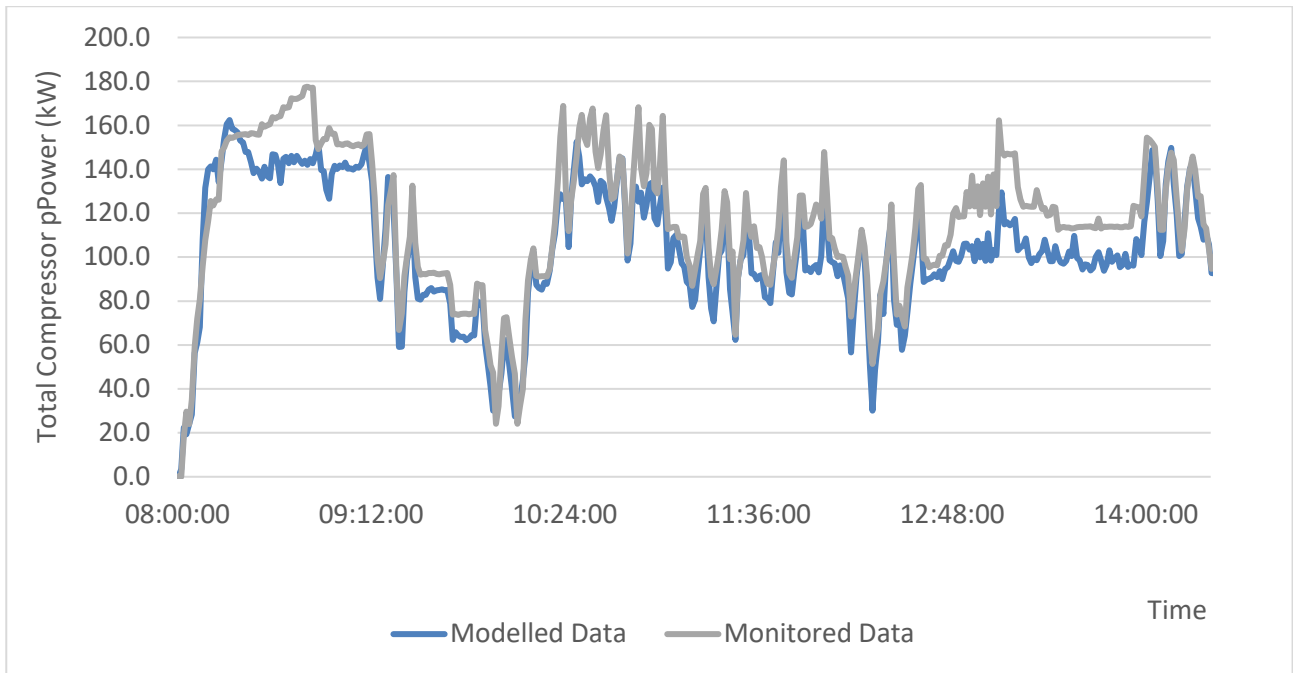


Figure 33 The measured and modelled total compressor power from the refrigeration system at the apple-packing site recorded over an 8 hour period on 01/06/2022.

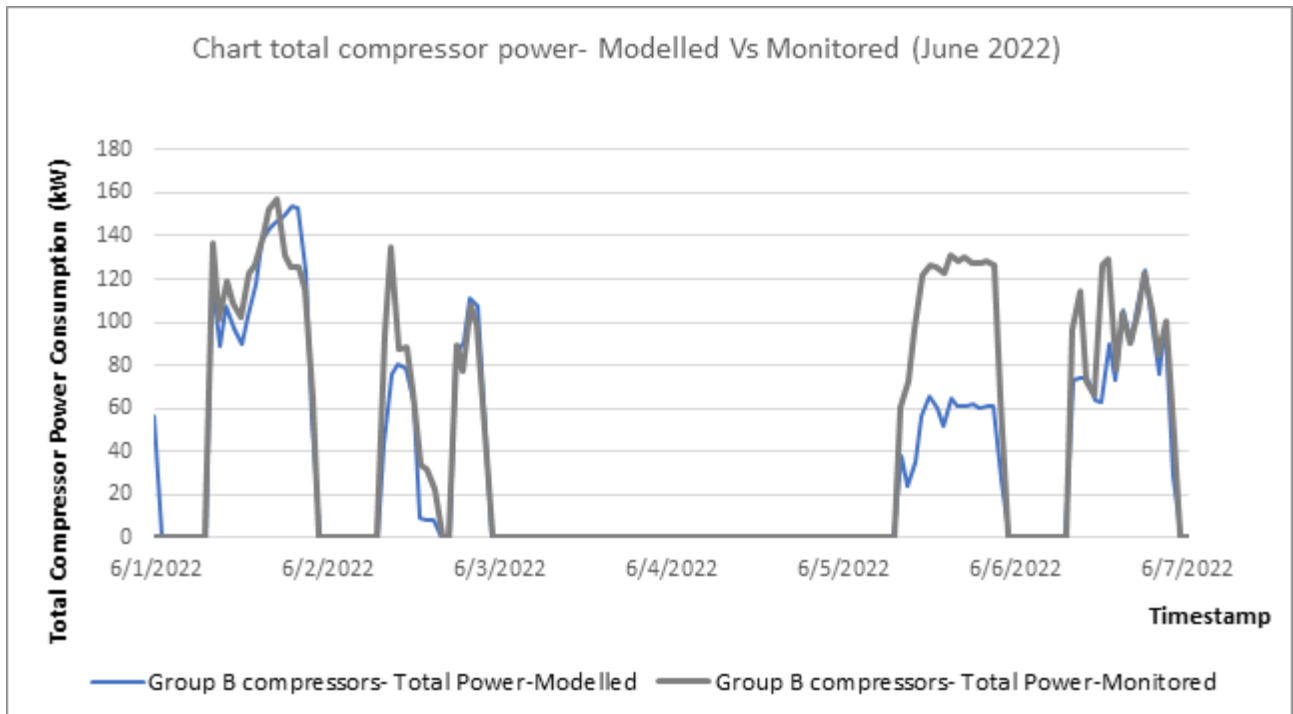


Figure 34 Comparison of monitored and modelled compressor data (hourly averages) for the first week of June 2022 for the refrigeration system at the apple-packing site.

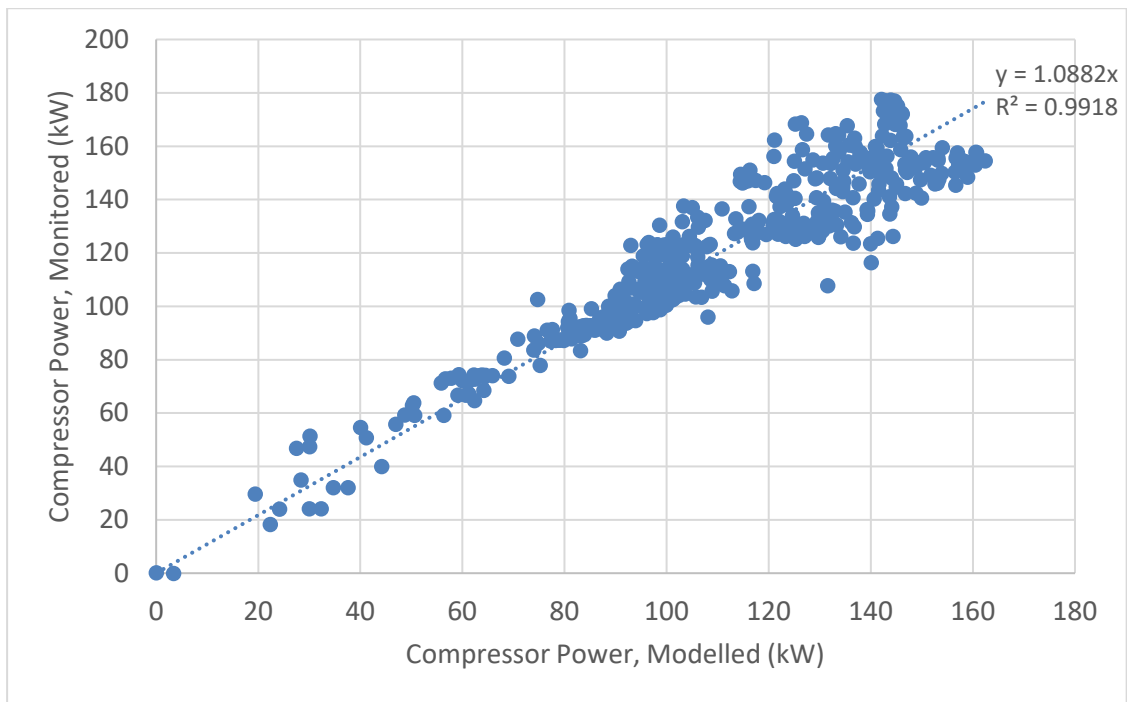


Figure 35 Modelled versus monitored total compressor power for the refrigeration system at the apple-packing site for the first week of June, 2022. Data points are hourly-averaged data. The dotted line shows a linear curve fit to the data.

## 4.2 Model for Extended Applications

The efficacy of the DP-CO<sub>2</sub> refrigeration system for different sectors was analysed by applying the model to a number of case studies informed by the IRG industry members. The case studies range across different sectors, and use different refrigeration configurations, including single and multiple suction groups, different ambient conditions, sizing and temporal cooling profiles. Case studies were based on real-world applications and data were supplied to the research team by engineers in those sectors in Australia (through the IRG). The case studies involved the modelling of the DP-CO<sub>2</sub> system in a typical operation within the following sectors:

- Kitchen cool rooms,
- Breweries,
- Abattoirs and meat processing,
- Hospital HVAC.

Note that techno-economic analyses were not included in these case studies as DP-CO<sub>2</sub> systems have only been installed in pilot systems to-date (and as such estimation of capital costs were not available) and no power-purchasing information was readily available for the different sectors analysed.

### 4.2.1 Case Study 1 – Hospital Kitchen Cool Room

The first case study analysed was for a series of kitchen cool rooms in a hospital setting in Brisbane, Australia. This was a medium-temperature (MT) refrigeration scenario where an evaporator at 2°C is used to cool separate cool rooms for dairy, fruit and vegetables, cooked food and dry food held near constant temperature in the range 3-5°C, dependent on produce type. The size of the refrigeration system is modest, with a peak refrigeration load of 14 kW<sub>t</sub>.

The refrigeration plant was located on a roof-top above the kitchen and is subjected to variations in outdoor temperature. However, the cool rooms were all located within the hospital kitchen which, in turn, is held at

approximately 22°C, resulting in no significant weather-dependent heat losses. A load profile was derived from the monitored data supplied and with the use of weather data for the location. The model was then used with the obtained weather and load data as inputs.

The monthly-averaged results across the whole year are presented in Figure 36. The orange curve represents the peak outdoor temperature, while the green and blue bars indicate monthly electricity consumption of the refrigeration system (only). The blue bar indicates the performance of the DP-CO<sub>2</sub> system determined from the model, while the green bar indicates the measured electrical data from the existing 4 packaged R134a systems.

The results show that for the summer months of December, January and February, the DP-CO<sub>2</sub> system uses 20-25% less electricity compared to the existing system. This demonstrates that the DP-CO<sub>2</sub> system can significantly reduce energy and peak demand during the peak summer months, even in the relatively humid conditions typical of Brisbane. It also demonstrates that the incorporation of the dew-point cooler to pre-cool the air to the gas cooler can reduce peak demand of the refrigeration system by up to 25%, consistent with the lab-scale results (Belusko et al., 2019).

However, in cooler winter months, despite the DP-CO<sub>2</sub> reaching a respectable maximum COP of 4.74, the results show that it remains less efficient than the existing R134a system installation, as the latter refrigerant is generally more efficient than CO<sub>2</sub>. In total, across the whole year, it was found that the energy savings realised using the DP-CO<sub>2</sub> system during the warmer months was not sufficient to offset the CO<sub>2</sub> refrigeration system's comparably lower COP during the winter months, with the total energy consumption across the whole year being approximately equal for both systems.

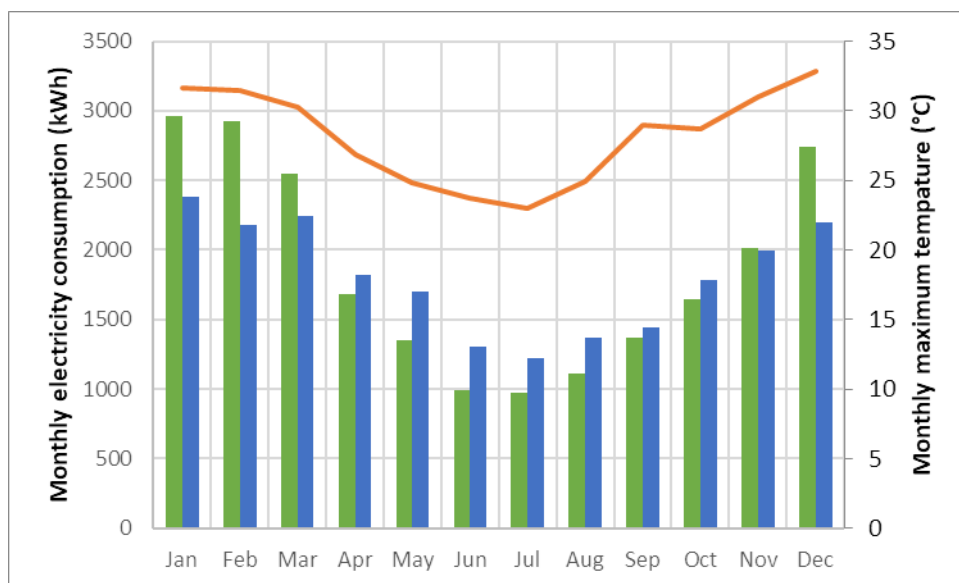
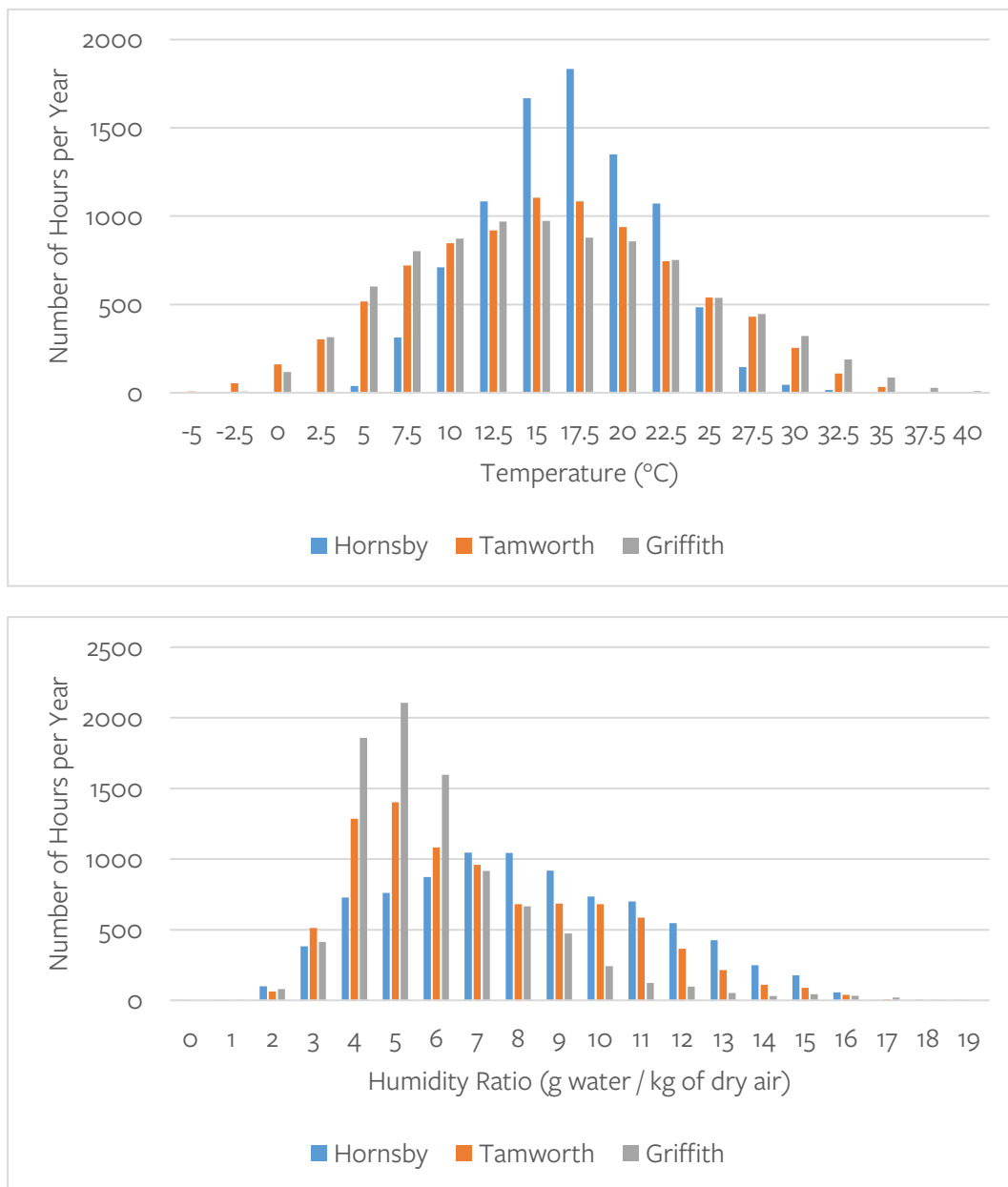


Figure 36 Monthly electricity usage (in kWh) over one year for a modelled 14 kW<sub>t</sub> DP-CO<sub>2</sub> refrigeration system (blue) compared against measurements of an existing refrigeration system (green) at the hospital location in Case Study 1. Maximum measured temperatures of each month are also shown (orange curve).

#### 4.2.2 Case Study 2 - Hospital HVAC

The second study compared similar load cases in three different regional locations and two different climate zones. The systems analysed in this case study provided chilled water for HVAC in three regional hospitals in the Australian state of New South Wales. The analysis used modelled cooling loads of real hospitals in these locations. In each case, the modelled system supplied 6°C chilled water, with a peak chiller capacity of 400 kW. In practice, it is likely that a CO<sub>2</sub> refrigeration system would be designed to provide simultaneous water heating

in such an application. However, hot water heating was not considered in this study as the focus was on the performance of the DP-CO<sub>2</sub> system.



**Figure 37** Histograms of temperature and humidity ratio measured at the three hospital locations (Hornsby, Tamworth and Griffith) in Case Study 2.

Figure 37 provides an insight into the different climates associated with the three regions considered in this case study. From the histograms, it can be seen that Hornsby has the mildest climate amongst the three considered towns, with it having the narrowest distribution of temperatures. While both Tamworth and Griffith have similar temperature profiles across the year, the former is significantly more humid than the latter, as evidenced by the larger number of hours per year where the humidity ratio is high. The result of the differing climate zones and their effect on the cooling loads and system performance can be seen in Figure 38 and Table 9. The results show that the refrigeration system in Tamworth uses significantly (up to a factor of 2 or more) energy than in Griffith and Hornsby in the warmer months, due to its more humid conditions. This highlights the sensitivity of the DP-CO<sub>2</sub> system to ambient humidity levels.

The results also show that the energy consumption of the refrigeration systems in Griffith is only slightly larger than in Hornsby, despite the former being significantly warmer than the latter. This is because the climate in

Griffith is relatively dry, which allows the DP-CO<sub>2</sub> system to work efficiently, resulting only a slight increase in energy consumption. However, by contrast, the annual water consumption in Griffith is relatively high (see Table 9), as the dew-point coolers use more water to provide cooling.

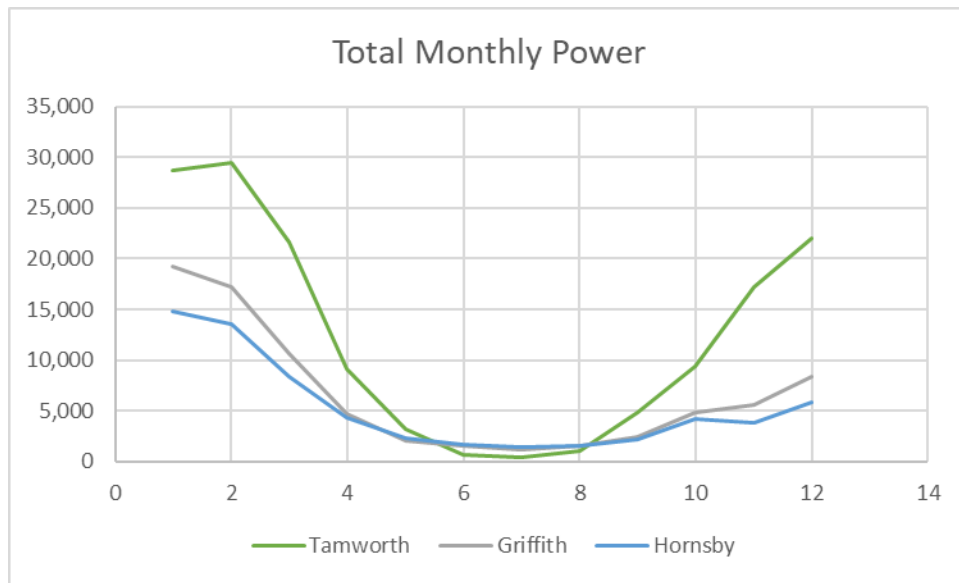


Figure 38 Mean monthly power consumption for the same DP-CO<sub>2</sub> system installed at three different hospital locations for Case Study 2.

Table 9 Comparison of annual energy and water usage for the same DP-CO<sub>2</sub> system installed at three different hospital locations for Case Study 2. Total electrical consumption of a DP-CO<sub>2</sub> is the sum of the compressor and DP cooler consumptions.

Site	Annual compressor energy (kWh <sub>E</sub> )	Annual DP-cooler energy (kWh <sub>E</sub> )	Annual water consumption (kL)
Griffith	68,000	3,000	206
Hornsby	56,000	2,000	115
Tamworth	109,000	20,000	112

#### 4.2.3 Case Study 3 - Brewery

The third case study comprises a commercial brewery located in Brisbane, Australia. The brewery operates different schedules on weekdays and weekends, in contrast to the steady cooling needs presented in Case Studies 1 and 2. As the specific brewery's refrigeration load was deemed to be too large for the application of the current DP-CO<sub>2</sub> system in its present form, the brewery cooling requirements were therefore scaled to 600 kW<sub>t</sub>. The model was again used to investigate cooling loads only, without any additional optimisation for hot water heating from the CO<sub>2</sub> system. In this case, the DP-CO<sub>2</sub> system is required to provide a cooling temperature of -8.9°C.

The results from the model shown that the DP-cooler fans consume at least 14.5% of electrical energy in any given month, up to 21% in both March (early autumn) and October (mid-spring). This contrasts with the 2.7-3.5% electrical demand of the DP-cooler fans in Case Study 1. A detailed analysis showed that in the brewery system the dew point cooler fans were required to operate for longer periods at a higher percentage of their peak design capacity.

Table 10 Brewery case study model results.

	Compressor Power (kWh)	DP Power (kWh)	Total Power (kWh)	System COP	Water Usage (kL)
Jan	64,600	14,809	79,408	2.79	200
Feb	57,203	12,058	69,261	2.78	176
Mar	69,710	18,557	88,266	2.82	236
Apr	47,223	10,146	57,368	3.17	186
May	37,423	6,324	43,747	3.37	115
Jun	31,057	5,376	36,434	3.72	90
Jul	29,361	5,158	34,519	3.91	90
Aug	33,578	6,271	39,849	3.70	118
Sep	40,785	9,533	50,318	3.51	197
Oct	53,938	13,907	67,844	3.17	219
Nov	57,155	13,694	70,849	2.96	186
Dec	63,295	15,211	78,506	2.85	217
<b>Total</b>	<b>522,031</b>	<b>131,042</b>	<b>716,369</b>		<b>2,032,422</b>

#### 4.2.4 Case Study 4 - Abattoir and Meat Processor

The final case study is a generic abattoir and meat processor plant. The thermal loads are adapted from RACE for 2030 report: Flexing industrial refrigeration (Stanley, et al., 2022). The loads were arbitrarily scaled to peak loads of 1 MW<sub>t</sub>. Such a system would be a potential replacement for meat processors currently using synthetic refrigerants. This case study offered the most complex refrigeration scenario of all the cases. The DP-CO<sub>2</sub> refrigeration systems required multiple cold process air temperatures, typically supplied by different suction groups (LT <-40°C>, MT <-12°C> and HT <-8°C>). In addition to this, the loads are highly dependent on the time of day and day of the week.

Table 11 Power consumption and water usage for a 1MW<sub>t</sub> abattoir at each capital city in Australia.

	Annual comp energy (kWh)	Annual DP- cooler energy (kWh)	DP power (% of total power)	Average COP	Annual water (kL)
Adelaide	850,000	279,000	25	3.1	3,356
Canberra	768,000	170,000	18	3.6	3,172
Brisbane	1,058,000	113,000	9.6	3.2	4,555
Darwin	1,397,000	196,000	12	2.6	5,896
Hobart	859,000	195,000	19	3.5	2,185
Melbourne	867,000	139,000	14	3.5	3,384
Sydney	972,000	151,000	13	3.2	5,000
Perth	898,000	145,000	14	3.4	5,872



There was a correlation between the efficiency of the system and the number of fans. Where more dew point coolers were used for a specific location, the dew point cooler power consumption and water consumption decreased. Increasing the number of DP-CO<sub>2</sub> units would increase overall COP, however, capital costs and complexity of the system would limit this ability in real applications.

The total energy consumption for the proposed abattoir in each Australian capital city was used to compare the performance of an alternative performance calculation method. The alternative method used weather bin hour based on the weather files in the .TMY files to predict annual performance. The bin hour method significantly reduces computational time. The faster computational calculation time allows the bin hour method to be used to produce performance charts for the whole of Australia, as shown in Figure 39. It was found that trans-critical CO<sub>2</sub> systems with adiabatic “spray type” precooling used between 4-27% more electricity over a 12-month period when compared to the proposed abattoir DP-CO<sub>2</sub> system, with the DP-CO<sub>2</sub> system showing the most significant improvement over the adiabatic spray pre-cooling systems in regions where the climate is hot and dry (e.g. central Australia). It should be noted that these values are only relevant for the abattoir case study, with different values expected for different applications.



Figure 39 The ratio of the annual energy consumption of the refrigeration system for the abattoir case study for the adiabatic spray pre-cooling system vs the DP-CO<sub>2</sub> for different regions across Australia.

## 5 Monitoring System Performance

The monitoring system of the DP-CO<sub>2</sub> system serves two main purposes. Firstly, the monitoring system collects data from the system in real life operation to substantiate the consistency and accuracy of the simulation results (i.e. model validation). Secondly, it ensures the effective operation of the DP-CO<sub>2</sub> system by capturing the state of the system, allowing sufficient system control and flagging any faults or abnormalities. These faults may include failures of pumps, fans or errors in the control system logic resulting in suboptimal operation. Since model validation typically requires significantly more data than required for system control alone, this report focusses on the performance of the monitoring system from the perspective of model validation.

The monitoring system consisted of multiple instruments measuring the key indicators of the dynamics of the processes governing the function of the system, while interfaced in a way such that the captured data can be logged, visualised, and analysed in real-time. The architecture of the monitoring system is described in Section 5.1.

### 5.1 Monitoring System Architecture

The DP-CO<sub>2</sub> refrigeration system can be divided into two sub-systems which interact with the cooling loads at one end and the outside climate at the other. The CO<sub>2</sub> refrigeration rack is the interface with the cooling loads and its function is to remove the heat through the evaporators. The indirect evaporative CO<sub>2</sub> condenser (also known as a gas cooler) is the interface with the climate. Its function is to reject the heat removed from the load to the atmosphere and its performance depends on the ambient conditions.

#### 5.1.1 The Refrigeration System

The CO<sub>2</sub> refrigeration system consists of multiple compressors operating in three different suction groups to meet the whole refrigeration requirement in a typical supermarket including freezers, cool rooms, display cases, and air conditioning. Figure 8 demonstrates a line diagram representing the refrigeration loop schematically. One key aspect of the design of the monitoring system is the identification of measurable parameters within this system which can be used to calculate the real-time cooling loads. The thermodynamic state of the system at each of the numerated points can be mapped on the pressure-enthalpy diagram as previously illustrated in Figure 27.

As shown in Figure 40 the compressor's refrigeration capacity (load) is a function of the operating condition and electrical input power. The operating conditions includes the condensing /discharge pressure, suction pressure, and superheat. All these variables as well as the electrical input power to the compressors are measurable with an acceptable accuracy.

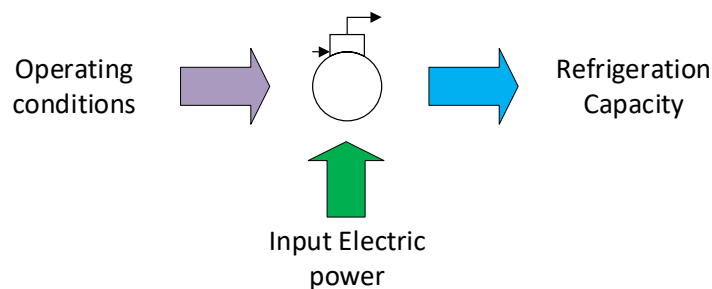


Figure 40 Compressor Model

Other ways of measuring the refrigeration load are either not feasible or extremely expensive (e.g. refrigerant flow meter on multiple load lines) as the system is not operating in a controlled environment.

### 5.1.2 Indirect evaporative CO<sub>2</sub> Condenser/ Gas cooler

The heat removed from the load through refrigeration effect is rejected to the atmosphere through the condenser in the refrigeration system. The operation of the CO<sub>2</sub> condenser integrated with the indirect evaporative cooler is a function of the Total Heat Rejection (THR) as well as the ambient condition. THR can simply be calculated as the sum of refrigeration load and the electrical input power to the compressors, Figure 41. The THR can also be determined by analysing the heat gained across the airside of the gas cooler.

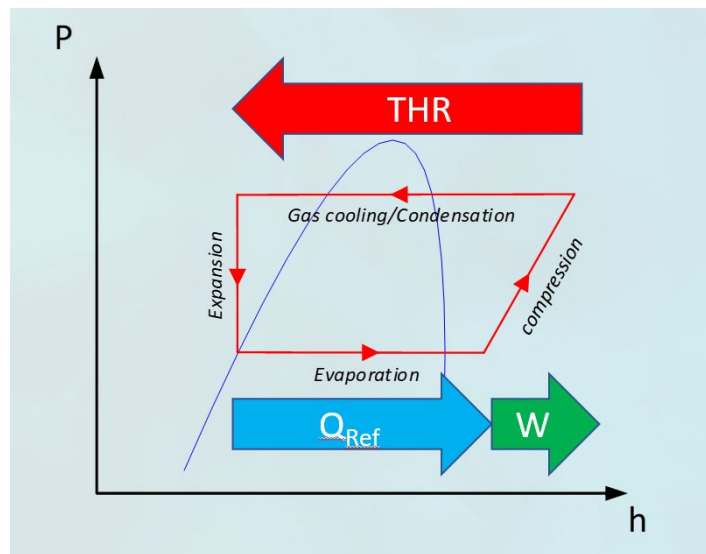


Figure 41: Refrigeration cycle- cooling energy, compressor work and total heat rejection

The function of the indirect evaporative cooler is to cool the condenser inlet air. The flow rate of air is controlled corresponding to the amount of heat to be rejected at each state of operation as well as the temperature of air cooled through the indirect pads. The cooling performance of the indirect evaporative cooler is a function of ratios between the dry and wet air channel flow rates as well as the ambient air dry-bulb temperature and humidity. A model has been developed and verified for an older generation of indirect evaporative coolers. However, in the current system, a new generation of indirect evaporative coolers is integrated with an additional step of direct cooling after the indirect pads. Therefore, the performance of the cooler should be monitored accurately to validate the new model and to ensure that the performance of the new configuration is predictable with reasonable accuracy in all conditions.

Notably, based on former tests and evaluations of the first prototype of the indirect evaporative condenser, an optimal control strategy has been engineered to govern the operation of the dew point cooler fans to maintain the condensing pressure such that the refrigeration system can operate with maximum efficiency (Belusko et al., 2019).

The new version of the indirect evaporative condenser is suitable for rejecting 120 to 150 kW of heat depending on the location and operating conditions. Based on the size of the supermarket rack at Coles, Norwood, three of these modules were required to meet the total heat rejection of the CO<sub>2</sub> system. One out of the three modules were monitored in more detail to evaluate the performance of the new design. This unit

was referred to as “the control unit” or “the control condenser/gas cooler”. Overall performance of the three units as a group was monitored to derive the efficiency of the system as a whole with sufficient instrumentation to establish the repeatability of the process across the three units.

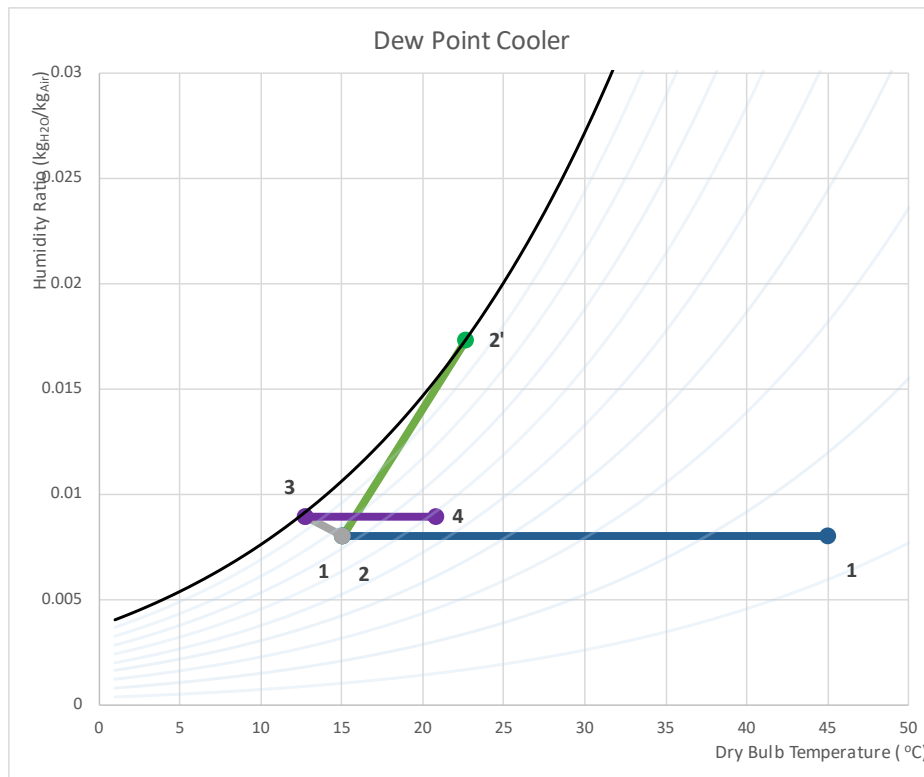


Figure 42: Psychrometric chart and process cycle for the dew point cooler

Figure 42 illustrates an example of the cooling cycle on the air through the Seeley international dew point cooler for an ambient air condition of 45°C, and a humidity ratio of 0.0075 kg<sub>h2o</sub>/kg<sub>air</sub>. There are 4 main processes in the cycle. The change in temperature and moisture content is calculated for each point in the process allowing for the calculation of energy transfer. These calculations allow for the determination of optimal running of the refrigeration. The processes are as follows:

**Process one:** 1-2, (blue) Air enters the dry side of the dew point cooler heat exchanger, cooling from ambient air temperature towards the dew point temperature. No moisture is removed from the air.

**Process two:** 2-2', (green) A portion of the air travels back along the wetted channel. This air is cooled via adiabatic cooling. As the air travels along the dew point heat exchanger, the temperature across the heat exchanger allows heat flow from the dry side to the now cooler wet side. Air exits the exhaust of the dew point cooler exhaust near saturation temperature and between the ambient temperature and the exit of the dry side of the cooler.

**Process three:** 2'-3, (grey) The remaining air from the dry side of the dew point cooler continues through an adiabatic cooler, further reducing the air temperature, tending towards the wet bulb temperature of state 2.

**Process four:** 3-4, (purple) Finally, the air from the dew point cooler is supplied to the condenser of the refrigeration system. Heat is transferred from the CO<sub>2</sub> in the condenser to the air side of the condenser. No change in moisture content occurs during this process.

## 5.2 Monitoring System Performance

### 5.2.1 Data logging

The Schneider Electrical PLC used for the data acquisition in this project is a rugged, industrial device. The device operated flawlessly throughout the monitoring period. Data was collected from the refrigeration system's pack controller and the DP-CO<sub>2</sub> PLC continuously. Had the monitoring period completed the expected 12-month period, this site would have had the most accurate, high fidelity monitored data of a supermarket site in Australia. Unfortunately, with the monitoring period being shortened to just 8 months, important periods of operating were not able to be monitored. The data that was collected was of high quality and can be used to validate the computer model developed in this study.

The use of this 10-second interval data provided great detail into the operation of the system. The detail obtained at 10s recording allows analysis of the performance of individual components and importantly, clear understanding of how major components in the system react to each other. Longer term trends could also be established by aggregating the 10s data into hourly data points.

The ability to see this data in real-time was imperative during the commissioning period where it allowed the research engineer to establish relationships between the dew point coolers and the refrigeration system that would not be possible with historical data alone.

There was a 1% loss of data which occurred as a result of the logging laptop being placed within the electrical control panel. It was assumed that the temperature within the cabinet would be satisfactory. The laptop shut itself down on 3 separate occasions before it was moved to a secure location with fresh airflow. The laptop has not shut down in the remaining period of monitoring.

Regular files transfers to a cloud operating system enabled researchers to continuously monitor long term performance trends remotely and efficiently. The cloud storage of data also provided data retention security.

### 5.2.2 Temperature, Pressure, Flow & Power Meters

All temperature sensors, pressure sensors and flow meters worked flawlessly throughout the monitoring period. The selection of these sensors was a result of 7 years' worth of development of this product between UniSA and the DP-CO<sub>2</sub> system manufacturer. With the reorganisation of the dewpoint cooler layout, it was necessary to adjust the positioning of the temperature sensors for the supply air temperature and add an additional, combined CO<sub>2</sub> gas cooler outlet temperature. It was found that radiant heat from the gas cooler affected the supply air temperature readings during periods of low airflow due to low ambient temperatures. The repositioning of this sensor and the addition of a minimum 10% fan power as adopted. The initial design of the CO<sub>2</sub> gas cooler outlet monitoring was to have one outlet temperature sensor on each of the modules and a combined CO<sub>2</sub> temperature sensor prior to the high pressure expansion valve. Due to local variabilities the average of the 3 module temperatures was found to be insufficient. Also, the distance between the gas coolers and the CO<sub>2</sub> rack was significant so the temperature sensor at the rack did not suffice either. To resolve these issues, an additional sensor was installed in a position that allowed for the measurement of the CO<sub>2</sub> after the flow from all 3 modules was allowed to mix.

### 5.2.3 24V Power Supply Failure

There was one instance of a power supply unit failure. The power supply module on one of the I/O modules on Unit 1 of the dew point coolers failed. The unit was not able to communicate with the rest of the plant. This

resulted in the unit not operating and data for that unit not being recorded. As the main PLC continued functioning, the manufacturer was able to observe the issue and have it rectified. The ability to be notified of system failure and to diagnose them before attending site is by far the greatest benefit of real time monitoring to cloud based systems.

#### 5.2.4 CO<sub>2</sub> Cycle /Load Calculation using Collected Data

The sheer number of thermal loads, freezers, fridges, air conditioning, water heating and their layout make it unfeasible to measure the actual load on the refrigeration system. For this reason, it was decided that the thermal loads on the cooling side of the system were to be calculated using computer model itself based on empirical performance data from Bitzer (the compressor manufacturer). This results in a slight decrease in accuracy of the modelling results, however, testing, and previous monitoring programs where evaporator loads have been monitored indicate that this method provides a satisfactory level of accuracy.

Figure 43 demonstrates the ability to visualise the monitored data on a pressure- enthalpy diagram. The blue lines display the base cycle parameters while the pink, grey and yellow dots show the MT compressor outlet, desuperheater outlet and gas cooler outlet conditions respectively. This clearly illustrates the operating window of the system and aids in the development of advanced control strategies.

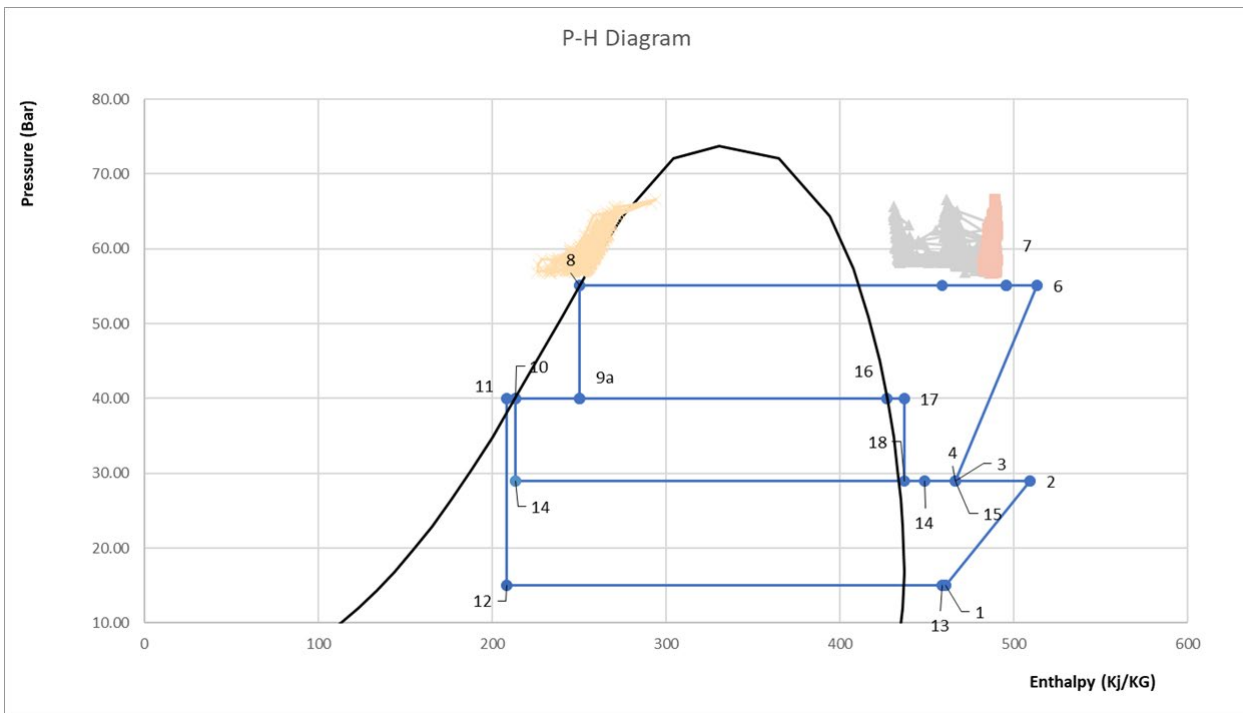


Figure 43 Visualisation of the gas cooler performance overlayed on a P-h diagram. The numbered points here refer to the locations within the DP-CO<sub>2</sub> system, as shown schematically in Figure 9.



## 6 DP-CO<sub>2</sub> System Performance

Modern Australian supermarket refrigeration systems are complex, integrated systems that can be difficult to monitor. The systems can provide cooling for over 50 separate cooling devices (fridges, freezers, display cases, air conditioning) while at the same time provide heating for “domestic” hot water. This study has monitored the refrigeration system at the Coles supermarket in Norwood, South Australia for 8 months of the year, between July 2023 and February 2024 (inclusive), providing the most detailed, monitored data for that period of any Coles supermarket. The original intention of the project was to provide full 12 months of monitoring, in addition to a detailed post-monitoring analysis, however due to the project being cut short only a preliminary analysis based on incomplete data was achievable. In any case, the data gathered provides clear evidence of the performance of the system for that period and will aid in the future development of the DP-CO<sub>2</sub> technology and can drive performance enhancements throughout all Coles sites.

### 6.1 Dew Point Cooler Efficiency

#### 6.1.1 Dew Point Effectiveness

The fundamental component of the efficacy of the DP-CO<sub>2</sub> system is the dew point cooler, and its ability to supply cool air to the gas coolers despite the warm/hot ambient conditions. An example of the dew point cooler performance for a single day is shown in Figure 44. Here the selected day is the 23<sup>rd</sup> of January, 2024, where the peak ambient conditions exceeded 40°C (red line). Despite this high temperature, the supply air to the gas coolers (the blue and black lines), was maintained below 17°C. In fact, throughout the day, the supply air temperature to the gas coolers closely followed the dew point temperature of the ambient air and was quite independent of the ambient dry-bulb temperature, as expected. This highlights the strong capability of the DP-CO<sub>2</sub> system for conditions where the ambient dew point conditions are low (i.e. conditions with low humidity), even under very high ambient dry-bulb temperatures.

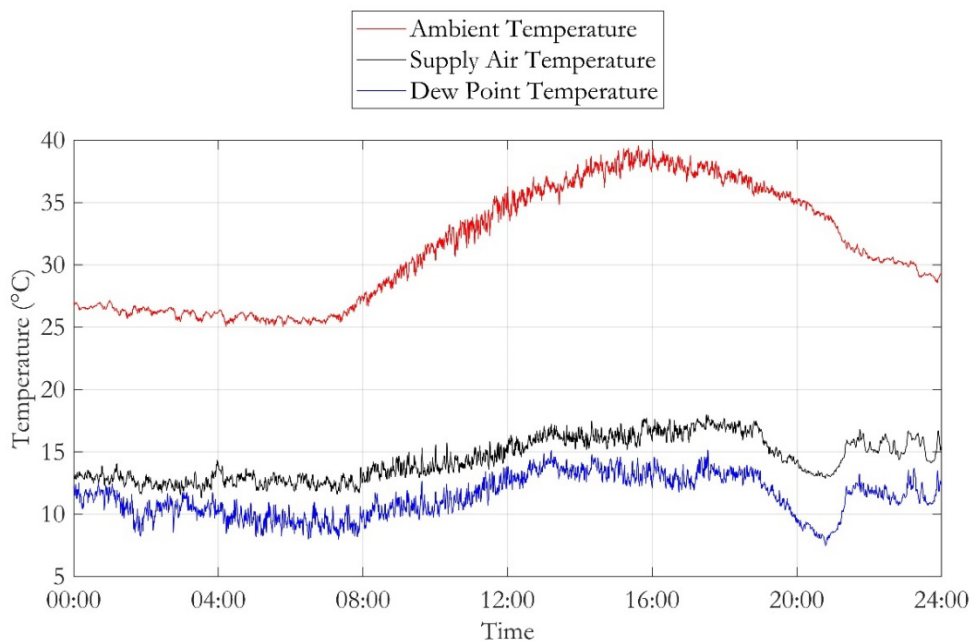


**Figure 44: Ambient and supply air temperatures for the installed system at Coles. Data was taken from the 23rd of January, 2024.**

It should also be re-iterated that there is a slight energy penalty with the operation of the dew-point coolers since the dew-point cooler fans need to operate to ensure pre-cooling. Hence, under sufficiently low ambient

conditions, it may be more efficient to turn the dew point coolers off. This is illustrated in Figure 45, which provides data for the 26<sup>th</sup> of January. In this case, the dew point coolers are turned off overnight (black line), and only turn when the ambient conditions exceeded 20°C (at approximately 11 am). It was the intention of the project to assess whether this 20°C cut-off temperature was the most optimal, however as the project was terminated early the project team did not have sufficient time to conduct this assessment.

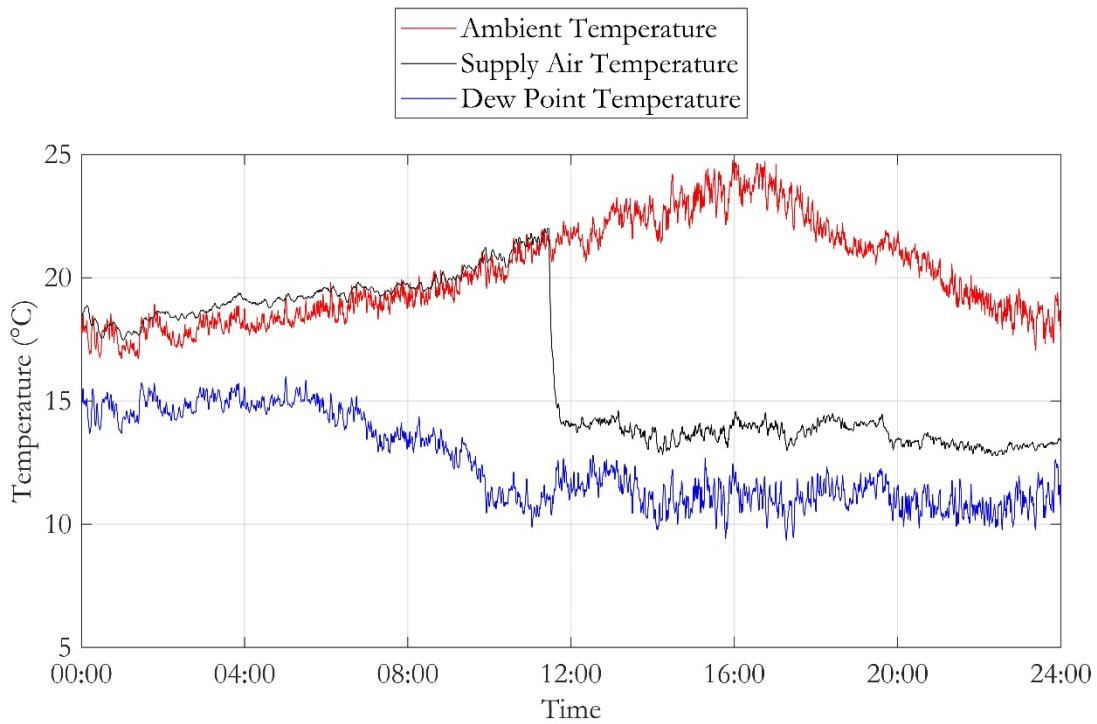


Figure 45 Air temperatures across the dew point cooler for DP-CO<sub>2</sub> system installed at Coles. Data taken from the 26<sup>th</sup> of January, 2024

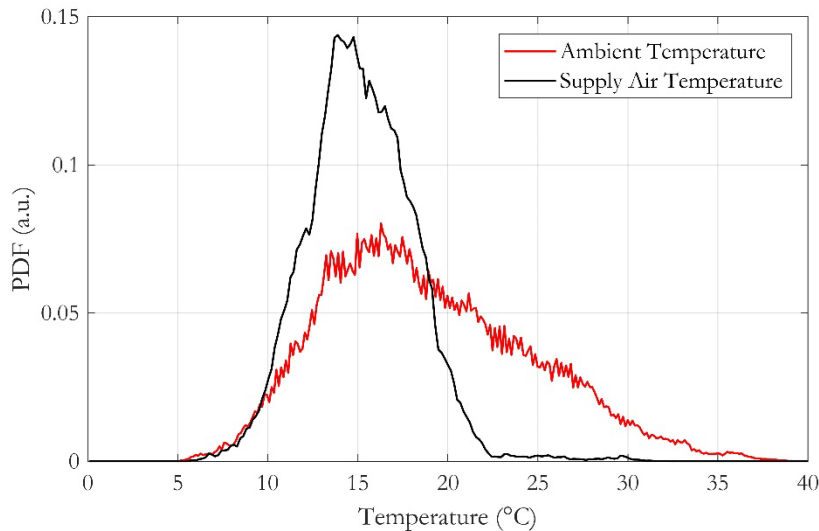
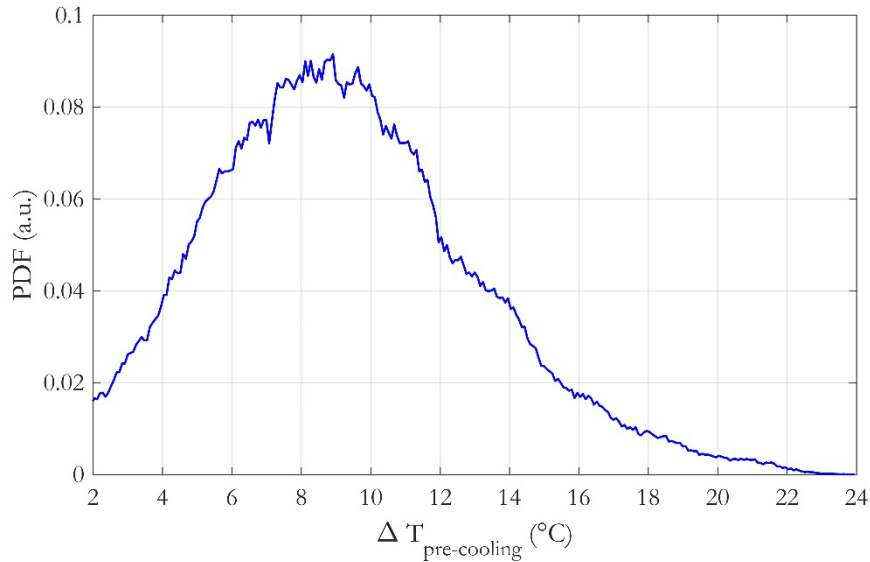


Figure 46 Probability distribution function (PDF) of the ambient and supply air temperatures. Data taken from the first 8 months of the monitoring period.

Figure 46 presents a probability distribution function (i.e. a histogram) of the ambient and supply air temperatures obtained from the monitoring data across the first 8 months of the monitoring period. As can be seen, the ambient temperatures (red line) are broadly distributed between approximately 5°C to 39°C, while the supply air temperatures to the gas cooler (i.e. the air pre-cooled by the dew point coolers) are more narrowly distributed in between approximately 5°C and 22°C. The maximum supply air temperature during

normal operation during the monitored period was 22°C, with the supply air temperatures cooled to below 20°C for 98.4% of the operating time. With a subcritical approach temperature of 6-8 °C (i.e. the temperature difference between the gas cooler CO<sub>2</sub> temperature and the supply air temperature to the gas cooler) at maximum capacity, this provides the ability for the system to run exclusively in the sub-critical mode for nearly 99% of the time.



**Figure 47** Probability distribution function of the difference between the ambient and supply air temperatures,  $\Delta T_{\text{pre-cooling}}$ . Data taken from the first 8 months of the monitoring period.

Figure 47 presents a histogram of the amount of pre-cooling done by the dew point cooler (i.e. the temperature difference between the ambient and supply air temperatures),  $\Delta T_{\text{pre-cooling}}$  for the duration of the monitoring period. Here, the data is limited to the times where the dew point cooler is turned on, noting that when the dew point cooler is turned off the supply air temperature will be equivalent to the ambient temperature (i.e. the temperature difference will be zero). The results show that the dew point coolers can produce supply air temperatures that are up to 24°C cooler than the ambient temperature, with the most common temperature difference being approximately 9°C.

### 6.1.2 Water Consumption

The monitoring system also measured the water consumption of the dew point coolers. The daily average water consumption is plotted against the daily maximum ambient temperature in Figure 48. The results show that for maximum daily ambient temperatures of 20°C or more (i.e. when the dew point coolers are turned on), the measured water consumption shows an approximate linear dependence on the ambient temperature, as expected (i.e. hotter ambient temperatures result in a greater dew point cooler water consumption). The measured slope of Figure 48 is 448 L/day/ $\Delta T$ , where  $\Delta T = T_{\text{amb}} - 20\text{°C}$ .

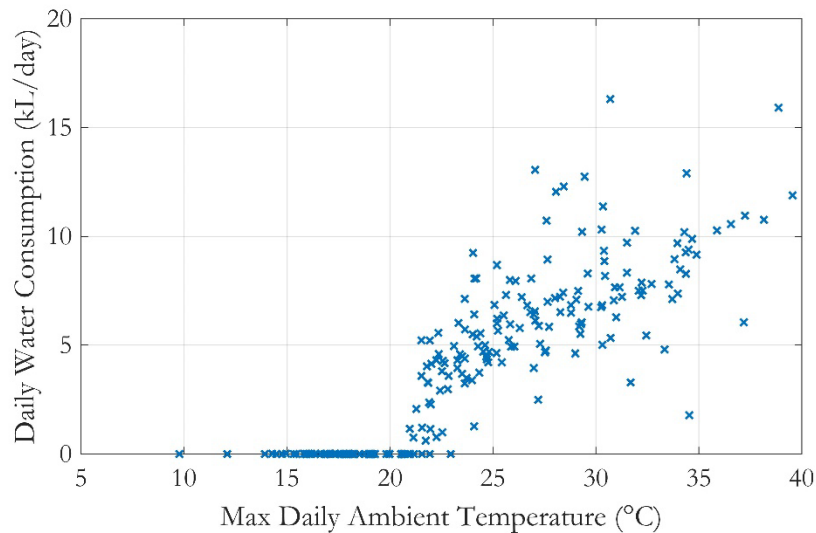


Figure 48 Daily average water consumption vs daily maximum ambient air temperature.

Across the 8 month monitoring period between July 2023 to Feb 2024, the total water consumption was 988 kL (i.e. an average of 4.07 kL per day). However, it should be iterated that the monitoring period does not include some of the warmer months, and therefore these values are expected to increase for a complete 12 month period.

## 6.2 CO<sub>2</sub> Refrigeration System Performance

The dew point cooler effectiveness directly impacts the performance of the refrigeration system by reducing the gas cooler outlet temperature. This effects the performance of the system in both sub-critical and trans-critical operation. In sub-critical operation, a lower gas cooler outlet temperature results in a reduced discharge pressure, which in turn reduces the compressor work. In trans-critical operation, where the discharge pressure may be raised to aid the performance of the production of hot water, lower gas cooler outlet temperatures can lower the vapor fraction of the receiver, which in turn increases the refrigerant mass flow to the evaporators (and therefore increases refrigeration capacity for the same amount of input work).

### 6.2.1 MT, HT Compressor Discharge Pressure

The discharge pressure of the compressors (i.e. how much the compressors have to compress the CO<sub>2</sub> refrigerant) is strongly correlated with the energy consumption of the compressors. Therefore, it is often desirable to reduce the discharge pressure where possible, particularly when the compressors operate in sub-critical mode. Figure 49 presents the correlation between supply air temperature from the dew point coolers and the compressor discharge pressure as measured from the monitoring system. As can be seen, the compressor discharge pressure increases, particular when the supply air temperatures to the gas coolers exceed approximately 15°C. This further highlights the value of the dew point coolers, as the DP coolers are able to supply air to the gas coolers below 20°C for the vast majority of the year, as previously discussed.

Additionally, the results from Figure 49 also show that for the vast majority of the time, the discharge pressure is below the critical pressure of CO<sub>2</sub>, which is 73.8 bar, allowing the refrigeration system to operate in the sub-critical mode. The discharge pressure only increases beyond the critical pressure when the supply air temperature is above approximately 24°C. That is, to ensure sub-critical operation, the dew point cooler needs to cool the ambient air to below 24°C, regardless of ambient conditions. As the lower limit of the supply air temperature is the dew point temperature of the ambient air (see also Figure 45), the DP-CO<sub>2</sub> system operates

best when the ambient dew point temperature does not exceed approximately 24°C. That is, the DP-CO<sub>2</sub> system would likely not be suitable for hot, humid climates where the dew point temperature regularly exceeds 24°C.

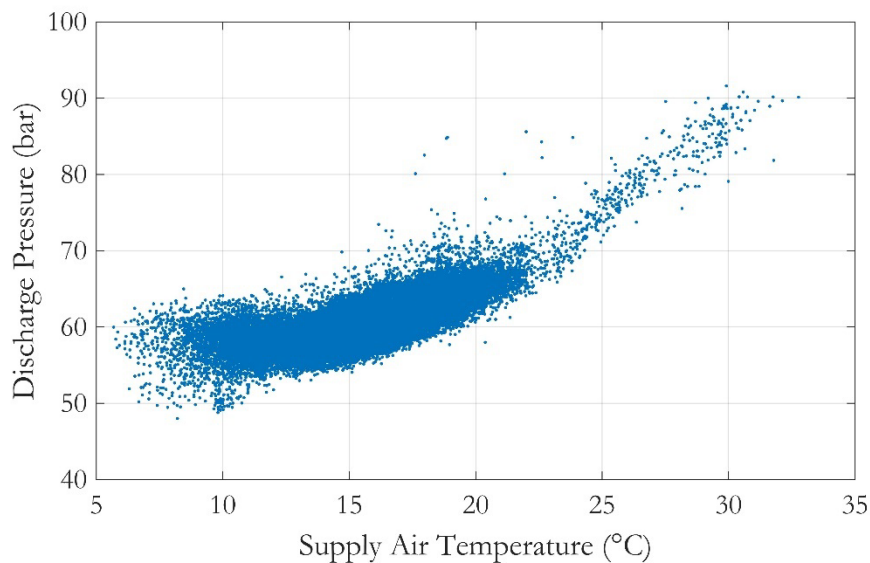


Figure 49 Measured discharge pressure vs supply air temperature for the installed DP-CO<sub>2</sub> system at Coles.

## 6.2.2 Flash Gas Bypass Vs Parallel Compression

In the present Coles refrigeration system, the CO<sub>2</sub> refrigerant leaving the gas coolers is cooled as it expands through the high pressure expansion valve (Figure 9– state 9). The expanded refrigerant, which is a mixture of liquid (Figure 9- state 10) and vapour (Figure 9– state 16), is collected in the receiver. While the liquid is used to produce useful cooling (e.g. for the LT and MT indoor freezer and fridge units), the installed refrigeration system at Coles allows for two options for the treatment of the vapour:

- 1) Flash gas bypass - Vapour is taken from the top of the receiver, travels through an expansion valve and is mixed with the vapour leaving the MT and LT evaporators (Figure 9- state 18). The mixed gasses are compressed by the MT compressors.
- 2) Parallel compression – Vapour from the receiver is fed directly to a HT compressor (Figure 9- state 19).

Parallel compression can improve the efficiency of the system by re-compressing the vapour from the receiver at a lower compression ratio than is possible with a flash gas cycle. At low discharge pressures, the volume of vapor in the receiver may be significant low enough such that it is more efficient to maintain a stable receiver pressure with the MT compressors and flash gas bypass than to cycle the HT compressors on and off.

With the addition of the dew point coolers, it was found that the vapour fraction in the receiver remained small enough for much of the monitored period and as such the system remained in flash gas bypass mode for much of the time. In an effort to quantify the performance gain operating in parallel compression, the changeover point was lowered from 50% to 40% (vapour fraction). It was noted that the compressor staging was not able to maintain receiver pressure. On investigation, it was found that the fixed frequency HT compressors were oversized for the loads associated with the DP-CO<sub>2</sub> system. As soon as the HT compressors were engaged, the receiver pressure dropped, and the system reverted back to flash gas bypass mode. Further

analysis is needed; however, the preliminary findings here suggests that the oversizing of the HT compressors, and the lack of a smaller “low-load” HT compressor has limited the ability of the refrigeration system to be more efficient. The compressors in this study were designed for systems that predominantly operate in trans-critical mode during high ambient conditions. Future designs of the refrigeration system can incorporate the DP-CO<sub>2</sub> systems ability to operate almost entirely in a sub-critical manner.

### 6.2.3 Energy and Water Comparison

The monitoring program was shortened from 12 months to 8 months, due to the early termination of the project. To estimate the energy saving and water usage for the full 12 months, monitored data was compared to the DP-CO<sub>2</sub> model developed for this study (see Section 3) where available. Figure 50 and Figure 51 compare the total energy and water consumption of the DP-CO<sub>2</sub> system predicted by the model relative to the monitored data. As can be seen, based on the available data, the model was able to predict the total system power to within 7%. Discrepancies in the calculation are likely to:

- The inherent assumptions and simplifications of the model, which was not designed to predict every single detail of all the components of the DP-CO<sub>2</sub> system (e.g. piping losses, inaccuracies in manufacturers data, electrical losses under part-load operation, etc.)
- The model did not include the “live” switch-over between flash gas bypass to parallel compression modes
- Inaccuracies in the estimated refrigeration load, with only simplified load values provided by Coles.

Notable discrepancies between the model and the monitored data include:

- 1) A significant underestimation of the water consumption data between September and December 2023. This was due to the implementation of an incorrect algorithm in the dew point cooling PLC, which did not account for the hysteresis on the dew point cooler activation temperature. It was observed that the dew point cooler would initiate, fill its buffer tank and start cooling. The air exiting the dew point cooler then would become sufficiently cold such that it would affect the ambient temperature, which in turn caused the dew point cooler to turn off and dump the water in the buffer tank. This process would repeat, resulting in a large, and unnecessary, water consumption in the real system. This was rectified in December 2023, and by Jan 2024 the water consumption of the real system matched more closely the modelled data;
- 2) The model underestimates the power consumption between July and Nov 2023. This was a result of the approach temperature difference between the supply air temperature and the gas cooler outlet being set too small (in the actual system). As a result, the dew point cooler started to activate more often in this period. This resulted in a large increase in fan power for a relatively small increase in air flow rate to the gas cooler. To address this, the approach temperature difference was increased in December 2023.

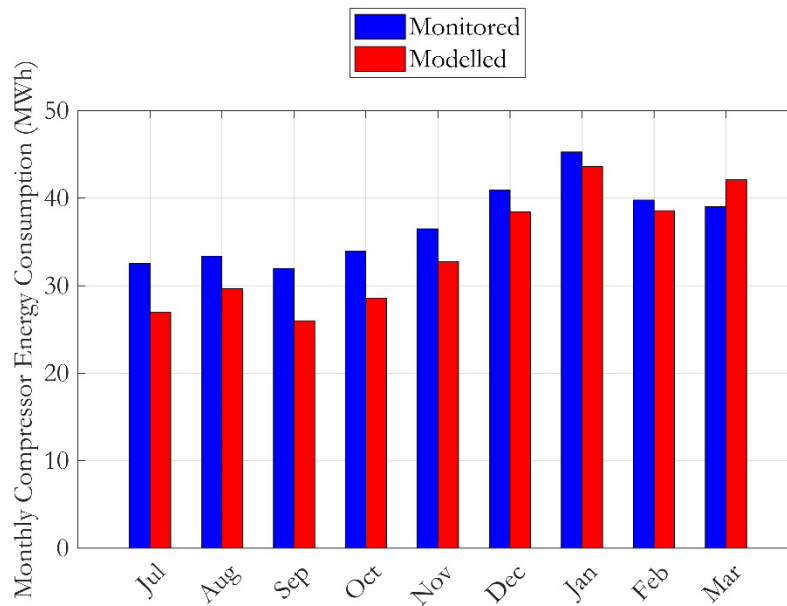


Figure 50 Modelled vs monitored electrical consumption for the Coles DP-CO<sub>2</sub> refrigeration system.

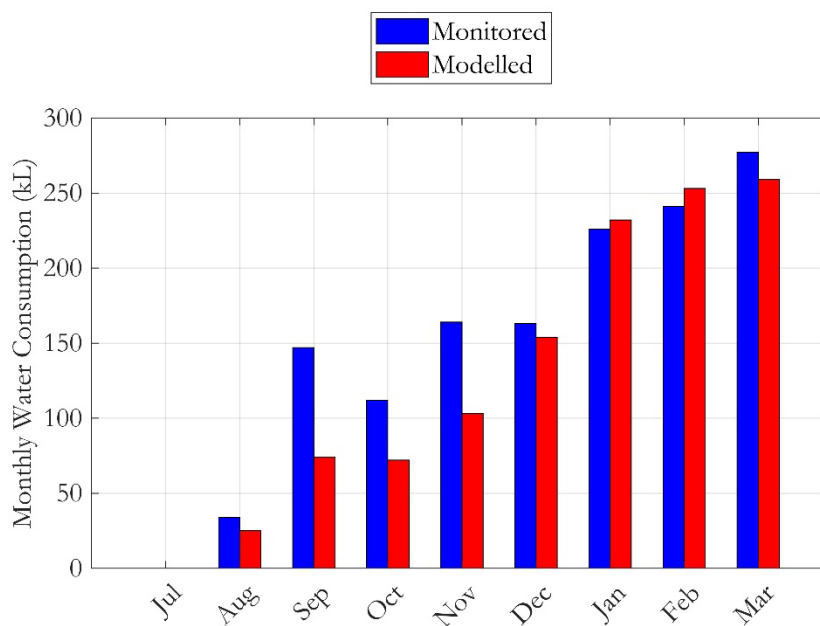


Figure 51: Modelled vs monitored monthly water consumption for the Coles DP-CO<sub>2</sub> refrigeration system

Nevertheless, as previously noted, the computational model of the Coles DP-CO<sub>2</sub> system is able to predict with reasonable accuracy the overall (total) power consumption across all measured months (including both winter, summer and shoulder seasons), providing confidence in the model.

The confirmation that the computer is able to reliably estimate the potential energy savings allows it to be used to compare the performance of the DP-CO<sub>2</sub> technology over a trans-critical CO<sub>2</sub> rack with misting style, adiabatic cooling that would be typically installed in a new build, Australian supermarket. The results of the total energy consumption of both systems applied to the current Coles conditions is shown in Figure 52.



The results show that the DP-CO<sub>2</sub> system significantly reduces refrigeration energy consumption, particularly in the warmer summer and shoulder seasons. The model estimates that the DP-CO<sub>2</sub> system reduces total refrigeration electricity consumption by 19.6% across the whole year compared to a typical adiabatic cooling system.

It should be noted that the values above are specifically for the Adelaide climate, and for the Coles refrigeration system configuration. The magnitude of reduction will depend on the specific system and the local climate. Nevertheless, these results clearly demonstrate, using a combination of monitored data under real conditions and high fidelity computational modelling, that a significant amount of electricity savings (and hence, reduction of CO<sub>2</sub> emissions) can be realised through the employment of DP-CO<sub>2</sub> systems over traditional adiabatically-cooled CO<sub>2</sub> refrigeration systems.

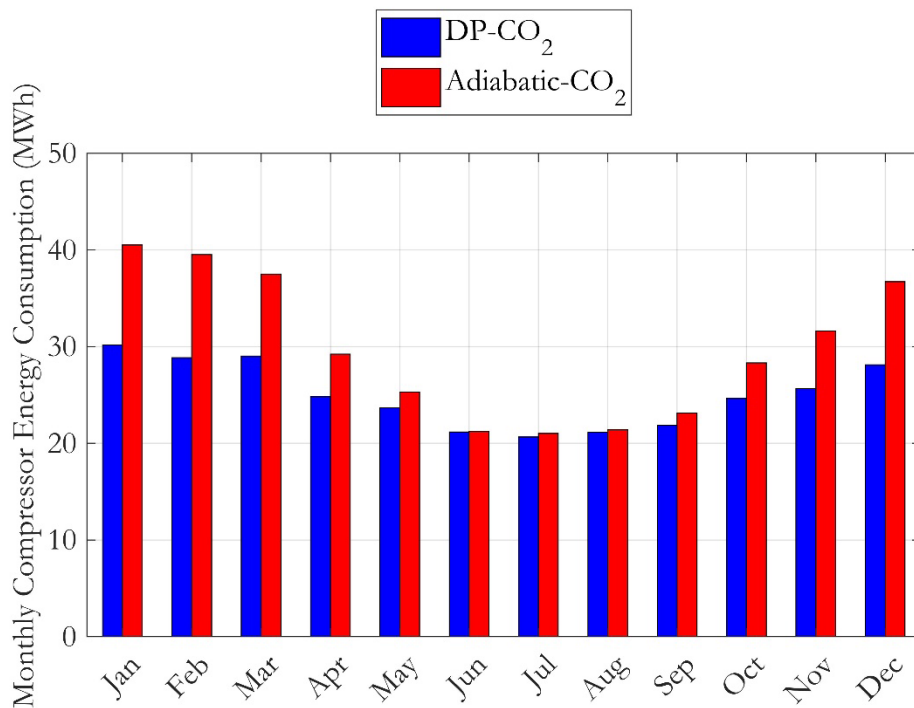


Figure 52 Modelled monthly energy consumption for DP-CO<sub>2</sub> and adiabatically-cooled CO<sub>2</sub> systems. The values here are for the current Coles system, under Adelaide weather conditions.

## 7 Conclusion

A novel dew point CO<sub>2</sub> refrigeration system that was actively monitored with 115 sensors was successfully deployed at a Coles supermarket in Adelaide, South Australia. The system has been monitored on a minute-by-minute basis right from the store opening date, which was the 21<sup>st</sup> of June, 2023. Concurrently, a detailed computational model of the DP-CO<sub>2</sub> system which integrates sub-models of both the dew point coolers and the CO<sub>2</sub> refrigeration system that is capable of modelling all the key parameters of the monitored system on an hourly basis has also been successfully developed and validated with existing data.

The results for the monitoring system during the 8 month monitoring period between July 2023 and February 2024 (inclusive) show that the dew point coolers are able to supply air temperatures that are up to 24°C cooler than the ambient air temperature, even when peak ambient conditions exceeded 40°C. The ambient temperatures were found to be broadly distributed between 5°C and 40°C, while the pre-cooled air supplied to the gas coolers were more narrowly distributed between 5°C and 22 °C. The maximum supply air temperature was found to be 22°C, with the supply air temperature found to be below 20°C for 98.4% of the time. This enables the CO<sub>2</sub> system to operate exclusively in the (more efficient) sub-critical mode for nearly 99% of the time. Importantly, the dew point coolers were found to pre-cool the ambient air to close to the ambient dew point temperature, which implies that the DP-CO<sub>2</sub> system is most effective in regions where the dew point temperatures (humidity) are low (regardless of the ambient dry bulb temperature).

The results also show that the installed DP-CO<sub>2</sub> system used a total of 988 kL of water during the 8 month monitoring period, at an average of 4.07 kL per day. During the same period, the DP-CO<sub>2</sub> system used 42.4 MWh to operate the dew point cooler fans (an average of 174.7 kWh per day), and 290.9 MWh to operate the CO<sub>2</sub> compressors (an average of 1,197 kWh per day).

The results from the model using a typical meteorological year (noting that a full year of monitored weather was not available) for Adelaide show that the DP-CO<sub>2</sub> system reduces total refrigeration electricity consumption by 19.6% across the whole year compared to an adiabatic CO<sub>2</sub> refrigeration system. The magnitude of improvement is more noticeable in the warmer months, with the DP-CO<sub>2</sub> system showing a 37% improvement in energy consumption compared to an equivalent adiabatically cooled system during summer. These improvements are despite the DP-CO<sub>2</sub> system consuming more fan energy, i.e., the reduction in compressor energy by the DP-CO<sub>2</sub> system is more than sufficient to offset the increase in the fan energy.

The model of the DP-CO<sub>2</sub> system was also applied to a number of desktop case studies in non-supermarket sectors in climates that are different to Adelaide. In particular, in a typical hospital kitchen room in Brisbane utilising package R134a refrigeration units, it was found that the DP-CO<sub>2</sub> was able to reduce cooling energy consumption by 20-25% during the summer months between December and February. However, the DP-CO<sub>2</sub> refrigeration system was less efficient than conventional R134a refrigeration systems during winter, such that the energy consumption of both systems across the whole year were approximately equal.

The model of the DP-CO<sub>2</sub> system was also applied to a representative abattoir across multiple climate zones across Australia. The results of the model show that the DP-CO<sub>2</sub> system was between 4-27% more efficient than adiabatically cooled CO<sub>2</sub> refrigeration systems, with the DP-CO<sub>2</sub> system showing most significant efficiency improvements in regions with dry climates, such as central and western Australia. However, even in cool and humid regions, such as Tasmania, the DP-CO<sub>2</sub> system was found to be at least 4% more efficient than adiabatic CO<sub>2</sub> systems.

In summary, it has been demonstrated that the installed DP-CO<sub>2</sub> system is capable of significantly pre-cooling the ambient air, resulting in the CO<sub>2</sub> refrigeration system operating in the more efficient sub-critical mode for the vast majority of the year, even when ambient temperatures may exceed 40°C. The resultant efficiency gains relative to conventional adiabatically cooled CO<sub>2</sub> refrigeration systems is approximately 20% across the whole year, even after taking into account the increased fan energy of the dew point coolers. These values are specifically for the DP-CO<sub>2</sub> system installed in Adelaide, but similar results are expected for regions where the dew point temperatures are typically low (e.g. hot, dry climates). Further improvements in energy efficiency may be possible, but further work and analysis of the measurements from the monitored system across a full 12 months will be required.

## References

- Bellos, E., Tzivanidis, C., 2019. A comparative study of CO<sub>2</sub> refrigeration systems. *Energy Conversion and Management*: X 1, 100002. <https://doi.org/10.1016/j.ecmx.2018.100002>
- Belusko, M., Liddle, R., Alemu, A., Halawa, E., Bruno, F., 2019. Performance Evaluation of a CO<sub>2</sub> Refrigeration System Enhanced with a Dew Point Cooler. *Energies* 12, 1079. <https://doi.org/10.3390/en12061079>
- Brodribb, P., McCann, M., 2018. Cold hard facts 3. Canberra.
- Denham, T., Xing, K., Dodson, J., Pears, A., Agrawal, H., Azar, B., Hossain, J., Indraswari, K., Katic, M., Liu, M., Rajakaruna, S., Shawon, M., Shi, L., Susilawati, C., 2021. Transforming energy productivity through value chains. Final report of the opportunity assessment for research theme B1. RACE for 2030 CRC.
- Ge, Y.T., Tassou, S.A., 2014. Control optimizations for heat recovery from CO<sub>2</sub> refrigeration systems in supermarket. *Energy Conversion and Management* 78, 245–252. <https://doi.org/10.1016/j.enconman.2013.10.071>
- Lau, T., Alemu, A., Bruno, F., Evans, M., Gilbert, R., Hadian, D., Hudson, J., Leak, J., Leonardis, C., Liddle, R., Liu, A., Rainey, T., Semsarilar, H., Xing, K., 2022a. Testing and monitoring of an energy efficient indirect evaporative CO<sub>2</sub> refrigeration system at a Coles supermarket: Milestone Report I. B1 for RACE for 2030.
- Lau, T., Alemu, A., Bruno, F., Evans, M., Gilbert, R., Hadian, D., Hudson, J., Leak, J., Leonardis, C., Liddle, R., Liu, A., Rainey, T., Semsarilar, H., Xing, K., 2022b. Testing and monitoring of an energy efficient indirect evaporative CO<sub>2</sub> refrigeration system at a Coles supermarket: Milestone Report II. B1 for RACE for 2030.
- Lau, T., Alemu, A., Bruno, F., Evans, M., Gilbert, R., Hudson, J., Leak, J., Leonardis, C., Liddle, R., Rainey, T., Semsarilar, H., Taghipour, A., Xing, K., 2022c. Testing and monitoring of an energy efficient indirect evaporative CO<sub>2</sub> refrigeration system at a Coles supermarket: Milestone Report III. B1 for RACE for 2030.
- Lau, T., Bruno, F., Evans, M., Gilbert, R., Leak, J., Leonardis, C., Liddle, R., Rainey, T., Taghipour, A., Xing, K., 2023. Testing and monitoring of an energy efficient indirect evaporative CO<sub>2</sub> refrigeration system at a Coles supermarket: Progress Report IV. B1 for RACE for 2030.
- Lecamwasam, L., Wilson, J., Chokolich, D., 2012. Guide to Best Practice & Maintenance & Operation of HVAC Systems for Energy Efficiency. Commonwealth of Australia.
- Li, D., Groll, E.A., 2005. Transcritical CO<sub>2</sub> refrigeration cycle with ejector-expansion device. *International Journal of Refrigeration* 28, 766–773. <https://doi.org/10.1016/j.ijrefrig.2004.10.008>
- Mahmood, M.H., Sultan, M., Miyazaki, T., Koyama, S., Maisotsenko, V.S., 2016. Overview of the Maisotsenko cycle – A way towards dew point evaporative cooling. *Renewable and Sustainable Energy Reviews* 66, 537–555. <https://doi.org/10.1016/j.rser.2016.08.022>
- Sarkar, J., Agrawal, N., 2010. Performance optimization of transcritical CO<sub>2</sub> cycle with parallel compression economization. *International Journal of Thermal Sciences* 49, 838–843. <https://doi.org/10.1016/j.ijthermalsci.2009.12.001>
- Span, R., Wagner, W., 1996. A New Equation of State for Carbon Dioxide Covering the Fluid Region from the Triple-Point Temperature to 1100 K at Pressures up to 800 MPa. *Journal of Physical and Chemical Reference Data* 25, 1509–1596. <https://doi.org/10.1063/1.555991>

Wang, J., Belusko, M., Semsarilar, H., Evans, M., Liu, M., Bruno, F., 2022. An optimisation study on a real-world transcritical CO<sub>2</sub> heat pump system with a flash gas bypass. *Energy Conversion and Management* 251, 114995. <https://doi.org/10.1016/j.enconman.2021.114995>

# Appendix A: Piping and Instrumentation Diagrams (P & ID) of the DP-CO<sub>2</sub> system

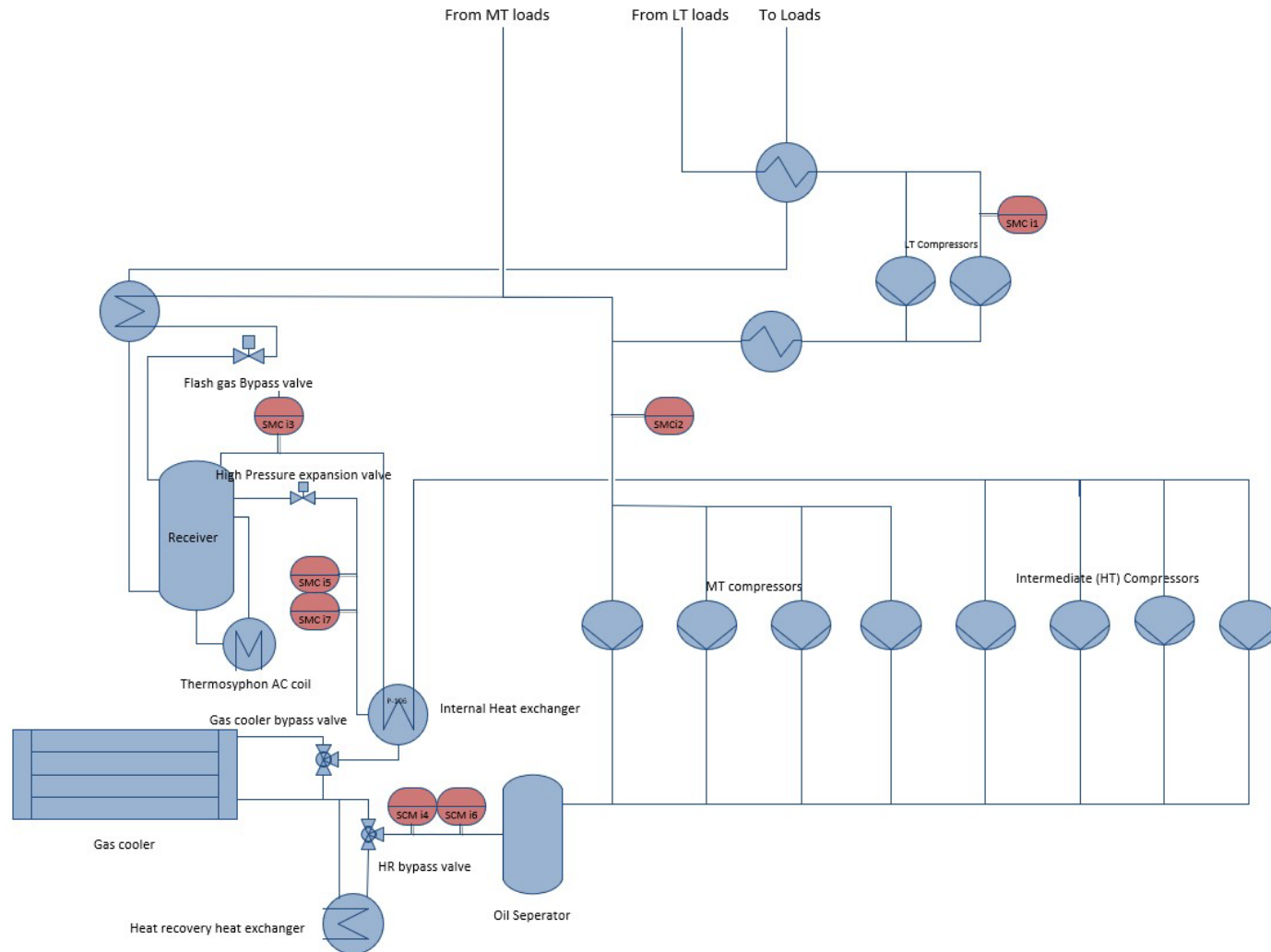


Figure 53: Piping and instrumentation (P & ID) diagram of the proposed Coles DP-CO<sub>2</sub> refrigeration system

From Refrigeration System

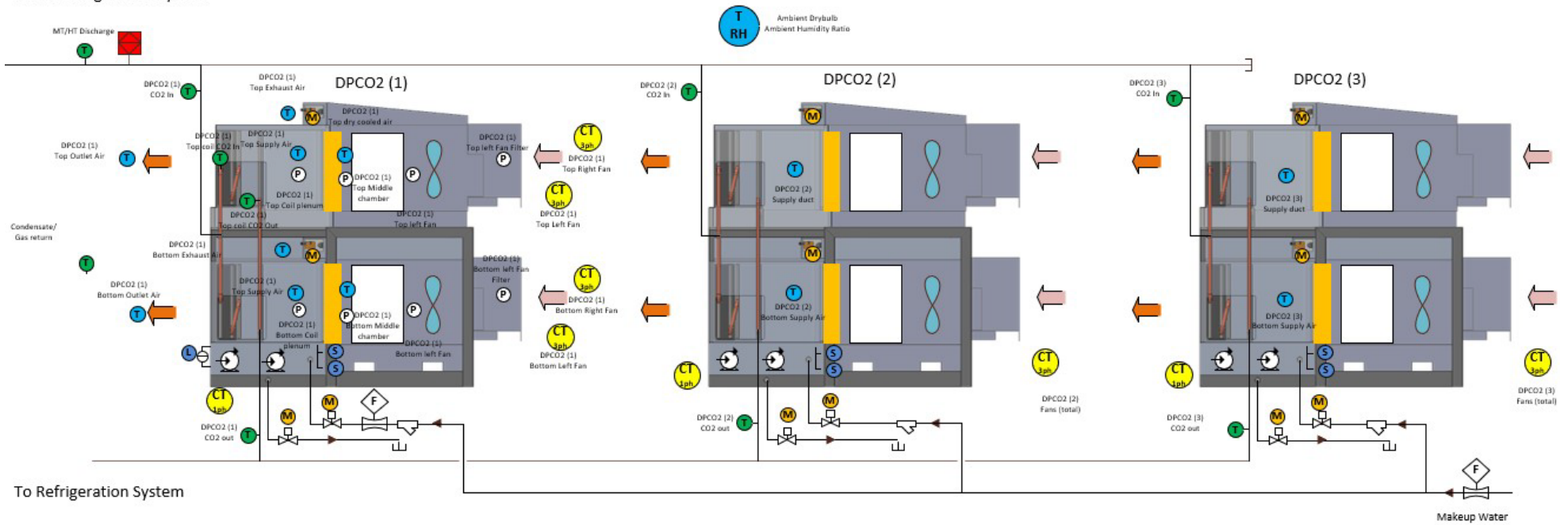


Figure 54: Piping and instrumentation diagram of the condensers and dew-point cooling units



## Appendix B: DP-CO<sub>2</sub> Monitoring Equipment Schedule

Table 12: Schedule of monitoring equipment for the proposed DP-CO<sub>2</sub> system

### Equipment List

Unit	Description	Manufacturer	Model Number	Signal	Total Qty	Default/ Model verification
1,2,3	CW H15 S Plus Fan	EBP Papst	R3G560-RA24-03	0-10V	12	Default
1,2,4	Pump (Direct pads)	Grundfoss	Unilift KP150	On/Off	3	Default
1,2,5	Pump (Indirect pads)	Grundfoss	Unilift KP150	On/Off	6	Default

### Valve List

Unit	Description	Manufacturer	Model Number	Signal	Total Qty	Default/ Model verification
1,2,3	Gas cooler water makeup solenoid valve	Process Solutions	PS B35M-4-14-1N (Brass, Seal: NBR Manual Override Pressure 0.3-16 Bar Normally Closed)	On/Off	3	Default
1,2,3	Gas cooler water Drain solenoid valve	Process Solutions	PS ES56-6-25-1N (Pressure 0-5 bar Normally Open)	On/Off	3	Default
1,2,3	Damper actuator	Belimo	Modulating actuators (0-10) 5 Nm 24V AC	0-10V	6	Default
CO <sub>2</sub> Rack	HPEV bypass valve	Refrigera, Belimo	Ball valve actuator	0-10V	1	Default

CO <sub>2</sub> Rack	Gas cooler bypass valve	Refrigera, Belimo	Ball valve actuator	0-10V	1	Default
CO <sub>2</sub> Rack	Flash gas bypass valve	Refrigera, Belimo	Ball valve actuator	0-10V	1	Default
CO <sub>2</sub> Rack	Desuperheater hot water inlet temp	Danfoss compatible	Pt100	0-10V	1	Default
CO <sub>2</sub> Rack	Desuperheater hot water outlet temp	Danfoss compatible	Pt100	0-10V	1	Default
CO <sub>2</sub> Rack	Rack Target Discharge Pressure	Danfoss Variable	-	0-10V	1	Default
CO <sub>2</sub> Rack	Rack Target gas cooler outlet temperature	Danfoss Variable	-	0-10V	1	Default

#### Instrument List

Unit	Description	Manufacturer	Model Number	Signal	Total Qty	Default/ Model verification
site inst.	Main CO <sub>2</sub> discharge Temp.	IFM	TS4759	PT100	1	Default
site inst.	Main CO <sub>2</sub> Gas return Temp.	IFM	TS4759	PT100	1	Default
1	CO <sub>2</sub> outlet Temp.	IFM	TS4759	PT100	1	Model Ver.
2	CO <sub>2</sub> outlet Temp.	IFM	TS4759	PT100	1	Model Ver.
3	CO <sub>2</sub> outlet Temp.	IFM	TS4759	PT100	1	Model Ver.
1,2,3	PT100/1000 Signal Convertor	IFM	TP3231	4-20mA	8	Model Ver.
1,2,3	Temp. Probe Cable & Socket	IFM	EVT001	N/A	8	Model Ver.
1,2,3	Variable Plug	IFM	EVC816	N/A	8	Model Ver.
1	Unit 1 top coil CO <sub>2</sub> inlet Temp.	IFM	TA2537	4-20mA	1	Model Ver.

1	Unit 1 top coil CO <sub>2</sub> outlet Temp.	IFM	TA2537	4-20mA	1	Model Ver.
1	Welding thermowell for Temp. sensors	IFM	E37421	N/A	2	Model Ver.
1	Temp. Probe Cable & Socket	IFM	EVT001	N/A	2	Model Ver.
1	CO <sub>2</sub> Discharge Pressure Transducer 0-250bar	IFM	PT5501	4-20mA	1	Default
site inst.	Pressure Transducer Cable	IFM	EVT004	4-20mA	1	Model Ver.
1	Humidity/Temp. sensor	Dwyer	RHP-2R11 (2 outputs)	4-20mA	1	Default
1	Top left indirect cooled Air Temp.	IFM	TA2262 (PT1000 inbuilt signal converter)	4-20mA	1	Model Ver.
1	Top coil Supply Air Temp. (Cooled air)	IFM	TA2262 (PT1000 inbuilt signal converter)	4-20mA	1	Default
1	Top coil discharge Air Temp. (dry heated)	IFM	TA2262 (PT1000 inbuilt signal converter)	4-20mA	1	Model Ver.
1	Top Exhaust Air Temperature (humid air)	IFM	TA2262 (PT1000 inbuilt signal converter)	4-20mA	1	Model Ver.
1	Bottom left indirect cooled Air Temp.	IFM	TA2262 (PT1000 inbuilt signal converter)	4-20mA	1	Model Ver.
1	Bottom coil Supply Air Temp. (Cooled air)	IFM	TA2262 (PT1000 inbuilt signal converter)	4-20mA	1	Default

1	Bottom coil discharge Air Temp. (dry heated)	IFM	TA2262 (PT1000 inbuilt signal converter)	4-20mA	1	Model Ver.
1	Bottom Exhaust Air Temperature (humid air)	IFM	TA2262 (PT1000 inbuilt signal converter)	4-20mA	1	Model Ver.
2	Top coil Supply Air Temp. (Cooled air)	IFM	TA2262 (PT1000 inbuilt signal converter)	4-20mA	1	Default
2	Bottom coil Supply Air Temp. (Cooled air)	IFM	TA2262 (PT1000 inbuilt signal converter)	4-20mA	1	Default
3	Top coil Supply Air Temp. (Cooled air)	IFM	TA2262 (PT1000 inbuilt signal converter)	4-20mA	1	Default
3	Bottom coil Supply Air Temp. (Cooled air)	IFM	TA2262 (PT1000 inbuilt signal converter)	4-20mA	1	Default
1,2,3	Temp. Probe Cable & Socket	IFM	EVT001	N/A	12	Model Ver.
1	PD sensor (Top left Fan pressure)	Dwyer	607D-04 or MS2-W102	4-20mA	1	Default
1	PD sensor (Top left middle chamber pressure)	Dwyer	607D-04 or MS2-W102	4-20mA	1	Model Ver.
1	PD sensor (Top left supply duct pressure)	Dwyer	607D-04 or MS2-W102	4-20mA	1	Default
1	PD sensor (Bottom left Fan pressure)	Dwyer	607D-04 or MS2-W102	4-20mA	1	Model Ver.
1	PD sensor (Bottom left middle chamber pressure)	Dwyer	607D-04 or MS2-W102	4-20mA	1	Default

1	PD sensor (Bottom left supply duct pressure)	Dwyer	607D-04 or MS2-W102	4-20mA	1	Model Ver.
1	PD sensor (Top left fan filter pressure)	Dwyer	607D-04 or MS2-W102	4-20mA	1	Default
1	PD sensor (Bottom left fan filter pressure)	Dwyer	607D-04 or MS2-W102	4-20mA	1	Model Ver.
1,2,3	level switch Water tank low level switch	SPX	Ultima switch (bilge pump)	24V DC	3	Default
1,2,4	level switch Water tank High level switch	SPX	Ultima switch (bilge pump)	24V DC	3	Default
1	Water tank Level sensor	IFM	LR2050	4-20mA	1	Model Ver.
1	Level sensor Cable	IFM	EVT004	4-20mA	3	Model Ver.
1	Unit 1 makeup water flow	IFM	SM8030	4-20mA	1	Model Ver.
site inst.	Total makeup water flow (This might not exist)	IFM	SM2000	4-20mA	1	Model Ver.

#### Power Measurement

Unit	Description	Manufacturer	Model Number	Signal	Total Qty	Default/ Model verification
	Power meter	Dent Inst.	PS48HD-C-D-N (Ethernet, Serial, Enclosure, & LCD Display)	MOD-BUS	1	Model Ver.
1	Current transducer (Top left Fan)	Dent Inst.	CT-HSC-20 (20A)	mA	1	Model Ver.
1	Current transducer (Top right Fan)	Dent Inst.	CT-HSC-20 (20A)	mA	1	Model Ver.
1	Current transducer (Bottom left Fan)	Dent Inst.	CT-HSC-20 (20A)	mA	1	Model Ver.
1	Current transducer (Bottom right Fan)	Dent Inst.	CT-HSC-20 (20A)	mA	1	Model Ver.

1	Current transducer (Total fan power)	Dent Inst.	CT-HSC-50 (50A)	mA	1	Model Ver.
1	Current transducer (Total pump power)	Dent Inst.	CT-HSC-20 (20A)	mA	1	Model Ver.
1	Current transducer (Total fan power)	Dent Inst.	CT-HSC-50 (50A)	mA	1	Model Ver.
1	Current transducer (Total pump power)	Dent Inst.	CT-HSC-20 (20A)	mA	1	Model Ver.
1	Current transducer (Total fan power)	Dent Inst.	CT-HSC-50 (50A)	mA	1	Model Ver.
1	Current transducer (Total pump power)	Dent Inst.	CT-HSC-20 (20A)	mA	1	Model Ver.
1	Current transducer (total system power)	Dent Inst.	CT-R16-A4-U (5000A)	mA	1	Model Ver.
1	Current transducer (LT compressors)	Dent Inst.	CT-HMC-100 (100A)	mA	1	Model Ver.
1	Current transducer (MT compressors)	Dent Inst.	CT-HMC-100 (100A)	mA	1	Model Ver.
1	Current transducer (HT compressors)	Dent Inst.	CT-HMC-100 (100A)	mA	1	Model Ver.

#### Control

Unit	Description	Manufacturer	Model Number	Signal	Total Qty	Default/ Model verification
1,2,3	Scada	CITEC	100 point licence +Program	MODBUS	1	Model Ver.
1	Main PLC with enough IOs for the monitored unit	Schneider	SCHNEIDER M251, DUAL ETHERNET PLC  - 16 x DIGITAL INPUTS	MODBUS	1	Model Ver.

			<ul style="list-style-type: none"> <li>- 16 x DIGITAL OUTPUTS</li> <li>- 32 x 4-20mA ANALOG INPUTS</li> <li>- 4 x 0-10V ANALOG OUTPUTS</li> </ul>			
2	Auxiliary Unit	Schneider	<p>Auxiliary DP unit</p> <p>ADVANTYS I/O</p> <ul style="list-style-type: none"> <li>- 6 x DIGITAL INPUTS</li> <li>- 6 x DIGITAL OUTPUTS</li> <li>- 8 x 4-20mA ANALOG INPUTS</li> <li>- 4 x 0-10V ANALOG OUTPUTS</li> </ul>	MODBUS	1	Default
3	Auxiliary Unit	Schneider	<p>Auxiliary DP unit</p> <p>ADVANTYS I/O</p> <ul style="list-style-type: none"> <li>- 6 x DIGITAL INPUTS</li> <li>- 6 x DIGITAL OUTPUTS</li> <li>- 8 x 4-20mA ANALOG INPUTS</li> </ul>	MODBUS	1	Default



			- 4 x 0-10V ANALOG OUTPUTS			
4	Auxiliary Unit	Schneider	Auxiliary DP unit  ADVANTYS I/O  - 6 x DIGITAL INPUTS  - 6 x DIGITAL OUTPUTS  - 8 x 4-20mA ANALOG INPUTS  - 4 x 0-10V ANALOG OUTPUTS	MODBUS	1	Default

### Pressure transducers

Converts pressure to an electrical output signal. These transducers are available commercially with high accuracy and response time. Depending on the position of the sensor on the CO<sub>2</sub> refrigeration cycle, sensors within a measuring range of 0 to 250 bar are selected. The response time of these sensors are 2 ms which is much faster than pressure variation in the system. The accuracy of 0.05% of the measuring range is acceptable for these sensors. A 0-250 bar IFM transducer is chosen (Figure 55) to measure the discharge pressure. This will also be available through the CO<sub>2</sub> rack pressure transducer.

The tag used in the diagram in the appendix to identify these instruments on the refrigeration loop and the

condenser / gas-cooler units is: 



Figure 55: IFM PT series pressure transducer

## Resistive Temperature Detector (RTD)

The relationship between change in resistance of specific material with their temperature is known and repeatable. A transmitter (signal converter) can generate a signal and measure the change of resistance and convert it to an output signal. These sensors are commercially available with various accuracies and response times. The two types of RTDs considered in the current project are the PT100 and PT1000. PT1000 RTDs can capture smaller variation in temperature. We have chosen both sensors for different measurements depending on the physical shape of the available sensors and the available space for mounting them. It should be noted that the temperatures will be measured within two mediums, i.e., CO<sub>2</sub> throughout the refrigeration loop and air at different stages of the condensing/ gas cooling process as listed in Table 3. The main difference between the two is that the measuring device is in direct contact with the medium in the case of air as opposed to CO<sub>2</sub> which is interfaced with the copper tube material. The thermal resistance of the intermediate material as well as the impact of outside temperature delays the correct measurement of the temperature value. The following 3 types are sensors are selected:


- a) IFM TA2262 probes (PT1000) with fast response time are selected to measure air temperature at different stages, namely, ambient temperature, cooled air through indirect pads, cooled air through direct pads and heated air through the condenser/ gas cooler coil. The sensor reaches 90% of the actual value in less than 2 seconds with an accuracy of 0.3% (Figure 56). A transmitter is embedded in these sensors to produce an analogue signal proportional to the measured value. The tag used in the diagram in the appendix to identify these instruments on the condenser / gas cooler units is: 



Figure 56 IFM TA2262 temperature sensor (RTD)

- b) IFM TS4759 are selected to measure the temperature of CO<sub>2</sub>. These PT100 RTDs are as accurate as the former model (0.3% of the measuring range) however slower in response time and takes less than 8 seconds to transmit 90% of the actual temperature value. These are particularly selected as they can be installed on the surface of the smaller copper tubes by means of a welded nut to enable a reliable and effective contact surface for heat transfer (Figure 57). This sensor is an RTD without a signal converter and requires an IFM evaluation unit (Figure 58) to generate the analogue output proportional to the temperature by measuring the resistance of the probe. The


tag used in the diagram in the appendix to identify these instruments on the refrigeration loop and the condenser / gas cooler units is: 



Figure 57 IFM TS4759 temperature sensor (RTD)



Figure 58 IFM TP3231 evaluation unit

- c) IFM TA2537 are as accurate and fast as TA2262s. These are selected to measure the discharge and gas return temperature of the controlled condenser/gas cooler coils. The tag used on the diagram in the appendix to identify these instruments on the refrigeration loop and the condenser/gas


cooler units is: 



Figure 59 IFM TA2537 temperature sensor RTD

## Ambient air Humidity

The ambient air humidity will be measured using a Dwyer RHP-2R11 sensor (Figure 60), which is a dual output sensor that is capable of measuring both humidity and temperature. Its measuring accuracy of  $\pm 2\%$  for a relative humidity range of 10-90% is acceptable. However due to poor response time of the embedded temperature sensor, the embedded temperature sensor will not be used to measure temperature (for temperature, the IFM TA 2262 sensor, as described in Section 0 will be used instead). The setup should be installed outside near the air intake of the gas cooler, preferably in shade for minimal impact from solar

radiation. The tag used on the diagram in the appendix to indicate this instrument is:



Figure 60 Dwyer RHP-2R11 humidity sensor

## Pressure Differential sensor

As explained in section 3.3.1, the air flow rate should be known when calculating the energy transfer through the indirect evaporative cooler condenser. However, it is difficult to measure the air flow rate accurately. This is due to inconsistency in the pressure drops at each section of the air flow profile. In addition, common air flow measurement instruments measure the flow by translating the cooling effect of the flow stream using a hot wire. Variation in the air flow temperature which is inherent in this system reduces the reliability and accuracy of the measurement. Instead, measuring the pressure difference at each section against the atmospheric pressure will give more accurate results. Measuring the pressure created by the condenser fans can be translated to air flow by using the fan curves. We will measure the pressure after the indirect pads as well as after the direct pads and at the exhaust of the dew point coolers. This an easy way to control the ratio of air split between the channels of the cooler. We have selected a Dwyer 607D-04 which is the most accurate (0.25%) with fast response time (1 ms) to measure the fan pressure for accurate calculation of flow rate. As air flow ratios and pad pressure drops can be measured at steady state at different flow rates, for other sections

the Dwyer MS2-W102 is selected with a slower response time (0-240 s). The tag used on the diagram in the appendix to identify these instruments on the system is: <sup>(P)</sup>



Figure 61 Dwyer 607D-04 pressure differential sensor



Figure 62 Dwyer MS2-W102 Pressure differential sensor

### Water level switch

The indirect evaporative cooler uses the cooling effect of evaporation of water. As with any other equipment that consumes water it is important to accurately manage and monitor its usage. Two types of sensors are selected in this project. Firstly, high- and low-level switches are used to fill the water tank and ensure there is always sufficient water available for spraying the pads. For this purpose, an SPX Ultima switch (Figure 63) which are capacitive level detectors are selected which are designed for harsher environments and will be reliable and low maintenance for our application. The tag used on the diagram in the appendix to identify these switches on the system is: <sup>(S)</sup>



Figure 63 XPS Ultima switch capacitive level switch

### Water level sensor


The second type of sensor is an IFM LR2050, a radar guided level sensor to continuously measure the level of water in the tank with 1 mm resolution (Figure 64). This level translates to the instantaneous volume of water in the tank. Values like the amount of water that is dumped for avoiding bacterial growth as well as the amount of water the pads hold while being sprayed or after being sprayed can be derived from its readings. This sensor will be mounted on the controlled unit. The tag used on the diagram in the appendix to identify this instrument on the system is: 



Figure 64: IFM LR050 radar guided level sensor

### Water flow meter

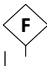
In order to verify the calculation of the actual evaporated water through the indirect evaporative cooling process the total volume of water supplied to the control unit will be measure with an IFM SM8030 magnetic flow meter. The accuracy is claimed to be 0.8% of the measuring range. A fast response time is not crucial as the makeup water flow rate is steady. The tag used on the diagram in the appendix to identify this instrument on the system is: 



Figure 65 IFM SM8030 Magnetic water flow meter

### Power meter

As explained in section 2.2.1.1, the evaluation of efficiency requires the instantaneous input electrical power to the system. Power measurement devices have become popular and commercially available in favour of energy

management strategies employed by power consumers. Dent Instruments provides a number of options for measuring the electrical power supplier to multiple devices. The major power consumers on our system are the compressors and fans. At the time of writing this report, the proposed DP-CO<sub>2</sub> system design has 10 compressors and 12 fans within system. A Dent Power Scout 48 with 48 measurement channels is selected to meet the requirement (Figure 66). The electrical current passing through each device is detected and transmitted to the power meter through current transformers mounted on the electrical input wires of each device. These are called current transformers or CTs in short. The input voltage is measured for each device as well. Values such as Power, Energy, Current, Power factor can be transmitted through multiple communication channels available on the PS48. The accuracy level of this instrument is class 0.2. The tag used on the diagram in the appendix to identify the CTs on each device is: **CT**



Figure 66: Dent Power Meter PS48



Figure 67: Dent HSC-20 Mini Hinged current transformer





## Appendix D: Summary of IRG Meetings

As part of the project, an Industry Reference Group (IRG) was established to provide independent feedback and perspectives. The IRG comprised of representatives from:

- The Australian Institute of Refrigeration Air Conditioning and Heating (AIRAH)
- Alfa Laval
- Americold
- The Australian Meat Processing Corporation (AMPC)
- Coca-Cola Europacific Partners
- Dairy Australia
- Health Infrastructure (New South Wales)
- Mater Group
- The Refrigerated Warehouse and Transport Association (RWTA)

The project team engaged with the IRG through scheduled workshops, and directly through email correspondence and individual video conferences. Outcomes of these meetings, workshops and correspondence have enabled the project team to apply their findings to a range of sectors and climates, as discussed in Section 4.

The project originally planned for a total of six IRG workshops to be held throughout the duration of the project, however due to the early termination of the project, only four workshops were held. These meetings are summarised in the sub-sections below.

### IRG Meeting #1

The first IRG meeting for the project was held on the 17<sup>th</sup> of February, 2022, and was conducted fully online via Microsoft Teams. The meeting was attended by all five project partners, five IRG member organisations and the RACE for 2030 Business Program Manager. The meeting lasted 2 hours, with a significant portion of the time allocated to discussion and Q&A.

The aim of the meeting was to introduce the project to the IRG members, and to discuss the overall project plan, including objectives, tasks, milestones and knowledge sharing plan. In particular, feedback from the IRG was sought about aspects of the project that are most relevant to the IRG, and to ascertain the key features of the project that may be the most useful to their own individual organisations.

Questions from the IRG focussed on the technical aspects of the project, including the details of the (at that time) proposed DP-CO<sub>2</sub> system that was going to be installed at Coles, such as control systems, material selection, operational temperatures, together with the serviceability and cost implications of the new system, particularly when retrofitted.

Additionally, the IRG also recommended that the project scope be expanded to include a comparison of the DP-CO<sub>2</sub> system against alternative systems, particularly those commonly utilised in the sector, including adiabatically cooled systems and Ammonia (NH<sub>3</sub>) based refrigerant systems. While the suggestion to include a comparison to adiabatically cooled systems was taken on board, with the results included in this report (see Section 6.2.3), a comparison against NH<sub>3</sub> systems was not conducted as this was outside the scope of the project.

A more detailed summary of the meeting outcomes can be found in Milestone Report I (Lau et al., 2022a).

## IRG Meeting #2

The second IRG meeting was held on the 19<sup>th</sup> of May, 2022, and was attended by all project partners, five IRG organisations and the RACE for 2030 Business Program Manager. The meeting was held online. The meeting focussed on discussing the latest outcomes of the preliminary model of the DP-CO<sub>2</sub> system, together with the preliminary design of the DP-CO<sub>2</sub> system to be installed at Coles (including the monitoring system). In particular, the project partners used the meeting as an opportunity to engage with the IRG members that could potentially volunteer their organisation as a case study in the application of the model. That is, the project team asked if any IRG members would be willing to provide basic data of their refrigeration system (such as loads, temperatures, usage profile) that the project team could input into their model. A number of IRG members responded positively to the request, with the results presented in Section 4 of this report.

The IRG also recommended that the model be expanded to include the ability to model water consumption, given that the DP-CO<sub>2</sub> system is expected to consume significantly more water than conventional refrigeration systems. This would allow organisations to balance the need to reduce energy consumption and conserve water. This feedback was taken on board, with the final model capable of estimated water consumption (see Section 3.2.2).

The IRG also noted that the utility of the model would be greatly expanded if the model was applied to a range of climatic conditions relevant to Australia, and not only limited to Adelaide (where the Coles supermarket is located). This feedback has also been addressed in the current report, with the results of the model applied to Australian-wide conditions shown in Section 4.2.4.

Further details of IRG Meeting #2 can be found in Milestone Report II (Lau et al., 2022b).

## IRG Meeting #3

The third IRG meeting was held on the 18<sup>th</sup> of November 2022 via Microsoft Teams. Key representatives from UniSA, QUT and RACE for 2030 attended, together with representatives from four IRG members. The aim of the meeting was to provide an update of the status of the DP-CO<sub>2</sub> system manufacturing and installation, and to discuss the results of the preliminary model applied to a range of non-supermarket conditions.

At the time of the meeting, the design of the DP-CO<sub>2</sub> system had been completed, with the key components of the system in the process of being procured. In particular, Seeley's dew point coolers had been procured, with the rack frames, dampers and stainless steel tanks installed. The sensors for the monitoring system, as well as the gas cooler units, were in the process of being installed. Images of the system being installed were shown to the IRG members.

The meeting also discussed the results of the model applied to a number of non-supermarket case studies, with the case studies including an orchard and an aquarium. The project team then demonstrated how the model can be used sectors represented by the IRG, including abattoirs, cold chain storage and hospitals. These results are presented in Section 4 of this report.

The IRG re-iterated the need for the model to be able to simulate conventional refrigeration systems, in particular adiabatic spray-type CO<sub>2</sub> systems and other low GWP refrigerants, such as ammonia and hydrofluoroolefins (HFOs). The IRG also noted that it would be useful to expand the model to include a costing tool, with the tool being able to estimate capital costs, reduction in ongoing energy costs and calculating a payback period. The project team noted that they are reluctant to develop a costing tool, given

the volatility in energy prices and the lack of reliable data on the true capital cost of the system given that the current DP-CO<sub>2</sub> system will be a world first.

A full review of IRG Meeting #3 can be found in Milestone Report III (Lau et al., 2022c).

## IRG Meeting #4

The fourth IRG meeting was held on the 23<sup>rd</sup> of August, 2023, and was held on Microsoft Teams. In attendance were representatives from UniSA, A2EP and RACE for 2030, together with five IRG members. The agenda for the meeting was to update the IRG on the installation and commissioning of the DP-CO<sub>2</sub> system at Coles, and to provide an overview of the operation of the monitoring system given that the Coles store opened a few months prior to the meeting.

In particular, the project team presented to the IRG the final (as-installed) design of the DP-CO<sub>2</sub> system, together with details of its final construction, assembly, transportation to site and commissioning. Furthermore, a demonstration of the monitoring system interface, including a brief overview of the type of data that the monitoring system can provide, was also presented.

The meeting agenda also included a brief discussion on the potential knowledge sharing and industry engagement activities that the project team were planning, given that the DP-CO<sub>2</sub> system was up and running at Coles.

The feedback from the IRG largely focussed on the costs of the system, with the IRG inquiring about the capital cost of the final as-installed system, the expected financial savings due to energy reduction, and the return on investment. There was also discussion on the scalability of the system, and whether there were any limitations on its maximum size and capacity.

The IRG also provided feedback that an interactive tool whereby users can self-assess for their own circumstances and conditions would be useful. The project team noted that they plan to develop such a simplified, user-friendly tool.

A full report of the outcomes of IRG Meeting #4 can be found in Progress Report IV (Lau et al., 2023).

# RACE for 2030

[www.racefor2030.com.au](http://www.racefor2030.com.au)